To: Prof. Jack Middelburg

Dear Jack,

Please find enclosed our revised manuscript entitled **"Do degree and rate of silicate weathering depend on plant productivity?"** by Oeser and von Blanckenburg

We would like to thank you and the reviewers for the very constructive reviews, allowing us to improve our manuscript and better readable for a wider audience.

In this revision we followed many of the reviewer's comments but not all as some of the structure and content was requested by the other reviewers. Below you will find the point by point replies to the comments and suggestions of the reviewer.

Despite the hard work for you, the reviewers, and for us, we enjoyed the discussion process at Biogeosciences which we hope in this case resulted in a hopefully though-provoking, yet acceptable version for an interdisciplinary readership. We would like to express our thanks for guiding us through this process.

In the name of Friedhelm von Blanckenburg and Ralf A. Oeser, yours sincerely,

Ralf

I had already reviewed the first version of the manuscript and appreciate the complete overhaul, which rendered the paper much clearer. However, I have still concerns with respect to (i) the unusual use of soil scientific terms, (ii) partly sloppy and even wrong use of plant nutritional terminology, (iii) the statistical data treatment, and (iv) the general structure of the paper, which is still overly long for its message. I regret that the authors seem to be resistant against some of the reviewer comments without presenting arguments that I find convincing.

REPLY: We are grateful nevertheless for the comments from this reviewer and the other three reviewers. They considerably helped to shape this paper, that was written from the view point of Geochemistry, but will hopefully be read by readers from other fields, for example ecologists and soil scientists. This task involved a whole range of issues, including time scales, terminology, and general scientific perspective. In this revision we followed many of the reviewer comments – but not all, as some of the structure and contents was requested by the other reviewers, whereas other content we deem necessary to make this work accessible to an interdisciplinary audience.

i. I think that the use of saprolite is not consistent with its usual meaning in Soil Science. Saprolite is the lowermost part of the deep, strongly chemically weathered soil in the humid inner tropics where desilication prevails. Saprolites are characterized by their intensive degree of weathering while at the same time the original structure is maintained because of the location under tens of meters of weathered material. Saprolites surround Woolsacks and occur as relics of the Tertiary at erosion-protected locations in temperate soils but according to the soil description at your study sites in Chile, there are no saprolites. As a consequence, the use of the term regolith does not seem to be necessary, because there is no part of the weathering mantle which is free of living organisms. What you are studying is the soil with A, B, C and perhaps even R horizons. I understand what you mean by “weathering front” when referring to deep cracks in the granitoid rocks, where initial weathering indeed takes place but in Soil Science the weathering front is usually seen at the contact interface between soil and bedrock, i.e. between the Cw and the (nearly) unweathered rock (i.e. R horizon). The latter does not need to be changed but it should be clear what you mean.

REPLY: We acknowledge that the use of certain terms differs between scientific fields. However, the terminology used in this manuscript is in line with a large number of geomorphic

articles and in particular with the article from Bernhard et al. (2018) on which the classification of the regolith profiles in the EarthShape study sites is based on. In order to be compatible with the other EarthShape papers and other geomorphic papers we retain the terminology used.

ii. Although the authors removed the part that I most criticized in my past review, there are still several issues with the plant nutritional terminology. First of all, it must be clearly recognized that the most limiting nutrient is N, which is not rock-derived. The demand for the rock-derived nutrients follow the N supply in little variable stoichiometric ratios. All essential nutrients are required at the same time. A common differentiation would be to distinguish plant mineral macronutrients (N, P, K, Ca, Mg, S) from micronutrients (Fe, B, Cl, Mn, Zn, Cu, Mo, Ni). It is problematic to generally include Al in the list of plant beneficial elements because for most plants Al is not beneficial but even more likely toxic. Moreover, as I already stated in my previous review, nutrient concentrations are mostly regulated in plants so that their concentrations vary by much less than a factor of 10. One of the most extreme cases is the comparison of straw with grain of wheat where the straw contains 5% N and the grain 20%, i.e. a variation by a factor of four. If the whole plant is considered, the variation of nutrient concentrations is usually even smaller. The same is true for element ratios. Consequently, if there is a deviation of a factor of 10 of element ratios between the so-called plant-available nutrient pool in soil and the plants, then this is clearly dissimilar. Moreover, it is not easily possible to characterize plant availability with a single extract, because a single extract does not consider the kinetic replenishment of nutrients after plants have taken up a nutrient and because the extract cannot mimick nutrient acquisition strategies like enhanced mineralization of organic matter by exoenzymes or local acidification by roots and mycorrhizae. This is particularly true for P.

REPLY: Based on the previous reviews we decided to remove any reference to nutrient limitation in the text, including the role of N. Following the reviewers' request in this revised version we introduce the general importance of N to plant nutrition despite not being rock-derived. We further decided to remove any reference on nutrient classification and have erased the terms 'plant-beneficial' and 'plant-essential' throughout the manuscript, figures, and tables accordingly.

We agree that sequential extractions do not mimic nutrient acquisition strategies by plants. Yet estimating plant available nutrients using sequential extraction methods is common

practice in geosciences (e.g. Brucker and Spohn, 2019; Bullen and Chadwick, 2016; Lang et al., 2017). We are not aware of other possibilities to determine plant availability within a reasonable effort.

iii. In principle, I find the approach to single out biological weathering with a statistical approach great. However, I see problems in the small number of independent data you have, i.e. n = 4. You are not transparent about the number of data considered in your analysis and I suspect that you have included more the four data pairs. If one considered the two soil profiles on the different slopes as independent from each other – which is debatable – you had n = 8. (But I would not recommend to do this.)

REPLY: We regret that our statistical data set is not sufficient in the reviewer's eyes. However, we cannot overcome these limitations by any means. Conducting this extensive analysis on even eight profiles represented a formidable effort- In order to address the concerns of the reviewer, we will tone down the corresponding text passages (i.e. removal of direct comparison of r-values as suggested by the reviewer).

We performed these statistical analyses on the basis that the two soil profiles at each site that are considered to be independent from each other. Further we did report p-values in APA style including the degree of freedoms which are directly linked to the independent variables. We believe that this approach was thus completely 'statistically honest'. In the revised version of the manuscript and tables we however explicitly mention the number of statistically independent variables instead.

iv. I think that the conceptual perspectives should be included into the introduction to avoid references to later sections such as in l. 78-79 and 91-94 and because you present your methods before you justify them. I also think that the introduction would become more concise (alone deleting the references to later section saves 5 lines). I therefore strongly suggest to combine and shorten Sections 1 and 2. Moreover, all results are still presented threefold, i.e. in tables, figures, and as numbers in the text. I had already previously suggested that the tables should be moved to the appendix and the numbers in the text deleted, while the figures should be kept and I still insist on this. This could be a really interesting paper. However, it is still cumbersome to read, because it is not sufficiently concise.

REPLY: After the first round of open discussion, we identified several priority revision items. One of which was the need for a section dedicated to the different concepts used in soil- and geosciences to characterize weathering profiles. We would prefer to retain 'Section 2

Conceptual perspectives' to make our concept of weathering and ecosystem nutrition accessible to a broader audience including soil scientists.

Another revision item that was raised by anonymous referee #1. The referee asked for a more rigorous presentation of uncertainties within the text. Therefore, we added uncertainties to the text which we retained in this version. However, to shorten the manuscript and address this referees' concern we suggest transferring the former Tables 4, 6, and 8 into the Appendix. They now become Table A1, A2, and A3.

We will be happy to receive guidelines from the editor on how to proceed in this respect.

Minor comments:

l. 11, 13, 167: Delete "substantial". If the work was not substantial, it should not be published.

REPLY: Done accordingly; the first "substantial" (describing the climate gradient) replaced by "major"

l. 82-83: Move to acknowledgments.

REPLY: Done accordingly

l. 90: Replace "nutritive element" by "mineral nutrient".

REPLY: Done accordingly

l. 97-98: Delete. At this point, this is an unsubstantiated claim and moreover a repetition from the abstract.

REPLY: Done accordingly

l. 125-127: This is not true. In many terrestrial ecosystem, biomass production is limited by N which is rarely (only in bituminous sedimentites) rock-derived but acquired by biological N2 fixation from the air.

REPLY: We agree with the reviewer with regards to N limitation in many terrestrial ecosystems as is the case in the EarthShape sites. We replaced "limitation" by "supply (of a mineral nutrient) needed to sustain an ecosystem over weathering time scales". Furthermore, we suggest adding the following text here: "Note that nitrogen (N), the most limiting nutrient in many ecosystems, is not an element addressed here. Although rocks have recently received attention as source of geogenic N (Houlton et al. 2018) this source is most prominent in sedimentary rock. This study explores ecosystems developed on granitoid rock where N is derived from the inexhaustible atmospheric pool by nitrogen-fixing bacteria, and limitation mostly arises by the energy required for fixation (Chapin III et al, 2011).

l. 127-129: I think that this is a too far-reaching generalization. There are e.g., biodiversity hotspots in mountainous areas, which are not particularly nutrient-poor.

REPLY: We reworded to say that supply by a specific mineral nutrient impacts plant diversity and nutrient acquisition strategies, for which there is ample evidence in the literature, even though of course mineral nutrient limitation is not an exclusive condition for biodiversity hotspots.

l. 156: The "geogenic nutrient pathway" rarely influences nutrient limitation in native ecosystems. I can only imagine that this would be the case if K was growth limiting. Even the P supply is governed by mineral dissolution and sorption-desorption equilibria, organic matter mineralization and biological acquisition strategies such as local acidification by plant roots and mycorrhiza. Of these processes, only mineral dissolution could be counted as weathering process but mostly of secondary minerals. In strongly weathered humid inner tropical ecosystems it is thought that the small losses of nutrients escaping from the close ecosystem cycling are replenished by deposition, while weathering does not play any role.

REPLY: We do not entirely understand the reviewer's comment. The loss of elements from ecosystems, amongst them the mineral nutrients through erosion and leaching has been documented by many studies, in particular for sloping landscapes. In ecosystems where atmospheric deposition does not suffice to balance these losses, nutrients must be replenished through weathering and this replenishment occurs over millennia. The reviewer refers to strongly depleted ecosystems in the tropics. In these erosion rates are way lower than in the EarthShape sites and the losses can indeed be compensated by atmospheric deposition (e.g. Arvin et al., 2017; Boy and Wilcke, 2008; Schuessler et al., 2018), even though the main nutrient source is recycling. These pathways (the geogenic nutrient pathway and the orgaic nutrient pathway were recently related to each other in a paper from our group (Uhlig and von Blanckenburg, 2019) and here we build on this conceptual framework.

l. 166: Start a new sentence after the references.

REPLY: Done accordingly.

l. 171: Mediterranean (with upper scale M).

REPLY: As mediterranean does not refer to the European region but is rather used as an adjective, we will retain the "M" as lower-case letter.

l. 178 (and in the whole paper): Replace "gC" by g m-2 yr-1 C.

REPLY: Done accordingly.

l. 229-230: Umbric Podzols, Orthodystric Umbrisols (mind the spelling including upper case letters).

REPLY: Done accordingly

l. 230: Do you mean an organic layer? Usually, there are several organic horizons (Oi, Oe, Oa).

REPLY: We mean the organic layer as we did not differentiate the single organic horizons. Changed accordingly.

l. 260: Delete "As is commonly the case in field studies", because this is not true. There are many field studies on root distribution even in forests.

REPLY: Deleted accordingly.

l. 262: What is the "litter layer"? Only the Oi horizon, i.e. the freshly fallen litter of the same or perhaps two years? Or the whole organic layer? Use consistent terminology.

REPLY: The litter layer comprised small woody debris and leaves fallen within the last two years. We amended the sentence accordingly.

l. 281: Where are the results of these quality controls?

REPLY: All data (including analysis of reference materials) are reported in an open access data repository (Oeser and von Blanckenburg, 2020). We mention the existence of this data supplement in the text.

l. 286 (and in the whole paper): The correct SI unit is mL (with upper case L).

REPLY: This journal asks to follow the recommendations of the SI and IUPAC. According to SI, both terms ml and mL are correct. Hence, we will retain ml throughout the manuscript.

l. 287 (and in the whole paper): Milli-Q is a brand name, which should not be used. Replace by "deionized water".

REPLYY: Done accordingly

l. 290 and l. 303: "rounds per minute" are meaningless without the knowledge of the geometry of your centrifuge or shaker. Delete or replace by g.

REPLY: Although we partially agree with reviewer we still prefer to retain the rpm as most lab centrifuges are similar and the reader thus gets a feel for the method.

l. 351: P and K are not the "most important nutrients" in a N-limited system like yours. It is N, and N supply does not depend on weathering at your study sites. This must be acknowledged and discussed.

REPLY: We are a little puzzled by this comment. We do explicitly use the term 'mineral nutrients' and although N can be derived though geogenic sources (Houlton et al., 2018), we

did not aim to include nitrogen into that group. However, we will highlight the particular role of N on gross primary production in line 133ff (see above).

l. 354: It is wrong to consider Al as a generally beneficial element for plants, only for a few and only at low concentrations. In Marschner (2012) it is stated: "Aluminum is beneficial to some plants, such as tea, and may alleviate proton toxicity and increase the activity of antioxidant enzymes."

REPLY: We did tone down this paragraph accordingly and removed any reference to plant-essential or plant-beneficial elements from the text and figures (see previous comment to point ii).

l. 355: It is wrong to include the micronutrient Fe into the group of beneficial elements. It does not make sense to refer to an arbitrary selection of nutrients as "plant-essential elements".

REPLY: Please see our comment above.

l. 356: It is wrong to consider Sr as a nutrient. It is at best a surrogate. However, its metabolism in plants differs from that of Ca for which it is used as surrogate (see e.g., Blum et al., 2012, Plant Soil 356, 303-314).

REPLY: Please see our comment above.

l. 364: I do not understand what you mean by "the shallowest mineral soil"?

REPLY: We mean the subsoil. Changed accordingly.

l. 382: element-specific

REPLY: Changed accordingly.

l. 395: The total stock of elements would include the organic layer, which plays a particular important role for plant nutrition, where present.

REPLY: The reviewer is right, elements contained in the organic layer would indeed contribute to the total stock of nutrients available. However, their total stock might be small compared to the mineral nutrients contained in bulk regolith. This is the theoretically maximum available amount of nutrients available. We changed the text to 'The maximum amount of mineral nutrients…'.

l. 403: If you just sum up the stocks of macro and micronutrients the result will be (almost) identical to that for the macronutrients. I do hard in seeing an additional value in this metric.

REPLY: Wo do not understand the reviewer's comment in that context. We believe it is worth mentioning that the total inventory of bio-available nutrients is highest in the arid site (where

demand in terms of NPP is lowest among the four sites) but lowest in the high-NPP site of Nahuelbuta. We discuss this pattern later in the manuscript.

l. 433-435: This is an example where numbers are mentioned in the text, which are additionally shown in Table 3 and Figure 4. It is sufficient to show the data once (preferably in the figure).

REPLY: Please see our comment to the referee's point iv. We are happy to receive guidelines from the editor on how to proceed.

l. 448: Is such a small difference really significant?

REPLY: In the framework of (radiogenic) isotope geochemistry even smaller differences are significant when resolvable. Resolution is dependent on the method applied but commonly variations on the 5th decimal are easily detectable.

l. 481: I believe that your estimate of the contribution of sea spray is not correct. At the short distance of 80 km to the ocean there must be a visible input of sea spray and this input should increase with increasing surface area of the canopy, i.e. from N to S. Couldn't the deviation of the Sr isotope ratio in the so-called bioavailable pool be caused by incorporation of Sr deposited from the sea? What is the Sr isotope ratio of sea spray? – I mentioned this already in my previous review and am not satisfied by the answer.

REPLY: We still do not entirely understand this comment. We have determined atmospheric contribution relative to weathering input from Sr isotopes using a two-component mixing calculation using bedrock and seaspray as endmembers. This is a commonly used approach. Accordingly, up to 93 and 43% of Sr derived from seaspray are incorporated in the regolith profiles of Pan de Azúcar and Santa Gracia, respectively. No such an input was found in the other two sites. Although we could not detect seaspray input in these sites, that does not mean this input is not existent. However, the **flux** of Sr derived from weathering likely exceeds the seaspray flux by orders of magnitude such that we cannot resolve this incorporation. Sr seaspray ratio is mentioned in Table A2 and Figure 5.

l. 489: This is pure speculation.

REPLY: The referee is right inasmuch as we have no direct mineral-specific measurements of $^{87}Sr/^{86}Sr$. However, we have no indications of a significant incorporation of external sources into the regolith profiles of La Campana and Nahuelbuta (neither $^{87}Sr/^{86}Sr$ nor τ-values would permit such a conclusion). If not from weathering of rock, what is the Sr-source? We will tone down this sentence.

l. 495: The most-demanded (in terms of limitation and quantitatively) is N, not P.

REPLY: Please see our previous comments on N. We do not regard N as a mineral nutrient simply because the majority of the N stem from Earth's largest N inventory, the atmosphere and is not limited by weathering rather than fixation. We addressed this misunderstanding by adding 'rock-derived'.

l. 501: One order of magnitude is more than nutrient concentrations and ratios in plants vary.

REPLY: We do not understand this comment. We found that with increasing NPP (and from saprolite to soil) the X:P ratio between the bio-available pool and plants increasingly approach the 1:1 line. We interpret these shifts as an increasing signature of plant material in the bio-available fraction, caused by higher recycling rates. We omitted making any further conclusions on plant stoichiometrical pattern.

l. 523: A large part of the nutrient recycling occurs via the organic layer which is not considered here. This could at least be acknowledged in the discussion.

REPLY: We acknowledge the loci of recycling by specifically mentioning organic bearing soil horizons: 'In the remaining sites $\mathrm{Rec}^{\mathrm{X}}$ **occurs in all organic-bearing soil horizons** and increases…'

l. 524-525: The plants take up nutrients from greater depth, primarily because they only find water there. Without water, there is no nutrient uptake via the roots.

REPLY: Deep nutrient uptake as nutrient acquisition strategy has only recently been shown by Uhlig et al. (2020). However, in order to account for the reviewer's concern, we changed the sentence into '…forage nutrients and water by deep…'.

l. 561: Organo-Al complexes are not bioavailable (and non-toxic).

REPLY: The wording is indeed a little bit confusing. We therefore change 'available' to 'abundant'

l. 567: This "dilution effect" is called "leaching" in Soil Science. **l. 570:** It is the pH value and leaching.

REPLY: We mean the "dilution effect" of solutes in water, as described in concentration-discharge relationships.

l. 595: Weathering only needs to replace the loss from plant nutrient cycling, not supply the whole required plant nutrients.

REPLY: This is exactly at the heart of the "geogenic nutrient pathay" - replacing the loss from recycling.

l. 636-641: What is the number of replicates? You need to mind that these replicates need to be statistically independent from each other. You need to add this number to Table A1. The maximum number of such data you have is in my view n = 4 (see above).

REPLY: Please see our response to reviewer's point iii. We treat the two regolith profiles at each site as natural (hence independent) replicates. In our view, n = 8. In Appendix B and the statistical tables, we now clearly state the number of replicates.

l. 667-669: Given the low number of independent correlation pairs, I would refrain from such a quantitative comparison of r values.

REPLY: We did refrain from mentioning r values in the text. Instead we only reference to the Table(s).

l. 685: How was this tested? Again, what was your number of replicates per site? Two?

REPLY: The description of the statistical procedures can be found in Appendix B. We tested for statistically significant differences in weathering pattern using Tukey's HSD test. The number of replicates per site is two.

l. 754-756: This is typical for the weathering regime of temperate soils where Si released from weathering is not leached but forms secondary minerals such as clay minerals. Thus nothing new.

REPLY: Please to see that interpretations from soil sciences and weathering geochemistry converge.

l. 769: Even though/Although

REPLY: Changed accordingly.

Table 2, Eq. (5): I think that you need to exchange numerator and denominator.

REPLY: We believe the equation is correct.

Arvin, L.J., Riebe, C.S., Aciego, S.M., Blakowski, M.A., 2017. Global patterns of dust and bedrock nutrient supply to montane ecosystems. Science Advances, 3: 1-10.

Bernhard, N. et al., 2018. Pedogenic and microbial interrelations to regional climate and local topography: new insights from a climate gradient (arid to humid) along the Coastal Cordillera of Chile. Catena, 170.

Boy, J., Wilcke, W., 2008. Tropical Andean forest derives calcium and magnesium from Saharan dust. Global Biogeochemical Cycles, 22(1): GB1027.

Brucker, E., Spohn, M., 2019. Formation of soil phosphorus fractions along a climate and vegetation gradient in the Coastal Cordillera of Chile. Catena, 180: 203-211.

Bullen, T.D., Chadwick, O., 2016. Ca, Sr and Ba stable isotopes reveal the fate of soil nutrients along a tropical climosequence in Hawaii. Chemical Geology, 422: 25-45.

Houlton, B.Z., Morford, S.L., Dahlgren, R.A., 2018. Convergent evidence for widespread rock nitrogen sources in Earth's surface environment. Science, 360(6384): 58-62.

Lang, F. et al., 2017. Soil phosphorus supply controls P nutrition strategies of beech forest ecosystems in Central Europe. Biogeochemistry, 136(1): 5-29.

Oeser, R.A., von Blanckenburg, F., 2020. Dataset for evaluation element fluxes released by weathering and taken up by plants along the EarthShape climate and vegetation gradient, GFZ Data Services.

Schuessler, J.A., von Blanckenburg, F., Bouchez, J., Uhlig, D., Hewawasam, T., 2018. Nutrient cycling in a tropical montane rainforest under a supply-limited weathering regime traced by elemental mass balances and Mg stable isotopes. Chemical Geology, 497: 74-87.

Uhlig, D., Amelung, W., von Blanckenburg, F., 2020. Mineral nutrients sourced in deep regolith sustain long-term nutrition of mountainous temperate forest ecosystems. Global Biogeochemical Cycles.

Uhlig, D., von Blanckenburg, F., 2019. How Slow Rock Weathering Balances Nutrient Loss During Fast Forest Floor Turnover in Montane, Temperate Forest Ecosystems. Frontiers in Earth Science, 7.

Do degree and rate of silicate weathering depend on plant productivity?

Ralf A. Oeser[1], Friedhelm von Blanckenburg[1,2]

[1] GFZ German Research Centre for Geosciences, Section Earth Surface Geochemistry, Potsdam, D-14473, Germany
[2] Freie Universität Berlin; Institute of Geological Science, Berlin, D-12249, Germany

Correspondence to: Ralf A. Oeser (oeser@gfz-potsdam.de)

Abstract. Plants and their associated below-ground microbiota possess the tools for rock weathering. Yet the quantitative evaluation of the impact of these biogenic weathering drivers relative to abiogenic parameters, such as the supply of primary minerals, of water, and of acids is an open question in Critical Zone research. Here we present a novel strategy to decipher the relative impact of these drivers. We quantified the degree and rate of weathering and compared these to nutrient uptake along the "EarthShape" transect in the Chilean Coastal Cordillera. These sites define a major north-south gradient in precipitation and primary productivity but overlie granitoid rock throughout. We present a dataset of the chemistry of Critical Zone compartments (bedrock, regolith, soil, and vegetation) to quantify the relative loss of soluble elements (the "degree of weathering") and the inventory of bio-available elements. We use $^{87}Sr/^{86}Sr$ isotope ratios to identify the sources of mineral nutrients to plants. With rates from cosmogenic nuclides and biomass growth we determined fluxes ("weathering rates"), meaning the rate of loss of elements out of the ecosystems, averaged over weathering timescales (millennia), and quantified mineral nutrient recycling between the bulk weathering zone and the bulk vegetation cover. We found that neither the degree of weathering nor the weathering rates increase systematically with precipitation from north to south along the climate and vegetation gradient. Instead, the increase in biomass nutrient demand is accommodated by faster nutrient recycling. In the absence of an increase in weathering rate despite a five-fold increase in precipitation and NPP, we hypothesize that plant growth might in fact dampen weathering rates. Because plants are thought to be key players in the global silicate weathering - carbon feedback, this hypothesis merits further evaluation.

hat gelöscht: substantial

hat gelöscht: substantial

1 Introduction

Ever since the emergence of land plants, their dependence on mineral-derived nutrients has impacted rock weathering (used here to mean the combined processes of primary mineral dissolution, secondary solid formation, and the loss of elements in aqueous solution). This impact results from three types of interaction. The first is mechanical processes, that weaken rock or change the depth of the weathering zone through roots and microbial symbionts (e.g. mycorrhizal fungi; Blum et al., 2002; Brantley et al., 2017; Hasenmueller et al., 2017; Minyard et al., 2012; Quirk et al., 2014; van Schöll et al., 2007). The second is a variety of biogeochemical processes that alter the susceptibility of minerals to weathering. These mechanisms include root respiration that releases protons and CO_2, lowering soil pH, the exudation of organic ligands through roots that increases the solubility of nutrients through complexation, and the uptake, uplift, and recycling of pore fluids and nutrients from solution (e.g. Berner et al., 2003; Brantley et al., 2012; Drever, 1994; Kump et al., 2000; Lee and Boyce, 2010; Jobbágy, 2001; Giehl and von Wiren, 2014). The third interaction affects the water cycle which is impacted by rooting depth and seasonal water storage in saprolite and evapotranspiration (Kleidon et al., 2000; Ibarra et al., 2019). All of these interactions impact weathering, either directly by aiding plant acquisition of mineral nutrients from rock, or indirectly by modifying the water cycle (e.g. Brantley et al., 2011; Porder, 2019; Moulton et al., 2000). This means the presence and growth rate of land plants is commonly thought to have strongly impacted the evolution of Earth's atmosphere over geologic time by strengthening the negative feedback between silicate weathering rates and atmospheric CO_2 concentrations (Beerling and Berner, 2005; Doughty et al., 2014; Lenton et al., 2012; Pagani et al., 2009; Porada et al., 2016).

While biota in general and plants in particular are undoubtedly key players in weathering and pedogenesis, a quantitative evaluation of their impact remains elusive. The reason is our inability to disentangle abiotic from biotic processes in field observations (Amundson et al., 2007). Almost all mass transfer in the weathering zone can have biotic and abiotic causes. An additional challenge is the difficulty in accounting for confounding effects. Environmental state variables shaping the Critical Zone (the zone of the Earth surface that extends from the top of unweathered bedrock to the top of the vegetation cover; the zone in which most biogeochemical reactions take place) can obscure or amplify the effects of biology, making the attribution of cause and effect challenging. Another reason for our inability to directly attribute

hat gelöscht: ,

hat gelöscht: .

weathering to plant growth arises from the ability of ecosystems to recycle nutrients through microbial mineralization from plant litter and organic matter, rather than acquiring fresh nutrient from rock (Chaudhuri et al., 2007; Lang et al., 2016; Lucas, 2001; Spohn and Sierra, 2018; Wilcke et al., 2002). Given the ability of ecosystems to buffer changes in nutrient fluxes (Spohn and Sierra, 2018) the dependence of weathering on plant growth and biomass distribution can be expected to be a highly non-linear one.

A classical strategy in field studies that aim to decipher how ecosystem functioning and weathering shape the Critical Zone relies on exploring the interactions along natural environmental gradients. Studies along a Hawaiian chronosequence (soils of variable discrete initial formation age) have evaluated the role of soil age in weathering and the distribution and cycling of cations through plants. These studies revealed the dependency of nutrient cycling on the degree of weathering (e.g. Bullen and Chadwick, 2016; Chadwick et al., 1999; Laliberte et al., 2013; Porder and Chadwick, 2009; Vitousek, 2004). Studies along a climosequence (gradients in climate whilst minimizing other environmental differences) have evaluated the effect of climate on ecological and pedogenic processes (Bullen and Chadwick, 2016; Calmels et al., 2014; Dere et al., 2013; Egli et al., 2003; Ferrier et al., 2012). These studies generally show an increase in weathering rates with increasing mean annual temperature (MAT) and mean annual precipitation (MAP), while vegetation plays a significant role in pedogenesis. Studies across different rock substrates have evaluated the availability of nutrients and the dissolution kinetics of minerals for ecosystem nutrient budgets (Hahm et al., 2014; Uhlig and von Blanckenburg, 2019) and indicate a 'bottom-up' lithological and mineralogical control on nutrient availability to ecosystems. Studies along gradients in erosion rates explored the supply of minerals to ecosystems and discovered an increase in nutrient supply through weathering with increasing erosion rates (Chadwick and Asner, 2016; Eger et al., 2018; Porder et al., 2007; Schuessler et al., 2018). Studies that have tried to isolate just the role of vegetation cover show that the weathering fluxes in adjacent areas in which only vegetation differs showed higher fluxes with more vegetation (Moulton et al., 2000). All these studies differ widely in their methodology, time scale, spatial scale, conceptual framework and even discipline. We return to this topic below by comparing our conceptual perspective to other approaches.

In this study we explore weathering, nutrient uptake, and nutrient recycling along one of the Earth's most impressive climate and vegetation gradients, located in the Chilean Coastal Cordillera (Oeser et al., 2018). Along this gradient we quantify the degree of weathering, (using chemical analyses of rock and regolith, Oeser et al., 2018), rates of weathering (using cosmogenic ^{10}Be, Schaller et al., 2018), and nutrient uptake (using net primary productivity, NPP and the chemical composition of the major plant species at each site). Sequential extraction protocols applied to bulk regolith were used to identify the stoichiometry of the main plant-available elements in the regolith. Radiogenic $^{87}Sr/^{86}Sr$ isotope ratios in bulk rock, regolith, the bio-available fraction in regolith (where regolith is used here to mean the sum of consolidated and unconsolidated material above the weathering front, including soil), and plant biomass were used to identify the sources of mineral nutrients. We were thus able to identify gains and losses of mineral nutrients in and out of these ecosystems and to quantify the efficiency of nutrient recycling. We applied the conceptual framework and parameterization of Uhlig and von Blanckenburg (2019) to place quantitative constraints on the "organic nutrient cycle" and the "geogenic nutrient pathway" as detailed in the next section. In a companion paper we exploited $^{88}Sr/^{86}Sr$ stable isotope fractionation in the materials studies here and established a stable isotope-based mass balance for Sr cycling in the critical zone including plants (Oeser and von Blanckenburg, 2020a).

Here, we specifically evaluated the following questions: (1) Do weathering rates increase along the north-south precipitation gradient because runoff, the main driver of weathering flux, increases? (2) Do the variations in NPP along the climate and vegetation gradient correlate with nutrient supply rates from weathering?

hat gelöscht: gradient

hat gelöscht: . The study was conducted within the framework of the priority program of the Deutsche Forschungsgemeinschaft "EarthShape: Earth Surface Shaping by Biota" (DFG-SPP 1803).

hat gelöscht: and

hat gelöscht:)

hat gelöscht: ,

hat gelöscht: nutritive elements

hat gelöscht: Specifically

hat gelöscht: We find that neither is the case. Rather than the expected increase in weathering rate, the recycling efficiency of nutrients increases instead along the north – south transect.

2. Conceptual perspectives

Two fundamentally different concepts describe the relationship between regolith formation and time, and their relationship to different geomorphic regimes (Lin, 2010; Smeck et al., 1983): the continuous evolution model and the steady-state model. The continuous evolution model describes regolith or soil evolution with time from an initial point and describes chronosequences, where soils evolve on stable (non-eroding) surfaces. These soils have a distinct age and undergo several phases of soil development (e.g. Chadwick et al., 1999; Vitousek and Chadwick, 2013). In contrast, the steady-state model assumes

all regolith state variables are independent of an initial point. In this concept, regolith is constantly rejuvenated by production at depth and its removal through erosion from above (e.g. Heimsath et al., 1997). In other words, the regolith is continuously turned over and has no distinct age, but rather a residence time. This concept applies to all sloping landscapes on Earth, on which typical regolith residence times ($\leq 10^4$ yrs) are often less than or equal to the timescales over which tectonics and climate vary ($\geq 10^4$ yrs). This suggests that much of the Earth surface operates in a manner that is consistent with the steady-state model of soil formation (Dixon et al., 2009; Ferrier et al., 2005; Riebe and Granger, 2013). The state variables do not necessarily vary linearly with age (in the continuous evolution model) or residence time (in the steady-state model). Thus, in the continuous evolution model, pedogenic thresholds have been deduced based on certain soil properties (Dixon et al., 2016; Vitousek and Chadwick, 2013). These have also been described to exist and strongly vary along the eroding surfaces in Chile explored in this study (Bernhard et al., 2018).

Although ecosystems respond over shorter time scales to environmental change, ranging from seasonal to decadal or longer climate cycles, their evolution can nevertheless be linked to the two regolith evolution models (Brantley et al., 2011). In the continuous evolution model, ecology and soil development are linked via progressive increases in soil stability and water retention capacity and a unidirectional decrease in mineral nutrient availability (Vitousek and Farrington, 1997). In contrast, in the steady-state model, regolith replenishment by uplift and erosion sets the upward advection of mineral nutrients (Buendía et al., 2010; Porder et al., 2007; Vitousek et al., 2003; Uhlig and von Blanckenburg, 2019) and availability of regolith moisture (Rempe and Dietrich, 2018). Thus, the combination of regolith residence time and mineral weathering rates determines whether supply by a specific mineral nutrient suffices to sustain an ecosystem over weathering time scales which in turn is thought to impact plant diversity and nutrient acquisition strategies. For example, ecosystems on strongly mineral nutrient-depleted soils seem to be characterized by high plant diversity (Laliberte et al., 2013; Lambers et al., 2008). Note that nitrogen (N), the most limiting nutrient in many ecosystems, is not an element addressed here. Although rocks have recently received attention as source of geogenic N (Houlton et al., 2018) this source is most prominent in sedimentary rock. This study explores ecosystems developed on granitoid rock where N is derived

hat gelöscht: an ecosystem is limited in

hat gelöscht: set

hat gelöscht: .

from the inexhaustible atmospheric pool by nitrogen-fixing bacteria, and limitation mostly arises by the energy required for fixation (Chapin III et al., 2011).

The methods employed to explore these processes span a range of time scales that are discipline specific. Plant ecology typically works on (sub-)annual timescales for ecosystem fertilization or manipulation experiments (Tielbörger et al., 2014; Tipping et al., 1999), while instrumental monitoring of water, gas, and nutrient fluxes between Critical Zone compartments in hydrology, soil ecology, and biogeochemistry can reach decadal timescales (Joos et al., 2010; Kelly and Goulden, 2016; Lang et al., 2016; Sprenger et al., 2019; Sohrt et al., 2019; Wilcke et al., 2017). Geochemical estimates of rock weathering or evolution of plant-available nutrient inventories typically integrate over millennial timescales (Buendía et al., 2010; Porder et al., 2007; Riebe and Granger, 2013; Uhlig and von Blanckenburg, 2019; Vitousek et al., 2003). To integrate these different time scales, some soil ecological models account for the coupled weathering – recycling – uptake systems by linking the short-term, biological cycle with the long-term, largely geological and hydrological-driven cycle (Porder and Chadwick, 2009; Powers et al., 2015; Vitousek et al., 1998). Such models have recently been complemented by concepts and methods from geochemistry (Uhlig and von Blanckenburg, 2019) that we pursue in this study. In this conceptual framework, the so-called "organic nutrient cycle" comprises a set of strategies for efficient nutrient re-utilization through microbial mineralization from plant litter and organic matter and entails rapid nutrient turnover. The "geogenic nutrient pathway" compensates the loss of nutrients by erosion and in solution through the slow but steady supply of nutrients from chemical weathering of rock (Buendía et al., 2010; Cleveland et al., 2013; Uhlig and von Blanckenburg, 2019). This concept is particularly relevant where atmospheric wet and dry deposition (e.g. Boy and Wilcke, 2008; Chadwick et al., 1999; Dosseto et al., 2012) do not suffice to balance the losses. These geogenic input fluxes are often minor compared to those in the organic nutrient cycle and may even be undetectable over the annual to decadal scales of ecosystem monitoring experiments. However, they sustain ecosystem nutrition over longer (decadal to millennial) time scales because they prevent mineral nutrient deficiency that may otherwise develop (Hahm et al., 2014; Schuessler et al., 2018; Uhlig et al., 2017; Uhlig and von Blanckenburg, 2019). Whether the geogenic nutrient pathway is sufficient to prevent development of mineral nutrient limitation over the millennial scale depends on the rate of supply of fresh rock into the weathering zone, the bio-availability of the

hat gelöscht: bioavailability

nutrients released, and whether plant roots and the associated mycorrhizal fungi can access them. Thus, any exploration of these links must constrain where nutrients are released in regolith relative to where plants obtain them. The aim of this study is to illustrate how these methods from geochemistry can be employed to assess the flux balances between the top of bedrock and the top of the vegetation canopy as integrated over millennia, and how plant growth affects these in comparison to the geologic drivers like uplift and erosion or climatic drivers like precipitation and runoff.

3 Study area and previous results

The study was conducted within the Critical Zone project "EarthShape: Earth Surface Shaping by Biota". The four study sites are part of the EarthShape study area which is located along the Chilean Coastal Cordillera. Three sites are located in national parks and one in a nature reserve, so human impact is minimized. The sites are located on the plutonic rocks of the Chilean Coastal Cordillera and are close to the Pacific coast (less than 80 km; Oeser et al., 2018). Two previous studies introduced the field area, its pedogenic and weathering characteristics, and a set of new soil- and geochemical data (Oeser et al., 2018; Bernhard et al., 2018).

The sites define a vegetation gradient controlled by climate, ranging over 1300 km. From north to south, they cover arid (Pan de Azúcar National Park, ~26°S), semi-arid (Santa Gracia Nature Reserve, ~30°S), mediterranean (La Campana National Park, ~33°S), and humid-temperate (Nahuelbuta National Park, ~38°S) climate conditions. The mean annual precipitation (MAP) increases from 10 mm yr^{-1} in Pan de Azúcar, 89 mm yr^{-1} in Santa Gracia, 440 mm yr^{-1} in La Campana, to 1100 mm yr^{-1} in Nahuelbuta, respectively. The mean annual air temperature (MAT) ranges from 18.1°C in the northernmost site in Pan de Azúcar to 14.1°C in the southernmost site in Nahuelbuta (Fig. 1, Table 1; Ministerio de Obras Públicas, 2017).

Net primary productivity (NPP), derived from a dynamic vegetation model (LPJ-GUESS) that simulates vegetation cover and composition during the Holocene (Werner et al., 2018), ranges from 30 g m^{-2} yr^{-1} C and 150 g m^{-2} yr^{-1} C in the arid shrubland of Pan de Azúcar and Santa Gracia, respectively, to 280 g m^{-2} yr^{-1} C in the sclerophyllous woodland of La Campana, and is highest (520 g m^{-2} yr^{-1} C) in the humid-temperate forests of Nahuelbuta (Fig. 1, Table 1). The vegetation cover (< 5%) in Pan de Azúcar

hat gelöscht: and are detailed in two
hat gelöscht: that
hat gelöscht: substantial
hat gelöscht: gc
hat gelöscht: gc
hat gelöscht: gc
hat gelöscht: ·
hat gelöscht: ·
hat gelöscht: gc

consists only of small shrubs, geophytes and annual plants (Armesto et al., 1993), which are mainly present in small ravines. The vegetation in Santa Gracia belongs to the "Interior Mediterranean desert scrub of *Heliotropium stenophyllum* and *Flourensia thurifera*" formation (Luebert and Pliscoff, 2006). Plants are affected by livestock grazing (mostly goats; Bahre, 1979), and vegetation cover is generally sparse. In La Campana the vegetation (almost 100% ground cover) is part of the "Coastal Mediterranean sclerophyllous forest of *Lithraea caustica* and *Cryptocarya alba*" formation (Luebert and Pliscoff, 2006). The dominant vegetation in Nahuelbuta is associated with the "Coastal temperate forest of *Araucaria araucana*" formation (Luebert and Pliscoff, 2006) and covers 100% of ground area. Ecosystems at all sites are primarily nitrogen-limited (Stock et al., 2019).

The basement at those sites is mainly composed of granitoid intrusions of late Carboniferous to Cretaceous age. The compositional variation ranges from monzo- to syenogranites in Pan de Azúcar (199 Ma; Berg and Breitkreuz, 1983; Berg and Baumann, 1985; Parada et al., 2007), pyroxene and hornblende-bearing diorites and monzodiorites in Santa Gracia (98 – 89 Ma; Moscoso et al., 1982), as well as tonalites and granodiorites in Nahuelbuta (Nahuelbuta complex, 294 Ma; Parada et al., 2007) and in the Caleu Pluton in La Campana with an intrusion age of 130 Myr (Molina et al., 2015; Parada and Larrondo, 1999; Parada et al., 2002).

For the soil pits studied here, denudation rates inferred from cosmogenic nuclides (*in situ* ^{10}Be), interpreted as soil production rates, are 8 – 11 t km^{-2} yr^{-1} in Pan de Azúcar, 16 – 22 t km^{-2} yr^{-1} in Santa Gracia, 54 – 69 t km^{-2} yr^{-1} in La Campana and 18 – 48 t km^{-2} yr^{-1} in Nahuelbuta (Schaller et al., 2018b). Catchment-wide denudation rates broadly agree with these soil-scale rates, except in La Campana. Here, they are higher, attributed to debris flows in valley tops due to the higher channel steepness than elsewhere (e.g. mean slope 23° in La Campana, 9° in Nahuelbuta; van Dongen et al., 2019). The relative consistency of these rates along the climate gradient is ascribed to consistent tectonic forces acting along the whole gradient (e.g. Blanco-Chao et al., 2014; Melnik, 2016), with the moderate increase in denudation rates at the two southern sites explainable with the combined effect of higher precipitation and increasing shielding by vegetation (Schaller et al., 2018b).

The architecture of the regolith profiles, their chemistry, mineralogy, and the physical properties of soils, saprolite, and the rocks beneath have been extensively described for four soil pits at each site by Bernhard

et al. (2018), Dal Bo et al. (2019), Oeser et al. (2018) and Schaller et al. (2018b). The regolith profiles in Pan de Azúcar are located between 330 and 340 m above sea level (asl) on steep (25 – 40°; Table 1) hill slopes. The soils on the north- and south-facing slopes were classified by Bernhard et al. (2018) as Regosols with only shallow A and B horizons of ~20 – 30 cm thickness, lacking any kind of organic and litter layer. In this area, the processes disintegrating rock and developing regolith are mainly physical weathering, specifically a combination of insolation- and salt weathering (Oeser et al., 2018). The regolith profiles in Santa Gracia are situated at almost 700 m asl on gently sloping hills (15 – 25°; Table 1). The soils on the north- and on the south-facing slope are a Leptosol and a Cambisol, respectively (Bernhard et al., 2018). Distinct O-horizons and a litter layer are not apparent. The Ah horizons in both profiles reach depths of 10 cm and the transition from the mineral soil (Bw) into saprolite occurs at 25 – 30 cm depth. Oeser et al. (2018) attribute this sites' high degree of elemental depletion (50% loss relative to bedrock as quantified by the CDF; Fig. A1; Data Table S2) despite low precipitation to the low abundance of quartz and the high abundance of readily weatherable plagioclase and mafic minerals. The regolith profiles in La Campana, located at 730 m asl and on gently sloping hills (12 – 23°), are classified as Cambisols. The O-horizon is ~5 cm thick and is followed by a Ah horizon, extending up to 40 cm depth (Bernhard et al., 2018). Here, the mineral-soil layer turns into saprolite at approximately 110 cm in both profiles (Table 1). The elemental depletion of Ca relative to bedrock increases from ~45% at the profiles' bottom towards ~70% at their top and can be classified as depletion (north-facing) or depletion and enrichment profiles (south-facing, Fig. A1; Table S2; Brantley and Lebedeva, 2011), respectively. The regolith profiles in Nahuelbuta are situated on gently sloping hills (~15°) at about 1200 m asl (Table 1). Bernhard et al. (2018) have classified the soils on the north- and south-facing slope as Umbric Podzols and Orthodystric Umbrisols, respectively. Here, the Ah horizons measure up to 50 cm (greater thickness on the south-facing slope) and are overlain by an organic layer of 5.5 cm thickness. In the two regolith profiles, the soil-saprolite transition is at 100 and 120 cm depth, respectively. The coarse-grained saprolite disaggregates readily. These two profiles are characterized by highly heterogeneous weathering patterns caused by the incorporation of the metamorphic basement at various parts (e.g. Oeser et al., 2018; Hervé, 1977). Along the EarthShape north-south transect, many of the soil properties indicate crossing of several distinct pedogenic thresholds (Bernhard et al., 2018). We note that while the detailed geochemical work

hat gelöscht: umbric Podsols

hat gelöscht: orthodystric

hat gelöscht: horizon

reported in this study is based on two profiles per site, the soil properties (Bernhard et al., 2018) and bulk geochemical data (Oeser et al., 2018) of these profiles are corroborated by two additional replicates per site as reported in these previous studies. A comprehensive summary of the characteristics of the eight regolith profiles and major plant types is given in Table 1.

4 Methods

4.1 Sampling

Regolith samples were collected in a continuous sequence of depth increments from bottom to top. Increments amount to a thickness of 5 cm for the uppermost two samples, 10 cm for the 3rd sample from top, and increase to 20 cm thickness for the 4th sample onwards. To account for the dependence on solar radiation, two regolith profiles on adjacent hillslopes (north- and south-facing) were sampled at each study site (see Appendix B for further information on sample replication).

The underlying unweathered bedrock was not reached in any of the regolith profiles and the depth to bedrock remains unknown. Thus, bedrock samples were collected from nearby outcrops. This sample set comprises the 20 bedrock samples already reported in Oeser et al. (2018) and 15 additional bedrock samples (in total 12 in Pan de Azúcar, 8 in Santa Gracia, 10 in La Campana, and 5 in Nahuelbuta).

Vegetation samples from representative shrubs and trees (grasses have been excluded) of each study site were sampled in the austral summer to autumn 2016. The sample set comprises material from mature plants of the prevailing species: *Nolana mollis* (Pan de Azúcar), *Asterasia* sp., *Cordia decandra*, *Cumulopuntia sphaerica*, and *Proustia cuneifolia* (Santa Gracia), *Aristeguietia salvia*, *Colliguaja odorifera*, *Cryptocarya alba*, and *Lithraea caustica* (La Campana), *Araucaria araucana*, *Nothofagus antarctica*, and *Chusquea coleu* (Nahuelbuta). From each sampled plant (n = 20), multiple samples of leaves, twigs and stem were collected, pooled together, and homogenized prior to analysis. These samples were either taken using an increment borer (stem samples) or plant scissors (leaf and twig samples) equipped with a telescopic arm to reach the higher parts of trees. Roots could not be sampled in a representative manner though we account for their influence on plant composition (see Appendix A). The

hat gelöscht: As is commonly the case in field studies, roots

litter layer, comprising recently fallen leaves (from within the last two years) and small woody debris, was also sampled in La Campana and Nahuelbuta.

hat gelöscht: was also sampled

4.2 Analytical methods

4.2.1 Chemical composition of regolith and bedrock

The concentration of major and trace elements in bedrock and regolith samples were determined using a X-Ray Fluorescence spectrometer (PANalytical AXIOS Advanced) at the section for "Inorganic and Isotope Geochemistry", GFZ German Research Centre for Geosciences. A detailed description of the analytical protocols and sample preparation is given in Oeser et al. (2018).

4.2.2 Chemical composition of vegetation

Major and trace element concentrations of vegetation samples were determined using a Varian 720-ES axial ICP-OES at the Helmholtz Laboratory for the Geochemistry of the Earth Surface (HELGES), GFZ German Research Centre for Geosciences (von Blanckenburg et al., 2016) with relative uncertainties smaller than 10%. Prior to analysis, all samples were oven-dried at 120°C for 12 hrs. Subsequently, leaves were crushed and homogenized. About 0.5 g of leaf and 1 g of woody samples were digested in PFA vials using a microwave (MLS start) and ultra-pure concentrated acid mixtures comprising H_2O_2 and HNO_3, HCl and HNO_3, and HF. In some plant samples Si-bearing precipitates formed upon evaporation after digestion. These sample cakes were redissolved in a mixture of concentrated HF and HNO_3 to ensure complete dissolution of Si prior to analysis. As some Si might have been lost by volatilization as SiF_4 in this process, we do not include these samples (indicated by a * in Data Table S5) for the compilation of the plants' Si budget. With each sample batch, the international reference material NIST SRM 1515 Apple leaves and a procedural blank were processed (Data Table S5).

hat gelöscht: .

4.2.3 Extraction of the bio-available fraction and its chemical analyses

The bio-available fraction of regolith samples was extracted using a sequential extraction procedure adapted from Arunachalam et al. (1996), He et al. (1995), and Tessier et al. (1979). The sequential extraction was performed in parallel on two regolith aliquots, and the supernatants were pooled together

for analyses. About 2 g of dried and sieved (< 2 mm) sample material were immersed in 14 ml 18 MΩ deionised H_2O (water-soluble fraction) and then in 1M NH_4Oac (exchangeable fraction; maintaining a sample:reactant ratio of ca. 1:7), and gently agitated. After each extraction, the mixture was centrifuged for 30 min at 4200 rpm and the supernatant was pipetted off. The remaining sample was then rinsed with 10 ml deionised H_2O and centrifuged again (4200 rpm, 30 min) and the rinse solution added to the supernatant. Subsequently, the supernatants were purified using a vacuum-driven filtration system (Millipore®; 0.2 µm acetate filter), evaporated to dryness, and redissolved with ultra-pure concentrated acid mixtures comprising H_2O_2, HNO_3, and HCl. With each sample batch, international reference materials (NIST SRM 2709a San Joaquin soil, CCRMP TILL-1) along with a procedural blank were processed.

The water-soluble fraction is comprised of elements contained in soil water in the form of free ions and ions which form complexes with soluble organic matter. It represents the most labile soil compartment and thus is most accessible to plants (e.g. He et al., 1995). This fraction was accessed by suspending the samples for 24 hrs in deionised H_2O at room temperature. The exchangeable fraction comprises elements that form weak electrostatic bonds between the hydrated surfaces of phyllosilicates (i.e. clays and micas), oxyhydroxide minerals (e.g. boehmite, diaspore, goethite, lepidocrocite, ferrihydrite), and organic matter. This fraction was extracted by suspending the samples in a mechanical end over end shaker at room temperature in 1 M NH_4OAc for 2 hrs at 60 rpm. Note that none of the further extraction steps described in Tessier et al. (1979) have been applied to the regolith samples as they are believed to make a negligible contribution to the bio-available fraction.

The element concentrations of the water-soluble and exchangeable fraction were determined using a Varian 720-ES axial ICP-OES at HELGES, following the analytical procedures described in Schuessler et al. (2016) with relative uncertainties estimated at smaller than 10%. Soil-P fractions were determined by Brucker and Spohn (2019). In this case, the bio-available fraction refers to the inorganic products of the modified Hedley sequential P fractionation method of Tiessen and Moir (1993), specifically the water-extractable P_i and labile P_i which was extracted by using 0.5 M $NaHCO_3$.

hat gelöscht: Milli-Q

hat gelöscht: /

hat gelöscht: Milli-Q

hat gelöscht: Milli-Q

4.2.4 $^{87}Sr/^{86}Sr$ isotope ratios

The radiogenic Sr isotope ratio was determined on bulk bedrock and regolith, the bio-available fractions of saprolite and soil, and on the different plant organs at each study site.

After sample digestion (bulk samples) or sequential extraction (bio-available fraction), Sr was separated from matrix elements using 200 µl Sr-Spec resin. Matrix elements were removed by elution with 2.5 ml 3 M and 2 ml 7.5 M HNO_3. Subsequently, Sr was eluted with 4 ml of 18 Ω Deionised H_2O. Any organic crown-ether which has been released from the Sr-spec resin was removed after evaporation and subsequent redissolution of the Sr fraction in 1 ml of a 1:1 mixture of concentrated H_2O_2 and HNO_3. This mixture was cooked in a tightly closed beaker at 150°C for at least 12 hrs. Within each sample batch, a minimum of one standard reference material and a procedural blank were processed.

$^{87}Sr/^{86}Sr$ was measured in a 50-ng g^{-1} pure Sr solution in 0.3 M HNO_3 using a multi collector inductively coupled plasma mass spectrometer (MC-ICP-MS, Thermo Neptune) in medium mass resolution. The MC-ICP-MS was equipped with an APEX-Q (ESI) desolvater and a nebulizer with an uptake rate of 70 µl min^{-1} and a nickel sampler cone. Radiogenic Sr isotope ratios were determined over one block of 20 cycles with an integration time of 16 seconds each. The sequence of a sample run was comprised of 10 to 12 blocks, where each block comprised a blank, four samples, and five SRM 987 which were not processed through chemistry. Blank correction of samples and reference material during the sequence was less than 0.4% of the sample signal. The intensities of the ion beams on the masses ^{82}Kr (L4), ^{83}Kr (L3), ^{84}Sr (L2), ^{85}Rb (L1), ^{86}Sr (central Cup), ^{87}Sr (H1) and ^{88}Sr (H2) were monitored using Faraday collectors equipped with 10^{11} Ω and one 10^{12} Ω (connected to L4 cup) resistors. Isobaric interference on the masses 84, 86, and 87 were corrected for with the Kr and Rb isotope ratios measured prior to the sequence run. To correct for any natural and instrumental isotope fractionation, the measured $^{87}Sr/^{86}Sr$ ratio was normalized to a $^{88}Sr/^{86}Sr$ ratio of 8.375209 (Nier, 1938's value) by using an exponential law. Finally, the $^{87}Sr/^{86}Sr$ ratios were corrected for a session offset that account for the differences between the certified and measured $^{87}Sr/^{86}Sr$ ratio of the SRM 987 reference material, which in any case where smaller than ± 0.00006 (2SD).

hat gelöscht: Milli-Q

4.3 Parameterizing geogenic and biogenic element fluxes in a terrestrial ecosystem

The parameterization of the "geogenic nutrient pathway" and the "organic nutrient cycle" (Fig. 2) to characterize element fluxes into, within, and from the Critical Zone and its ecosystem components is thoroughly described in Uhlig and von Blanckenburg (2019). Here, we only briefly summarize the metrics, which are shown in Table 2. Calculations and parameters used for these metrics are presented in Appendix A, including the propagation of uncertainties. A statistical analysis (i.e. ANOVA, Pearson correlation coefficients) of the weathering parameters is presented in Appendix B.

4.4 Data reporting

The original data and that pertaining to the companion paper (Oeser and von Blanckenburg, 2020a) can be found in a separate open access data publication (Oeser and von Blanckenburg, 2020b). These tables are referred to "Data Tables S1 to S5" from here on.

5 Results

We structure the presentation of our results in the following sequence: (1) the element fluxes of the geogenic nutrient pathway; (2) the availability of elements in regolith to plants; and (3) the plant chemical composition along with the element fluxes that couple the geogenic nutrient pathway to the organic nutrient cycle. The fluxes are presented as study-site averages, with the full dataset available in an associated open access data publication (Oeser and von Blanckenburg, 2020b).

We focus the detailed presentation of these results on P and K, the two most important rock-derived mineral nutrients to plants. Further data is provided for Al, Ca, Fe, Mg, Mn, Na, Si, and Sr. All metrics are defined in Table 2.

hat gelöscht: 2020

hat gelöscht: We focus the detailed presentation of these results on P and K, the two most important mineral nutrients to plants. Further data is provided for other plant-beneficial and plant-essential elements. Whether an element is considered as beneficial or essential to plants, however, is species-dependent (Marschner, 1983). Following Marschner (1983) we refer to the elements Al, Na, and Si as plant-beneficial elements and include the micronutrient Fe in this group. We refer to the elements Ca, K, Mg, and Mn as plant-essential elements. In this presentation, we treat Sr as a plant-essential element due to its similar (bio-)chemical behavior to Ca (e.g. Blum et al., 2012; Faure and Mensing, 2005; Faure and Powell, 1972; Poszwa et al., 2002). All metrics are defined in Table 2.

5.1 Element fluxes contributing to the geogenic nutrient pathway

5.1.1 Degree of weathering and elemental gains and losses

The chemical depletion fraction (CDF; Table 2, Eq. 5 and Appendix A) and elemental mass transfer coefficient (τ; Table 2, Eq. 6 and Appendix A) disclose the total and the element-specific loss, respectively, of soluble elements relative to bedrock. Thus, both metrics quantify the degree of weathering. The average CDF of the shallowest subsoil (combined analysis of north- and south-facing profiles) in Pan de Azúcar, Santa Gracia, La Campana, and Nahuelbuta amounts to 0.03, 0.54, 0.50, and 0.25, respectively (Fig. 3; Data Table S2). At all four sites, the elemental losses (Fig. A1; Data Table S2) can be attributed to a "kinetically limited weathering regime" (Brantley and Lebedeva, 2011). This means that the erosion rate is at a sufficient level to continuously replenish the weatherable primary minerals that transit vertically through the weathering profile.

Systematic differences in chemical depletion (i.e. CDF and τ) are not discernible between north- and south-facing slopes. Anomalously high Zr concentrations throughout the entire north-facing profile at La Campana cause one exception to this rule. Moreover, we found that neither CDF nor τ^X differ significantly between Santa Gracia, La Campana, and Nahuelbuta, despite both increasing precipitation and increasing biomass growth.

A comprehensive presentation of these data can be found as Appendix in Fig. A1 and in the supplementary Data Table S2.

5.1.2 Elemental chemical weathering fluxes

The soil weathering rate W quantifies the bulk weathering flux from rock and regolith. This flux is lowest in Pan de Azúcar (0 – 0.9 t km^{-2} yr^{-1}) and highest in La Campana (53.7 – 69.2 t km^{-2} yr^{-1}). In Santa Gracia (7.2 – 11.9 t km^{-2} yr^{-1}) and Nahuelbuta (3.5 – 7.5 t km-2 yr-1, Table 1; Oeser et al., 2018; Schaller et al., 2018b), these fluxes are at a similarly intermediate level.

$W^X_{regolith}$ (Table 2, Eq. 3 and Appendix A) quantifies element-specific release fluxes from rock and regolith by weathering. It thus assesses the maximum possible weathering supply of nutrients to plants by the "geogenic pathway", as some of this flux is potentially lost into groundwater before being

hat gelöscht: mineral soil

hat gelöscht: A1 and in the supplementary Table S2 (Oeser and von Blanckenburg, 2020).

hat gelöscht: elemental

accessible to roots. The weathering-release fluxes for phosphorus ($W^{P}_{regolith}$) amount to 1.3 ± 0.4, 12 ± 3, 19 ± 6, and 11 ± 4 mg m^{-2} yr^{-1} and of potassium ($W^{K}_{regolith}$) to 30 ± 30, 80 ± 50, 840 ± 220, and 100 ± 120 mg m^{-2} yr^{-1} (Fig. 4, Table 3) in Pan de Azúcar, Santa Gracia, La Campana, and Nahuelbuta, respectively. Similar trends are seen for Al, Na, and Si along with Fe and Sr. The rates of supply of P, K, and the aforementioned elements are thus similar at both Santa Gracia and Nahuelbuta despite the differences in MAP, NPP, and vegetation cover. $W^{Ca}_{regolith}$ and $W^{Mg}_{regolith}$ deviate from this general pattern: the highest Ca and Mg weathering-release fluxes occur in Santa Gracia followed by La Campana, Nahuelbuta, and Pan de Azúcar. These elevated fluxes in Santa Gracia are attributed to the initial bedrock mineralogy, with their high Ca and Mg concentration (Data Table S1).

hat gelöscht: the plant-beneficial elements

hat gelöscht: plant-beneficial

5.2 Availability of mineral nutrients to plants

The maximum amount of mineral nutrients present can be assessed by determining their inventory in bulk regolith (I^{X}_{bulk}; Table 2, Eq. 8 and Appendix A). For most elements I^{X}_{bulk} is by far greatest in Santa Gracia (apart from K and Si; Table A1). I^{X}_{bulk} at the other three study sites are at similar levels. Element concentrations in the bio-available fraction are orders of magnitude lower than in the bulk regolith (Fig. A2 & A3, Data Table S3). Bio-available P in saprolite ($I^{P}_{bio\text{-}av,\ sap}$) is virtually absent in Pan de Azúcar and amounts to 21, 39, and 23 g m^{-2} in Santa Gracia, La Campana, and Nahuelbuta, respectively (Table A1). $I^{K}_{bio\text{-}av,\ sap}$ equals 253 in the northernmost, and 23, 70, and 19 g m^{-2} at the sites progressively southwards. The inventory of the remaining mineral nutrients in saprolite generally decreases from north to south. Accordingly, the total inventory (i.e. the sum of all determined inventories) is highest in Pan de Azúcar (5100 g m^{-2}), intermediate in Santa Gracia (2100 g m^{-2}) and La Campana (1600 g m^{-2}), and lowest in Nahuelbuta (140 g m^{-2}; Table A1). Note that $I^{X}_{bio\text{-}av,\ sap}$ was calculated over the uppermost 1 m of saprolite, whereas in fact the zone of mineral nutrient extraction might extend deeper (Uhlig et al., 2020). Bio-availability in soil features a similar trend. The total inventory is highest in Pan de Azúcar (2100 g m^{-2}), on par in Santa Gracia (960 g m^{-2}) and La Campana (1000 g m^{-2}), and despite featuring the thickest soils, lowest in Nahuelbuta (200 g m^{-2}). P deviates from this general trend: $I^{P}_{bio\text{-}av,\ soil}$ amounts to 3.3 g m^{-2} in Pan de Azúcar, 22 g m^{-2} in Santa Gracia, 28 g m^{-2} in La Campana, and 31 g m^{-2} and Nahuelbuta

hat gelöscht: 4

hat gelöscht: 4

hat gelöscht: Table 4). Note that $I^{X}_{bio\text{-}av,\ sap}$ was calculated over the uppermost 1 m of saprolite, whereas in fact the zone of mineral nutrient extraction might extend deeper.

(Table A1). $I^{K}_{bio\text{-}av,\,soil}$ behaves differently, and amounts to 53, 38, 90, and 38 g m^{-2} in Pan de Azúcar, Santa Gracia, La Campana, and Nahuelbuta, respectively. Thus, K is almost equally available to plants in all four study sites.

hat gelöscht: 4

5.3 Plant element composition and nutrient-uptake fluxes

Average elemental concentrations in bulk plants generally decrease from Pan de Azúcar towards Nahuelbuta. For example, the Al and Na concentrations in the plants of Pan de Azúcar reach 2700 and 34600 µg g^{-1}, respectively, compared with minima of 70 and 80 µg g^{-1} in Nahuelbuta. However, element specific deviations from this pattern exist (Table 4). The most prominent exceptions are those of P and K. Average P concentration increases from 290 µg g^{-1} in Pan de Azúcar to 1400 µg g^{-1} in Nahuelbuta. The average K concentration amounts to 6900, 6400, 12000, and 5400 µg g^{-1} along the north-south gradient. Thus, in Pan de Azúcar, Santa Gracia, and Nahuelbuta, average K concentrations are in a similar range, whereas in La Campana, K concentration in plants is almost 2x higher than in the other sites (Table 4). In Pan de Azúcar and Santa Gracia some elemental concentrations in plants are exceptionally high. This elevated mineral-nutrient storage is typical for plants growing in infertile habitats (Chapin III et al., 2011). Accumulation of such an internal nutrient pool allows for plant growth when conditions improve, e.g. during rare rain events (e.g. Chapin III, 1980; Chapin III et al., 2011; Vitousek et al., 1998). For example, high amounts of Al and Na are incorporated into plants tissues, though they may hinder plant growth at high concentrations (e.g. Delhaize and Ryan, 1995; Kronzucker and Britto, 2011). However, Al-toxicity is prevented in these plants by accumulation of correspondingly high amounts of Si that compensates the effects of Al (Liang et al. (2007). The exceptional high Na concentration in *N. mollis* in Pan de Azúcar is typical of the metabolism of *N. mollis* which is known to be covered with salt glands on their leaves, aiding to retrieve water by directly condensing moisture from unsaturated air (Rundel et al., 1980; Mooney et al., 1980).

hat gelöscht: (Table 5).

hat gelöscht: (Table 5).

The nutrient-uptake fluxes (U^{X}_{total}; Table 2, Eq. 4 and Appendix A) of P and K increase from north to south, such that U^{P}_{total} amounts to 5 ± 2, 70 ± 20, 170 ± 90, and 350 ± 100 mg m^{-2} yr^{-1} and U^{K}_{total} to 110 ± 40, 500 ± 200, 2000 ± 1000, and 1400 ± 400 mg m^{-2} yr^{-1} in Pan de Azúcar, Santa Gracia, La Campana, and Nahuelbuta, respectively (Table 3). U^{X}_{total} of the elements Ca, K, Mg, Mn, P, and Sr exceed

hat gelöscht: plant-essential

$W^X_{regolith}$ up to several times. U^X_{total} and $W^X_{regolith}$ are similar for Mg, Mn, and Sr in La Campana (Fig. 4; Table 3). U^X_{total} of the remaining elements are, with the exception of Fe and Na in Pan de Azúcar, always lower than their release by weathering.

5.4 $^{87}Sr/^{86}Sr$ isotope ratios

Radiogenic Sr isotope ratios on bulk bedrock and regolith samples disclose mineral-weathering reactions and the incorporation of external sources into the regolith profiles. Moreover, $^{87}Sr/^{86}Sr$ in the bio-available fraction and plants reveal the plants' mineral nutrient sources.

In Pan de Azúcar, the $^{87}Sr/^{86}Sr$ ratio of average bedrock is 0.726 ± 0.002 (Fig. 5, Table A2). In regolith, $^{87}Sr/^{86}Sr$ differs significantly between the two profiles (0.728 ± 0.003 and 0.733 ± 0.003 on the north- and south-facing regolith profile, respectively) which can be attributed to varying degrees of atmospheric deposition ($^{87}Sr/^{86}Sr_{seaspray}$ = 0.7092; Pearce et al., 2015). The $^{87}Sr/^{86}Sr$ ratios in the bio-available fraction of saprolite and soil deviate by 0.02 from those of bulk bedrock and regolith but do not vary considerably between saprolite and soil, or between the north- and south-facing slopes. Bulk plant samples yield $^{87}Sr/^{86}Sr$ ratios of 0.710 and are thus indistinguishable from the $^{87}Sr/^{86}Sr$ ratio in the bio-available fraction (0.710 ± 0.001; Fig. 5, Table A2).

In Santa Gracia, the $^{87}Sr/^{86}Sr$ ratios in both bedrock and the regolith profiles do not differ significantly ($^{87}Sr/^{86}Sr_{rock}$ = 0.7039 ± 0.0004, $^{87}Sr/^{86}Sr_{regolith}$ = 0.7043 ± 0.0003; Fig. 5, Table A2). The radiogenic Sr composition of the bio-available fractions in saprolite and soil are identical within uncertainty, and no differences in $^{87}Sr/^{86}Sr$ between the north- and south-facing regolith profile are apparent. Plants yield an average $^{87}Sr/^{86}Sr$ ratio of 0.7062 ± 0.0001 and are thus indistinguishable from the bio-available fractions in saprolite and soil (Fig. 5, Table A2).

The bulk regolith $^{87}Sr/^{86}Sr$ ratio in La Campana ranges from 0.7051 in the north-facing to 0.7055 in the south-facing regolith profile. These ratios are lower than bedrock (0.7063 ± 0.0003; Fig. 5, Table A2) which can be attributed to the loss of a mineral with a high $^{87}Sr/^{86}Sr$ isotope ratio (e.g. biotite) beneath the sampled regolith profiles. The radiogenic Sr composition of the bio-available fraction in saprolite and soil amounts to 0.7051 and 0.7053, in the north- and south-facing slopes, respectively, and is within the range of bulk regolith. The average $^{87}Sr/^{86}Sr$ ratio in plants is 0.7059 and can be as high as 0.7063 in

hat gelöscht: plant-beneficial

hat gelöscht: 6

hat gelöscht: 6

hat gelöscht: 6

hat gelöscht: 6

hat gelöscht: , Table 6)

Cryptocaria alba (Data Table S7) and is thus higher than the soil and saprolite bio-available fractions. All these ratios are lower than in bulk bedrock.

In Nahuelbuta the radiogenic Sr isotope ratio in bedrock (0.716 ± 0.007) is in good agreement to those reported by Hervé et al. (1976) for the granitoid basement (0.717). However, the large spread among the bedrock samples implies petrological and geochemical heterogeneity of the Nahuelbuta mountain range (e.g. Hervé, 1977). Thus, $^{87}Sr/^{86}Sr$ in regolith is also variable (Fig. 5, Table A2 & S2). The $^{87}Sr/^{86}Sr$ ratios in both bio-available fractions in Nahuelbuta are restricted to a relatively narrow range in both regolith profiles, equal to 0.711 ± 0.002 and are indistinguishable from the mean ratio in plants (Fig. 5, Table A2). Individual plants' radiogenic Sr signature are distinct from each other and reflect the slope's bio-available fraction they grow on.

hat gelöscht: 6

hat gelöscht: 6

6 Discussion

6.1 The source of mineral nutrients

Comparing the radiogenic Sr composition of the bio-available fractions in saprolite and soil with that of bulk plant serves as a proxy for the nutrient sources of plants. At all four sites, the $^{87}Sr/^{86}Sr$ ratio in plants is largely indistinguishable within uncertainty to the bio-available fraction they grow on (Table A2), and no differences in $^{87}Sr/^{86}Sr$ between leaves, to twig, or stem are apparent (Data Table S5). Neither the plant $^{87}Sr/^{86}Sr$ ratio nor the $^{87}Sr/^{86}Sr$ ratio of the bio-available fraction is identical to that of bedrock or of bulk regolith. We conclude that plants obtain their Sr from the bio-available fraction rather than directly from primary minerals or from the atmosphere through leaves. Only La Campana showed evidence for a deep nutrient source (i.e. somewhere between the bottom of the regolith profile and unweathered rock) in the elemental-depletion pattern (Fig. A1). Here, deep-rooting plants (e.g. *Lithraea caustica*; Canadell et al., 1996) bypass the bio-available fraction of saprolite and soil and take up Sr with a higher proportion of radiogenic ^{87}Sr which has been released through biotite weathering beneath the regolith profiles. We can also use the $^{87}Sr/^{86}Sr$ ratio to identify the ultimate source of bio-available Sr. In the southernmost mediterranean and humid-temperate sites of La Campana and Nahuelbuta, the bio-available Sr is supplied by release from rock and regolith through weathering. In arid Pan de Azúcar the Sr pool in the bio-

hat gelöscht: (Table 6),

hat gelöscht: , albeit from specific minerals rather than bulk rock.

available fraction is formed by deposition from atmospheric sources (up to 93% seaspray contribution; Table A2). In semi-arid Santa Gracia, we found a possible combination of both sources (up to 43% seaspray contribution; Table A2).

Expanding our analysis of the source of mineral nutrients, we normalized both the mineral nutrient concentrations in plants (Table 4) and those in the bio-available fraction in saprolite and soil (Data Table S3) by the most-demanded rock-derived mineral nutrient P (Fig. 6). This normalization removes differences in concentrations induced by the very different matrices of regolith and plant. In this analysis, an element X that plots on the 1:1 line would have the same X:P ratio in plants and in the bio-available fraction. In turn, any deviation from that line would indicate positive or negative discrimination of an element contained in the regolith bio-available fraction by plants relative to P. We find a good correlation in the X:P ratios for all elements, and the ratios found in plants reflect those in the bio-available regolith fraction to within one order of magnitude. We interpret this correlation to confirm nutrient uptake mainly from the bio-available fraction. We also note that the X:P ratios increasingly approach the 1:1 line with increasing NPP from Pan de Azúcar to Nahuelbuta and the agreement is more pronounced in soil than in saprolite. We interpret these shifts to denote the increasing significance of recycling, a topic we return to in the next section.

6.2 An increase in nutrient recycling with NPP

In Section 5.1.2 we established that neither total weathering rate W, nor elemental weathering rates $W^{X}_{regolith}$, correlate with NPP. Only at La Campana weathering rates are elevated, as expected from the higher denudation rate. Santa Gracia and Nahuelbuta, have similar denudation rates and element release rates by weathering $W^{X}_{regolith}$, yet elemental uptake rates U^{X}_{total} of P, K, and Ca increase between a factor of two and five (Figure 4). We examine these correlations in more detail in Section 6.5. Here we first focus on the question: How is mineral nutrient demand satisfied at the more vegetated sites?

Recycling of mineral nutrients from organic material is the key mechanism enabling differences in NPP. We quantified recycling by the nutrient recycling factor Rec^{X} (Table 2, Eq. 7 and Appendix A; Table 5; note that in this discussion we use the Rec^{X} calculated for $W^{X}_{regolith}$ from rock weathering, whereas in Table 5 and Fig. A4 we also show Rec^{X} including atmospheric inputs in Pan de Azúcar). The amplitude

hat gelöscht: 6

hat gelöscht: 6

hat gelöscht: to include other plant-essential (P, K, Ca, Mg, Mn) and plant-beneficial (Al, Fe, Na, Si) elements

hat gelöscht: (Table 5)

hat gelöscht: the plant-essential nutrients

hat gelöscht: 7

hat gelöscht: 7

of recycling varies from nutrient to nutrient and site to site. In the arid Pan de Azúcar, nutrients are primarily recycled via photodegradation of shrubs (e.g. Gallo et al., 2006; Day et al., 2015). In the remaining sites Rec^X occurs through all organic-bearing soil horizons and increases from Santa Gracia to Nahuelbuta and is highest for Ca (increasing from 1 to 6), K (increasing from 6 to 15), and P (increasing from 5 to 30; Table 5). Thus, despite having the smallest nutrient inventory of bio-available nutrients (Table A1) but the highest NPP, Nahuelbuta can at least partially satisfy its nutrient requirements through efficient nutrient recycling. In the mediterranean site La Campana, nutrient requirements are satisfied through recycling and uptake from depth – a mechanism which has just recently been shown to balance losses by erosion and contributing to ecosystem nutrition (Uhlig et al., 2020). In contrast, in the (semi-) arid sites, where the bio-available pool is larger, plants forage nutrients and water by deep rooting from depth (McCulley et al., 2004).

The Rec^X metric reflects a mass balance between the total weathering zone and the total vegetation cover but does not yield insight to the mechanisms of recycling. The elemental stochiometric considerations presented above show that recycling is indeed fed from plant material accumulated in soil (Lang et al., 2017). With increasing recycling the nutrient pools in the soil bio-available fraction are increasingly dominated by the pool of recycled nutrients, thus shifting the X:P ratio in the bio-available fraction successively towards the X:P ratio in vegetation (Fig. 6). In other words, over the course of several recycling loops, the chemical composition of the bio-available fraction and biota eventually approaches a ratio close to the relative requirement of the ecosystem for the different nutrients (Vitousek et al., 1998).

6.3 Processes that set the size of the bio-available pool

In none of our sites is the bio-available nutrient pool entirely depleted (Table 3), but its elemental concentrations strongly shift along the gradient. The concentrations of the mineral nutrients K, Ca, and Mg in saprolite are highest in the arid site, lower in the semi-arid and mediterranean site, and lowest in the humid-temperate site. The element concentration in the bio-available fraction translates into the size of the inventory, quantifying the pool size (note, however, that the true inventory can in fact be larger than the 1 m inventory that we have used for its calculation. This is suggested by the elevated $^{87}Sr/^{86}Sr$ ratios in plants at La Campana suggesting extraction of a pool beneath the bio-available upper saprolite.

hat gelöscht: the plant-essential elements

hat gelöscht: 7

hat gelöscht: (Table 4)

hat gelöscht: In contrast, in the (semi-) arid sites, where the bio-available pool is larger, plants forage nutrients

hat gelöscht: 4

hat gelöscht: plant-essential

hat gelöscht:).

Nutrient uptake from greater depths have recently been demonstrated by (Uhlig et al., 2020). The bio-available pool represents the link between the organic and the geogenic pathway. That is because weathering in the geogenic pathway supplies elements that plants take up and recycle in the organic pathway (Uhlig and von Blanckenburg, 2019). We thus briefly review the potential processes that may set the pool size.

If a bio-available pool is in conceptual steady state, input fluxes and loss fluxes balance. Over millennial time scales or longer, we consider that such a balance must exist, as otherwise a pool might become depleted. In this case the inventory of the pool is set by the input fluxes of an element and a first-order rate constant that describes the relationship between the loss flux as a function of element inventory and thus the retention capacity. Essentially it is the inverse of the turnover time of an element. Biotic processes likely contribute towards setting this retention capacity directly or indirectly, a topic we return to below. Given that elemental weathering fluxes $W^{X}_{regolith}$ do not correlate with pool size we assume that retention capacity sets the pool size.

A first potential control over element retention capacity are pedogenic properties. The decrease of soil pH from 8 at the arid site to 4 at humid-temperate site (Bernhard et al., 2018) might cause the decrease in the bio-available divalent base cations Mg, Ca, and Sr. Conversely, the decrease in pH could be the result of the loss of these elements and thus their pH buffering capacity. Another possibility is the degree of complexing of elements to organic molecules. Such complexing might lead to either higher retention, or higher loss, depending on the element. Organic complexing is likely more pronounced in the mediterranean and humid-temperate sites where soil organic carbon concentrations are higher compared to the (semi-) arid sites (Bernhard et al., 2018). However, elements like Al and P, which are readily complexed, are abundant in higher concentration in the humid-temperate and mediterranean sites than in the other two sites. Differences in water flow is the third cause we discuss. Where fluid residence times are long, concentrations of solutes are more likely to be at equilibrium with secondary minerals (Maher and Chamberlain, 2014) and the bio-available fraction, formed by precipitation and sorption from pore fluids, can build up. We consider this to be the case in the low-precipitation sites. At sites with high MAP regolith fluids may be diluted, and thus desorb elements from the bio-available pool (i.e. leaching). Such dilution effect might be in effect at Nahuelbuta for elements like Mg and Ca. At Nahuelbuta these are

hat gelöscht: available

hat gelöscht: .

hat gelöscht: a

also the elements with the lowest bio-available inventory. We consider the pH and water flow to be the main factor governing the size of the bio-available pool.

6.4 Concepts for biotas role in setting fluxes in the geogenic and the organic nutrient cycle

Even if negligible on ecological timescales, ecosystems experience losses of nutrients through erosion (e.g. Heartsill Scalley et al., 2012) and as solutes (e.g. Chaudhuri et al., 2007). To prevent bio-available nutrients becoming depleted over longer timescales, the pool must be replenished (Uhlig and von Blanckenburg, 2019). Biological mechanisms comprise two means to regulate this delicate balance between nutrient replenishment by weathering and plant uptake. The first is by adjusting the recycling of nutrients, as shown in Section 6.2. At Nahuelbuta, where the bio-available pool is smallest, nutrient recycling rates are the highest. If the bio-available pool is small, plants may invest energy into re-using P and other elements from leaf litter, rather than foraging P at depth which is associated with higher energy expenditure (Andrino et al., 2019). This is a component of the organic nutrient cycle. The biochemical mechanisms of nutrient-recycling are beyond the scope of this paper, but are thought to be related to leaf litter quality (Hattenschwiler et al., 2011), soil fungal and bacterial communities (Fabian et al., 2017; Lambers et al., 2008), and plant diversity (Lambers et al., 2011; Oelmann et al., 2011; van der Heijden et al., 1998).

The second means for biota to influence the bio-available pool is via the geogenic pathway. Nutrient replenishment may take place either by exogenous inputs (e.g. Boy and Wilcke, 2008; Porder et al., 2007; Vitousek, 2004; Vitousek et al., 2010), or by weathering of primary minerals (Uhlig et al., 2017; Uhlig and von Blanckenburg, 2019). In arid Pan de Azúcar, where weathering-release fluxes are low, these pools are being replenished by the deposition of atmospheric sources (up to 93%; Table A2). In the other study sites the bio-available pools are replenished by weathering of rock and regolith. The timescales $T^{x}_{bio-av,W}$ of replenishment from weathering are long, and typically orders of magnitude longer than their turnover times with respect to plant uptake $T^{x}_{bio-av,U}$. For example, the inventory of K in the bio-available soil pool at Nahuelbuta is turned over every 30 years between soil and plants, but it takes 400 years to be replenished in its entirety by weathering (Table A3). Previous models in ecosystem science (e.g. Bormann et al., 1969; Vitousek and Reiners, 1975; Vitousek et al., 1998) suggest that increasing mineral-nutrient

hat gelöscht: thus

hat gelöscht: Table 6).

hat gelöscht: 8

demand will eventually lead to tightly coupled recycling loops such that nutrient losses will be minimized, and plant nutrition is sustained. Our data is also consistent with a relationship between demand (i.e. NPP) and recycling efficiency.

If recycling indeed exerts the dominant role in the supply of mineral nutrients, then we need to revisit the significance of biogenic weathering towards the nutrition of plants. The direct and indirect impacts of plants and their associated microbiota on weathering is well-documented and can be categorized into four suites of processes: (*A) Direct primary mineral dissolution by ectomycorrhizal fungi.* Ectomycorrhizal fungi can directly extract nutrients such as P, K, Ca, Mg, and Fe from minerals distant from the root, even under dry conditions, and thereby actively increase mineral dissolution kinetics. Laboratory dissolution experiments (Balogh-Brunstad et al., 2008b; Gerrits et al., 2020; Kalinowski et al., 2000), plant growth mesocosms (Bonneville et al., 2011; Smits et al., 2012), and deployment of minerals within the soil of natural ecosystems (Balogh-Brunstad et al., 2008a) all show either evidence for mineral dissolution by mycorrhiza, or quantify an increase in mineral dissolution over abiotic controls. Whether these short-term experiments can be extrapolated to the millennial time scales of the geogenic nutrient pathway is not obvious (review by Finlay et al., 2020). Over these time scales, mineral dissolution is often slowed by the development of nanoscale layers at the interface (Gerrits et al., 2020) or coatings by secondary precipitates (Oelkers et al., 2015). Slowing of mineral dissolution with time, known from weathering zone studies, has also been attributed to coating by secondary precipitates (White and Brantley, 2003), or to chemical saturation of pore fluids (Maher, 2010). *(B) Roots deepening regolith thickness*. Tree roots can physically penetrate and biogeochemically alter the immobile regolith underlying mobile soil (Brantley et al., 2017). They can take water up from depth, recycle water to depth for storage, or provide pathways in which water bypasses rather than infiltrating the shallow regolith (Fan et al., 2017). Deep roots aid nutrient transfer from the subsoil to shallow levels (Jobbágy and Jackson, 2004). *(C) Canopy and roots converting precipitation into evapotranspiration* (Drever and Zobrist, 1992). In sites with higher vegetation cover, water vapor is recycled and does not immediately enter runoff. By providing canopy, trees both modulate infiltration while turning water back into transpiration (Ibarra et al., 2019). For example Ibarra et al. (2019) have shown that total runoff can decrease by up to 23% as vegetation cover increases from barely vegetated to highly vegetated sites. Water recycling hence decreases total runoff

and potentially reduces weathering-release fluxes in the highly vegetated sites. (D) *Increasing mineral solubility by release of soil CO_2 and organic complexing agents.* Through the respiratory release of soil CO_2 and excretion of organic complexing agents, plants, hyphae, and their associated microbiota can increase the solubility limits of primary and secondary minerals by a factor of up to <10 (Perez-Fodich and Derry, 2019; Winnick and Maher, 2018). If dissolution is not kinetically limited, we would indeed expect higher solute concentrations with higher soil CO_2, and hence higher dissolution rates of primary minerals (Winnick and Maher, 2018).

Studies of biogenic weathering in natural Critical Zone systems struggle to disentangle expressions of these biogenic drivers of weathering rates from various competing drivers of weathering. Although the sites were selected to minimize potential confounding effects, this study also faces this challenge. We turn to a statistical approach in isolating any potential biogenic weathering signal.

6.5 Is weathering modulated by biota? A statistical analysis

To single out the possible biogenic weathering driver from the confounding factors at the EarthShape sites we used correlational statistics between indicators of weathering and metrics for its potential drivers along the EarthShape gradient. We determined Pearson correlation coefficients to determine how the degree of weathering (CDF, τ^X) and the flux of weathering (W, $W^X_{regolith}$) depend on denudation rate D, water availability (approximated by mean annual precipitation, MAP), and biomass growth as quantified by net primary productivity (NPP). See Appendix B for a detailed description on statistical analysis and Table A4, A5, and A6 for the results. We used these statistics to evaluate three starting hypotheses that reflect the basic confounding factors: (1) Where denudation rate D is high bulk weathering fluxes are high, since minerals with fast dissolution kinetics, such as plagioclase and P-bearing apatite, are supply-limited (Dixon et al., 2012; Porder et al., 2007). Where D is high, regolith residence times are low such that τ^X for elements not mostly contained in rapidly dissolving minerals are not depleted. (2) At sites at which MAP and hence runoff is high, weathering fluxes are high. This is because weathering rate is proportional to runoff for the chemostatic elements that comprise the bulk of the weathering flux, amongst them Si that contributes roughly half of the flux (e.g. Godsey et al., 2019; Maher and Chamberlain, 2014). As a result, CDF and τ^X will also be high. τ^X of soluble elements (e.g. Na) will be higher at higher runoff

hat gelöscht:

hat gelöscht: Table A1, A2

hat gelöscht: A3

than τ^X of elements that strongly partition into secondary phases. (3) If NPP is high the degree (CDF, τ^X) and rate of weathering (W, $W^X_{regolith}$) will be high (e.g. Berner et al., 2003; Brantley et al., 2011; Buss et al., 2005; Kelly et al., 1998; Porder, 2019; Schwartzmann, 2015), for the reasons predicted in Section 6.4.

In support of hypothesis (1) we find that total and elemental weathering rates correlate well with D (Table A4) and only a weak correlation relates denudation rate with the degree of weathering and elemental depletion. Thus, denudation rate is the predominant driver of weathering rate. However, D itself is also correlated with MAP and NPP. To evaluate whether D is nevertheless the main driver we exclude the La Campana site of unusually high D. The correlations between W, $W^X_{regolith}$, and D are still significant (Table A5) confirming that D is the main driver of weathering rate. Concerning hypothesis (2), neither the degree nor rates of weathering correlate with MAP. Only the soluble element Na becomes more depleted (Table A5) at higher MAP. Thus, a competing effect seem to counteract the expected increase in weathering rate with precipitation. As NPP is an output of the LPJ-GUESS model for which MAP is the basis, it is no surprise that both parameters are strongly correlated (Table A4 & A5). We would thus expect the same strong relationship between the degree and rates of weathering and NPP as with MAP. This is indeed the case. However, weathering release rates $W^X_{regolith}$ for elements like Na, P, and Si correlate slightly more strongly with NPP than with MAP (Table A5). This is the only indication that biomass growth exerts any control over weathering at all. In summary, neither MAP nor NPP seem to have a major impact on the degree and rates of weathering, and D is the main driver of total and elemental weathering rate at the EarthShape sites.

In this analysis we have not evaluated the potential confounding effects of differences in bedrock mineral composition. Because of the lack of an unequivocal metric allowing a statistical evaluation of the resulting differences in rock weatherability we focus on a comparison between the two study sites in semi-arid (Santa Gracia) and humid-temperate climate (Nahuelbuta). At these two sites, denudation rates (15 – 48 t km^{-2} yr^{-1}) and soil residence times (22 – 28 kyr; Schaller et al., 2018b) are similar. Although both granitoid, bedrock between the two sites differs. Santa Gracia is underlain by diorite, a mafic rock, while Nahuelbuta is underlain by granodiorite (Oeser et al., 2018). Thus, the suite of primary minerals in Santa Gracia is more prone to weathering than in Nahuelbuta. Specifically, this means a higher amount of plagioclase and amphibole, and less unreactive quartz, at Santa Gracia. These differences in

hat gelöscht: the average of the correlation coefficients is r (10) ~ .88, p < .01; Table A1)

hat gelöscht: the average of the correlation coefficients is r (7) ~ .72, p < .05; Table A2)

hat gelöscht: τ^{Na}: r (7) = .73, p < .05;

hat gelöscht: A2

hat gelöscht: r (7 – 10) ~ 1.00, p < .01;

hat gelöscht: A1 & A2

hat gelöscht: (the average of the correlation coefficients is r (7) ~ .62, p < .05; Table A2) than with MAP (the average of the correlation coefficients is r (7) ~ .51, p > .05; Table A2).

predominantly Ca- and Mg-bearing minerals are reflected in higher Ca and Mg inventories in bulk regolith in Santa Gracia (Table A1) , that also translate into higher Ca and Mg weathering fluxes (Table 3). Total soil weathering rates (5 – 10 t km^{-2} yr^{-1}; Table 1), and differences in weathering properties are not statistically significant (Table A6). The weathering-release fluxes (Fig. 4, Table 3) for K, Na, P, and Si are similar despite massive differences in vegetation cover, NPP, and even MAP (Table 1 & A6). These similarities, and the higher weathering fluxes of Ca and Mg at Santa Gracia can be explained with the confounding effects of higher rock weatherability at Santa Gracia and the higher precipitation at Nahuelbuta. A comparison of concentration-discharge relationships between catchments underlain by mafic (basaltic) and granitoid rock (Ibarra et al., 2016) shows higher solute concentrations for all major elements in the basaltic catchments at a given runoff, and the preservation of chemostatic solute concentrations to higher runoff than in granitoid catchments. As a result, weathering fluxes in mafic catchments at low runoff are similar to fluxes from granitoid rock subjected to high runoff, as we observe at Santa Gracia and Nahuelbuta. Regardless, an increase in either weathering rate or degree of weathering at Nahuelbuta resulting from the 3.5 times higher NPP at Nahuelbuta is not discernible.

hat gelöscht: (Table 4)

hat gelöscht: (Table A3).

hat gelöscht: A3

hat gelöscht: (Ibarra et al., 2016)

6.6 Do negative feedbacks decouple biomass growth from weathering rate and degree?

Why do neither the degree nor the rate of weathering increase with NPP or MAP, nor does higher biomass growth overwhelm differences in rock mineralogy? Nutrient recycling may be the mechanism that decouples weathering from NPP, as shown in Section 6.2. Even so, the higher runoff results in a greater loss of nutrients from the bio-available pool and thus requires higher weathering rate to balance the loss. We thus speculate that the increased vegetation cover might even counteract a potential increase in weathering that would be caused by the increase in MAP, essentially damping the geogenic pathway. We return to the four suites of processes as outlined in Section 6.4 on the direct and indirect impacts of plants and their associated microbiota on weathering and discuss their potential operation at the EarthShape sites.

(A) Direct primary mineral dissolution by ectomycorrhizal fungi. As yet we have no direct observations on nutrient foraging by fungi and other microbes in regolith from the EarthShape sites as obtained on other mountain sites in Chile (Godoy and Mayr, 1989). Proxies for total microbial biomass in saprolite

do not increase along the gradient: total gene copy numbers have similar ranges from Santa Gracia to Nahuelbuta, and DNA amounts even decrease slightly (Oeser et al., 2018). Common strategies of microbial symbionts with tree roots suggest that energy investment into nutrient recycling from leaf litter is more advantageous than dissolving primary minerals (Andrino et al., 2019). Thus, we would expect that mycorrhiza predominantly aid recycling in Nahuelbuta. In Santa Gracia, however, the absence of a litter layer may prompt the subsurface fungal network to invest in primary mineral dissolution, adding microbial weathering to total weathering at that that site.

(B) Roots deepening regolith thickness. A detailed survey of rooting depth along the gradient has not been completed, but deep roots were not observed in Santa Gracia whereas in Nahuelbuta and La Campana, individual roots reach several meters into the saprolite. A and B horizons in Santa Gracia are shallow (20 – 40 cm), whereas they are deep in Nahuelbuta (80 – 100 cm; Bernhard et al., 2018; Oeser et al., 2018). We do not know the depth of the weathering front which appears to be at least a dozen of meters depth or more at both sites. Thus, deep rooting can benefit plant growth by increasing the size of the bio-available pool.

(C) Canopy and roots converting precipitation into evapotranspiration. Along the EarthShape transect the potential 23% reduction in runoff predicted by Ibarra et al. (2019) is minor considering the 100-fold increase in precipitation over the entire gradient. A larger effect may occur if roots provide preferential flow paths such that infiltrating water bypasses the regolith matrix available for weathering (Brantley et al., 2017). However, given the deep weathering fronts - likely beneath rooting depth - we consider this effect to be minor, or even acting to increase deep weathering. Thus, we consider the hydrological impact of plants on weathering to be minor along the gradient.

(D) Increasing solubility by release of soil CO_2 and organic complexing agents. Although with increasing NPP soil respiration of CO_2 should lead to increased primary mineral dissolution, plants potentially impose a negative feedback onto this dependence by influencing the silicon cycle. Because silicon is the most abundant element in felsic rock and regolith (besides oxygen), it exerts a major control on the total weathering fluxes. The Si concentration in the bio-available pool is key in setting the saturation with respect to the various dissolving and precipitating minerals in regolith. Plants can impact this pool in both directions. Some plant species accumulate Si by active transporter-mediated uptake or through passive

uptake within the transpiration stream, whole others exclude Si and avoid accumulation (Ma and Yamaji, 2008; Schaller et al., 2018a). Enhanced Si uptake from soil solution by Si accumulating plants would result in Si undersaturation of solutions with respect to secondary minerals and would thus result in an increase in weathering rates. However, this increase may be damped. That is because these plants would also convert silicon into biosilica (e.g. phytoliths). If returned to soil in plant debris this biosilica becomes a key factor in the stability of secondary minerals (e.g. kaolinite; Lucas, 2001). However, neither factor seems to be the case: In the EarthShape sites, the average Si concentration in the above-ground living ecosystems ranges from 110 µg g^{-1} in Nahuelbuta to 2500 µg g^{-1} in Pan de Azúcar (Table 4). Thus, the Si weathering flux $W^{Si}_{regolith}$ exceeds the Si uptake flux U^{Si}_{total} throughout (Table 3) and uptake from soil solution by plants equates to only 5%, 0.2%, and 2% of the Si release flux in Santa Gracia, La Campana, and Nahuelbuta, respectively. Only in Pan de Azúcar, relative uptake of Si is higher (25%).The ecosystems at our sites can thus be regarded to be below the threshold considered for Si accumulators (Schaller et al., 2018a). We can therefore exclude plant Si uptake and recycling of Si as a factor that increases weathering rates substantially. Rather, if plants in these ecosystems are discriminating against Si uptake whilst taking up water, the residual pore waters will get oversaturated with respect to secondary minerals. In this regard a key observation is provided by the analysis of pedogenic oxides (i.e. dithionite-extractable Al, Si extracted by oxalate, dithionite, and pyrophosphate; Oeser et al., 2018) and cation exchange capacity (Bernhard et al., 2018). These analyses suggest high amounts of amorphous precipitates and secondary minerals in the regolith of Nahuelbuta. We thus argue that Si is effectively captured in these barely soluble secondary minerals after initial dissolution from rock and regolith. In turn, $W^{Si}_{regolith}$ in Nahuelbuta is subdued despite elevated solubility of primary minerals due to increased CO_2 respiration by roots.

Ecosystems thus exert substantial control over weathering by both directly and indirectly modulating processes. These processes can either enhance or reduce weathering fluxes and result, in combination with effective recycling loops of plant-litter material, in well-balanced nutrient cycles. From our field data, we did not find evidence for coupling of silicate weathering fluxes with the mineral-nutrient demands of biota to an extent that exceeds other controlling factors of weathering. Our data suggests that the combination of recycling and negative feedbacks on weathering by secondary mineral formation

hat gelöscht: (Table 5).

hat gelöscht: (Schaller et al., 2018a)

within the regolith decrease weathering rates in areas of high vegetation cover and net primary productivity from what they would be in the absence of high biomass density.

7 Conclusions

Even though the EarthShape study sites define a north-south gradient in precipitation and biomass production, no such gradient is apparent for weathering rates and weathering intensity between the study sites situated in semi-arid, mediterranean, and humid-temperate climate.

At all four sites we locate the primary mineral nutrient source to plants in the bio-available fraction. This pool of mineral nutrients is initially fed by geogenic sources, which comprise the weathering of primary minerals. It is further fed from organic sources, which involves recycling of nutrients from leaf litter. The size of the bio-available nutrient pool decreases from north to south and while pedogenic properties (e.g. pH) likely contribute to set its size, we attribute its decrease mainly to an increase in the below-ground water flow. To fulfill their mineral-nutrient demand at increasing NPP but decreasing pool size, ecosystems increase nutrient recycling rather than enhancing biogenic weathering. We consequently find that the organic nutrient cycle intensifies, whereas the geogenic nutrient pathway is steady despite increasing MAP and NPP.

In fact, the presence of plants might even counteract a potential weathering increase along the gradient by inducing secondary mineral formation rather than nutrient-acquisition through weathering. Due to nutrient buffering by recycling and a potential biological dampening of weathering, any additional contribution to weathering by NPP is unresolvable in our data and is certainly smaller than abiotic controls like denudation, rainfall, or bedrock mineralogy. The global silicate-weathering cycle may thus not be as sensitive to plant growth as commonly thought and cannot be simulated in a straightforward manner in weathering models. This non-linear behavior is of relevance for models of the global weathering and the linked carbon cycle, of which accelerated weathering by land plants since the Ordovician is a common component.

hat gelöscht: While

8 Appendices

Appendix A: Calculation of fluxes and inventories in terrestrial ecosystems

Weathering indices (CDF & τ)

Zr, Ti, and Nb are commonly used to estimate mass losses to the dissolved form during weathering (Eqs. 5 & 6) as they are presumed to be the least mobile elements during weathering (Chadwick et al., 1990; White et al., 1998). The suitability of these elements for the EarthShape study sites has been evaluated and thoroughly discussed on a site to site basis in Oeser et al. (2018). Based on possible Ti-mobility in some samples and the fact that Zr is used as a reference element in the majority of weathering and soil production studies worldwide (e.g. Fisher et al., 2017; Green et al., 2006; Hewawasam et al., 2013; Riebe and Granger, 2013; Riebe et al., 2001; Schuessler et al., 2018; Uhlig et al., 2017), Zr was taken as immobile reference element in this study.

The calculations of these weathering indices rely on a good approximation of the chemical composition of the initial bedrock from which regolith formed. To this end, any regolith sample with a Zr concentration that was lower than the mean of unweathered bedrock by more than one standard deviation (1SD) was excluded from further consideration. Because a lower Zr concentration cannot be due to weathering, such regolith samples likely originate from chemically distinct bedrock or small-scale bedrock heterogeneities (e.g. a pegmatitic vein). Saprolite samples were also excluded from our data set if Cr and Ti concentrations were twice those of unweathered bedrock (+ 1SD). Elevated concentrations of these elements imply the presence of mafic precursor rock such as commonly present in bedrocks' mafic enclaves. All such excluded samples are marked in grey color in Figs. 3 & A1, and mainly affect only the lower section of the south-facing Nahuelbuta profile.

The concentration of K throughout the entire regolith profiles in Santa Gracia is three-fold higher than K contained in local bedrock samples (Oeser et al., 2018). We thus assume that the K concentration in the bedrock samples of Santa Gracia as determined by Oeser et al. (2018) underestimates the actual occurring K concentration of local bedrock. Thus, τ^K has been calculated using published values for K and Zr concentration from a study nearby (Miralles González, 2013).

Weathering fluxes

To estimate elemental release fluxes from regolith (Eq. 3) for each study site, the most negative τ-values from the shallowest mineral-soil sample of each regolith profile were used (red-circled symbols in Fig. A1). This practice is common in eroding regolith, where the loss indicators τ and CDF represent the integrated mass loss over the time and depth interval that a given sample moved from bedrock reference level to its present position (Brantley and Lebedeva, 2011; Ferrier et al., 2010; Hewawasam et al., 2013; Uhlig and von Blanckenburg, 2019). The elemental chemical weathering flux ($W^{X}_{regolith}$) at each study site has been averaged. Because not all of this flux might not be within reach of plant roots (e.g. if a fraction is lost into deep groundwater), this is an upper estimate of the nutrient supply from rock into vegetation. $W^{X}_{regolith}$ is reported in Table 3.

Ecosystem nutrient uptake fluxes

Total ecosystem nutrient uptake fluxes (U^{X}_{total}) have been evaluated using Eq. 4 and are reported in Table 3. Because we compare these to the weathering fluxes that integrate over several millennia, we estimate uptake fluxes that are representative for the Holocene. Net primary productivity (NPP), has been derived from a dynamic vegetation model (LPJ-GUESS) simulating vegetation cover and composition during the Holocene (Werner et al., 2018) and is reported in Table 1. Biomass production was estimated from NPP(C) by assuming that dry biomass consists of 50 wt% carbon. To obtain the element-specific uptake rate U^{X}_{total}, NPP is multiplied with the bulk concentration of X in the plants $[X]_{Plant}$.

The sampling and analyses of roots was not done in this study, because of the difficulties in obtaining entire roots or representative root segments from a specific tree or shrub including fine roots. For elemental analysis this difficulty is compounded by the need to remove any remaining soil particles or attached precipitates that might bias measured concentrations. To nevertheless estimate bulk plant elemental composition, we applied the dimensionless organ growth quotients GL/GS (leaf growth relative to stem growth) and GL/GR (leaf growth relative to root growth) in accordance with Niklas and Enquist (2002). This estimation invokes several assumptions: (1) Roots biomass growth contributes little to total plant growth, namely 9% in angiosperms and 17% in gymnosperms (Niklas and Enquist, 2002). We thus

treat roots and stem/ twig as one plant compartment. In total, the pooled growth of root, stem, and twig amounts to 68% and 52% of relative growth in angiosperms and gymnosperms, respectively. (2) Differences in biomass allocation are relevant only between angiosperms and gymnosperms and not between single plant species of a given class. (3) The pattern of relative growth and standing biomass allocation holds true across a minimum of eight orders of magnitude of species size (Niklas and Enquist, 2002). We thus adapted the organ growth quotients from the work of Niklas and Enquist (2002), such that we only differentiate between the growth rate of leaves and stem, respectively, and the adapt these quotients between angiosperms and gymnosperms. The bulk elemental ecosystem composition (Table 4) has been determined by weighting the averaged elemental composition for each sampled plant for their relative abundance in the respective ecosystem.

hat gelöscht: 5

Inventories

The inventories for the bio-available fraction ($I^X_{bio\text{-}av.}$) and in bulk regolith (I^X_{bulk}) have been calculated using Eq. 8 and are reported in Table A1. $I^X_{bio\text{-}av.}$ was determined for both the bio-available fraction in soil (comprised of the A and B horizon; $I^X_{bio\text{-}av,\,soil}$) and saprolite of 1m thickness ($I^X_{bio\text{-}av,\,sap}$). For the calculation of all inventories we used the soils' bulk density determined by Bernhard et al. (2018). I^X_{bulk} is comprised of elements contained in fine-earth material and in fragmented rocks and coarse material (e.g. core stones). We derive the relative amount of coarse material of each depth increment from Bernhard et al. (2018) and allocate them the bedrocks' chemical composition (Data Table S1). If information on either bulk density or the relative amount of coarse material was unavailable, the respective horizons' average has been used for the calculation of $I^X_{i,j}$. In none of the eight regolith profiles is the depth to unweathered bedrock known. Thus, for comparison purposes, we calculated the inventories of the bio-available fraction in saprolite ($I^X_{bio\text{-}av,\,sap}$) and in bulk regolith ($I^X_{bulk}$) to the depth of the respective regolith profile and normalized this value to the arbitrary value of 1 m.

hat gelöscht: 4

Nutrient recycling factor

We call the ratio of nutrient uptake to nutrient supply by weathering the "nutrient recycling factor" Rec^X which was calculated using Eq. 7 and is reported in Table 5. Importantly, as defined, this factor ratios fluxes between entire regolith and total uptake into the entire vegetation cover (the same rationale as used by Cleveland et al., 2013 for the inverse; the "new" fraction of P). Rec^X represents a minimum estimate as some fraction of $W^X_{regolith}$ will bypass nutrient uptake by plants if it is drained directly via groundwater into streams. Rec^X might represent an underestimate for some elements that are returned to soil by stem-flow or throughfall. According to e.g. Wilcke et al. (2017), these fluxes are generally highest for K compared to other elements. Rec^X might also be an overestimate, if a substantial fraction of nutrient is eroded by leaf litter and other plant debris after uptake, rendering it unavailable for recycling (Oeser and von Blanckenburg, 2020a).

In Pan de Azúcar, where atmospheric deposition (Dep^X_{dry} and Dep^X_{wet}) is known to be an important component of ecosystem element budgets (e.g. increasing τ-values towards the profiles top in absence of bio-lifting of elements and field observation; Oeser et al., 2018) we need to consider these inputs in addition to the weathering release fluxes ($W^X_{regolith}$). Thus, to account for all potential sources of elements available for plant uptake, the nutrient recycling factor in Pan de Azúcar is given as:

$$Rec^X = \frac{U^X_{total}}{W^X_{regolith} + Dep^X_{wet} + Dep^X_{dry}}$$

Atmospheric deposition fluxes have been estimated by determining the absolute difference between the lowest τ-value in the shallowest mineral-soil sample and the highest τ-value in the soil profile above it. Further, we assume that elemental gains (i.e. increasing τ-values) in the regolith profiles are attributed solely to atmospheric deposition. We test these estimates for atmospheric depositional fluxes by placing the elemental gains in proportion to the initially determined weathering release fluxes ($W^X_{regolith}$, Eq. 3; Table 3).

hat gelöscht: 7

hat gelöscht: plant-essential

hat gelöscht: .

Uncertainty estimation of nutrient fluxes

The analytical uncertainty of measured samples and certified international reference materials are reported in section "Analytical methods" and in the data publication Oeser and von Blanckenburg (2020b).

The uncertainties on the nutrient fluxes of $W^X_{regolith}$ and U^X_{total} were estimated by Monte Carlo simulations in which 20 000 random data sets were sampled within the standard deviation of all input parameters using a Box-Muller transformation (Box and Muller, 1958). The simulation of each regolith profiles' $W^X_{regolith}$ incorporates the SD of the average soil denudation rate D (Table 1), the SD of the concentration of the element of interest in bedrock (Data Table S1), and 3% relative uncertainty on the element concentration in regolith samples. In the case of U^X_{total} the SD of the respective study sites' NPP and the SD of the chemical composition of the weighted plants (Table 4) were used. The resultant uncertainties on both fluxes are reported in Table 3.

Appendix B: Data presentation and Statistical analyses

Replication

We present our results on nutrient fluxes, inventories, and turnover times as study-site averages for synthesis reasons only. Indeed, at each study site four replicate regolith profiles have been analyzed in previous studies. Within a given site, these profiles show no significant differences in chemistry and pedogenic properties (Bernhard et al., 2018; Oeser et al., 2018). In this study we focused on two regolith profiles situated on opposing slopes (north- and south facing midslope profiles) to account for the variations in substrate and/ or the effects of insolation and microclimate on weathering and nutrient uptake by plants. However, these profiles are natural replicates and are considered independent from each other.

Statistical analysis

An analysis of variance (ANOVA) was performed to evaluate how denudation rate (D), the chemical depletion fraction (CDF), soil weathering rate (W), and the elemental weathering rates for Ca, K, Na, P, and Si ($W^X_{regolith}$) vary among sites. Variance homogeneity was tested using Levene's Test before applying

hat gelöscht: Oeser and von Blanckenburg (2020).

hat gelöscht: 5

ANOVAs and pair-wise differences were assessed using Tukey's HSD test. In these, p values ≤ 0.1 were considered as significant. The correlations between D, MAP, NPP, and the degree (CDF, τ^X) and rate (W, $W^X_{regolith}$) of weathering were evaluated using Pearson's correlation coefficients. To test for the significance of D on these weathering parameters, Pearson's correlation coefficients were evaluated twice: with (Table A4) and without La Campana (Table A5). This test is possible because of the high denudation rate of this site which originates from the steepest relief of all sites (Oeser et al., 2018; Schaller et al., 2018b; van Dongen et al., 2019). The sample set comprises the tested parameters for each regolith profile and each regolith profile is considered independent from each other (i.e. n = 8). Statistical analyses were conducted using the statistics packages included in the software OriginPro (Version 2020). Given the small sample size (n = 8), test for equal variances failed. Still, overall ANOVA showed all weathering patterns (except for $W^K_{regolith}$) differed among sites on the total population (Table A6). However, post-hoc comparisons indicated that sites did not always differ, and that differences between sites varied for the different weathering parameters (Table A6). Particularly, few statistically significant differences exist between the semi-arid Santa Gracia, the mediterranean La Campana and humid-temperate Nahuelbuta. In these three sites the weathering release fluxes do not differ significantly (Table A6) despite massive differences in D, MAP, and NPP (Table 1).

hat gelöscht: 05

hat gelöscht: (Table A1)

hat gelöscht: (Table A2).

hat gelöscht: includes study site average values from all

hat gelöscht: and those of the single

hat gelöscht: profiles.

hat gelöscht: Equal

hat gelöscht: could be assumed throughout and

hat gelöscht: (Table A3).

hat gelöscht: A3

hat gelöscht: two

hat gelöscht: for K ($W^K_{regolith}$), Na ($W^{Na}_{regolith}$), P ($W^P_{regolith}$), and Si ($W^{Si}_{regolith}$)

hat gelöscht: A3

9 Sample availability

All sample metadata are already available on a public server using unique sample identifiers in form of the "International Geo Sample Number" (IGSN).

10 Author contributions

R.A. Oeser conducted field sampling, analyzed samples, interpreted data, and wrote text. F. von Blanckenburg designed the study, selected the study sites, interpreted data, and wrote text.

11 Competing financial interests

The authors declare no competing financial interests.

12 Additional information

Supplementary data tables are available at GFZ data services (Oeser and von Blanckenburg, 2020b).

hat gelöscht: Supplementary data tables are available at GFZ data services (Oeser and von Blanckenburg, 2020).¶

13 Acknowledgements

The study was conducted within the framework of the priority program of the Deutsche Forschungsgemeinschaft "EarthShape: Earth Surface Shaping by Biota" (DFG-SPP 1803; http://www.earthshape.net). R.A. Oeser and F. von Blanckenburg are grateful for funding. We thank Leandro Paulino (Departamento de Suelos y Recursos Naturales, Universitad de Concepción, Chile) and Kirstin Übernickel for managing the priority program and Todd Ehlers (both Institute for Geosciences, Universität Tübingen, Germany) for its co-coordination.We acknowledge CONAF in Chile for providing us with the opportunity to work in the national parks of Pan de Azúcar, La Campana, and Nahuelbuta. We also thank CEAZA for facilitating access to the Reserva Natural Santa Gracia. We are grateful to J. Boy (Soil Sciences, Leibniz Universität Hannover, Germany) for discussions, and D. Uhlig (Institute of Bio- and Geosciences, Forschungszentrum Jülich, Germany), Michaela Dippold (Department of Crop Sciences, Georg-August University Goettingen, Germany), Matthew Winnick (Department of Geosciences, University of Massachusetts, USA), and Patrick Frings (Section "Earth Surface Geochemistry", GFZ German Research Centre for Geosciences, Germany) for informal reviews of the text. We thank the three anonymous referees and Marjin van de Broeck and his MSc students for their detailed critique of our work which led us to revise the manuscript with the aim of attempting to avoiding the pitfalls emerging when working across disciplines.

hat gelöscht: R.A. Oeser and F. von Blanckenburg are grateful for funding by the German National Science Foundation Priority Program DFG-SPP 1803 (EarthShape; http://www.earthshape.net). We thank Leandro Paulino (Departamento de Suelos y Recursos Naturales, Universitad de Concepción, Chile) and Kirstin Übernickel for managing the priority program and Todd Ehlers (both Institute for Geosciences, Universität Tübingen, Germany) for its co-coordination.

14 References

Amundson, R., Richter, D. D., Humphreys, G. S., Jobbágy, E. G., and Gaillardet, J. r. m.: Coupling between Biota and Earth Materials in the Critical Zone, Elements, 3, 327-332, doi:10.2113/gselements.3.5.327, 2007.

Andrino, A., Boy, J., Mikutta, R., Sauheitl, L., and Guggenberger, G.: Carbon Investment Required for the Mobilization of Inorganic and Organic Phosphorus Bound to Goethite by an Arbuscular Mycorrhiza (Solanum lycopersicum x Rhizophagus irregularis), Frontiers in Environmental Science, 7, doi:10.3389/fenvs.2019.00026, 2019.

Armesto, J. J., Vidiella, P. E., and Gutiérrez, J. R.: Plant communities of the fog-free coastal desert of Chile: plant strategies in a fluctuating environment., Rev. Chil. Hist. Nat., 66, 271-282, 1993.

Arunachalam, J., Emons, H., Krasnodebska, B., and Mohl, C.: Sequential extraction studies on homogenized forest soil samples, The Science of the Total Environment, 181, 147-159, doi:10.1016/0048-9697(95)05005-1, 1996.

Bahre, C. J.: Destruction of the natural vegetation of north-central Chile, Univ of California Press, 1979.

Balogh-Brunstad, Z., Keller, C. K., Gill, R. A., Bormann, B. T., and Li, C. Y.: The effect of bacteria and fungi on chemical weathering and chemical denudation fluxes in pine growth experiments., Biogeochemistry, 88, 153-167, doi:10.1007/s10533-008-9202-y, 2008a.

Balogh-Brunstad, Z., Kent Keller, C., Thomas Dickinson, J., Stevens, F., Li, C. Y., and Bormann, B. T.: Biotite weathering and nutrient uptake by ectomycorrhizal fungus, Suillus tomentosus, in liquid-culture experiments, Geochim. Cosmochim. Acta, 72, 2601-2618, doi:10.1016/j.gca.2008.04.003, 2008b.

Beerling, D. J., and Berner, R. A.: Feedbacks and the coevolution of plants and atmospheric CO2, Proc Natl Acad Sci U S A, 102, 1302-1305, doi:10.1073/pnas.0408724102, 2005.

Berg, K., and Breitkreuz, C.: Mesozoische Plutone in der nordchilenischen Küstenkordillere: petrogenese, geochronologie, Geochemie und Geodynamik mantelbetonter Magmatite, Geotectonic Research, 66, Schweizerbart Science Publishers, 1983.

Berg, K., and Baumann, A.: Plutonic and metasedimentary rocks from the Coastal Range of northern Chile: Rb-Sr and U-Pb isotopic systematics, Earth. Planet. Sci. Lett., 75, 101-115, doi:10.1016/0012-821X(85)90093-7, 1985.

Berner, E. K., Berner, R. A., and Moulton, K. L.: Plants and Mineral Weathering: Present and Past, in: Treatise on Geochemistry, 169-188, doi:10.1016/b0-08-043751-6/05175-6, 2003.

Bernhard, N., Moskwa, L.-M., Schmidt, K., Oeser, R. A., Aburto, F., Bader, M. Y., Baumann, K., von Blanckenburg, F., Boy, J., van den Brink, L., Brucker, E., Canessa, R., Dippold, M. A., Ehlers, T. A., Fuentes, J. P., Godoy, R., Köster, M., Kuzyakov, Y., Leinweber, P., Neidhard, H., Matus, F., Mueller, C. W., Oelmann, Y., Oses, R., Osses, P., Paulino, L., Schaller, M., Schmid, M., Spielvogel, S., Spohn, M., Stock, S., Stroncik, N., Tielbörger, K., Übernickel, K., Scholten, T., Seguel, O., Wagner, D., and Kühn, P.: Pedogenic and microbial interrelations to regional climate and local topography: new insights from a climate gradient (arid to humid) along the Coastal Cordillera of Chile, Catena, 170, doi:10.1016/j.catena.2018.06.018, 2018.

Blanco-Chao, R., Pedoja, K., Witt, C., Martinod, J., Husson, L., Regard, V., Audin, L., Nexer, M., Delcaillau, B., Saillard, M., Melnick, D., Dumont, J. F., Santana, E., Navarrete, E., Martillo, C., Pappalardo, M., Ayala, L., Araya, J. F., Feal-Perez, A., Correa, D., and Arozarena-Llopis, I.: The rock coast of South and Central America, in: Rock Coast Geomorphology: A Global Synthesis., 1, The Geological Society, London, 155-191, doi:10.1144/m40.10, 2014.

Blum, J. D., Klaue, A., Nezat, C. A., Driscoll, C. T., Johnson, C. E., Siccama, T. G., Eagar, C., Fahey, T. J., and Likens, G. E.: Mycorrhizal weathering of apatite as an important calcium source in base-poor forest ecosystems, Nature, 417, 729-731, doi:10.1038/nature00793, 2002.

Bonneville, S., Morgan, D. J., Schmalenberger, A., Bray, A., Brown, A., Banwart, S. A., and Benning, L. G.: Tree-mycorrhiza symbiosis accelerate mineral weathering: Evidences from nanometer-scale elemental fluxes at the hypha–mineral interface, Geochim. Cosmochim. Acta, 75, 6988-7005, doi:10.1016/j.gca.2011.08.041, 2011.

Bormann, F., Likens, G., and Eaton, J.: Biotic regulation of particulate and solution losses from a forest ecosystem, Bioscience, 19, 600-610, doi:10.2307/1294934, 1969.

Box, G. E. P., and Muller, M. E.: A note on the generation of random normal deviates, Ann. Math. Statist., 29, 610-611, doi:10.1214/aoms/1177706645, 1958.

Boy, J., and Wilcke, W.: Tropical Andean forest derives calcium and magnesium from Saharan dust, Global Biogeochem. Cycles, 22, GB1027, doi:10.1029/2007gb002960, 2008.

Brantley, S. L., and Lebedeva, M.: Learning to Read the Chemistry of Regolith to Understand the Critical Zone, Annual Review of Earth and Planetary Sciences, 39, 387-416, doi:10.1146/annurev-earth-040809-152321, 2011.

Brantley, S. L., Megonigal, J. P., Scatena, F. N., Balogh-Brunstad, Z., Barnes, R. T., Bruns, M. A., Van Cappellen, P., Dontsova, K., Hartnett, H. E., Hartshorn, A. S., Heimsath, A., Herndon, E., Jin, L., Keller, C. K., Leake, J. R., McDowell, W. H., Meinzer, F. C., Mozdzer, T. J., Petsch, S., Pett-Ridge, J., Pregitzer, K. S., Raymond, P. A., Riebe, C. S., Shumaker, K., Sutton-Grier, A., Walter, R., and Yoo, K.: Twelve testable hypotheses on the geobiology of weathering, Geobiology, 9, 140-165, doi:10.1111/j.1472-4669.2010.00264.x, 2011.

Brantley, S. L., Lebedeva, M., and Heimshath, E. H.: A Geobiological View of Weathering and Erosion, in: Fundamentals of Geobiology, edited by: Knoll, A. H., Blackwell Publishing, doi:10.1002/9781118280874.ch12, 2012.

hat gelöscht: Blum, J. D., Hamburg, S. P., Yanai, R. D., and Arthur, M. A.: Determination of foliar Ca/Sr discrimination factors for six tree species and implications for Ca sources in northern hardwood forests, Plant Soil, 356, 303-314, doi:10.1007/s11104-011-1122-2, 2012.¶

Brantley, S. L., Eissenstat, D. M., Marshall, J. A., Godsey, S. E., Balogh-Brunstad, Z., Karwan, D. L., Papuga, S. A., Roering, J., Dawson, T. E., Evaristo, J., Chadwick, O., McDonnell, J. J., and Weathers, K. C.: Reviews and syntheses: on the roles trees play in building and plumbing the critical zone, Biogeosciences, 14, 5115-5142, doi:10.5194/bg-14-5115-2017, 2017.
Brucker, E., and Spohn, M.: Formation of soil phosphorus fractions along a climate and vegetation gradient in the Coastal Cordillera of Chile, Catena, 180, 203-211, doi:10.1016/j.catena.2019.04.022, 2019.
Buendía, C., Kleidon, A., and Porporato, A.: The role of tectonic uplift, climate, and vegetation in the long-term terrestrial phosphorous cycle, Biogeosciences, 7, 2025-2038, doi:10.5194/bg-7-2025-2010, 2010.
Bullen, T. D., and Chadwick, O.: Ca, Sr and Ba stable isotopes reveal the fate of soil nutrients along a tropical climosequence in Hawaii, Chem. Geol., 422, 25-45, doi:10.1016/j.chemgeo.2015.12.008, 2016.
Buss, H. L., Bruns, M. A., Schultz, D. J., Moore, J., Mathur, C. F., and Brantley, S. L.: The coupling of biological iron cycling and mineral weathering during saprolite formation, Luquillo Mountains, Puerto Rico, Geobiology, 3, 247-260, doi:10.1111/j.1472-4669.2006.00058.x, 2005.
Calmels, D., Gaillardet, J., and François, L.: Sensitivity of carbonate weathering to soil CO2 production by biological activity along a temperate climate transect, Chem. Geol., 390, 74-86, doi:10.1016/j.chemgeo.2014.10.010, 2014.
Canadell, J., Jackson, R., Ehleringer, J., Mooney, H., Sala, O., and Schulze, E.-D.: Maximum rooting depth of vegetation types at the global scale, Oecologia, 108, 583-595, 1996.
Chadwick, K. D., and Asner, G. P.: Tropical soil nutrient distributions determined by biotic and hillslope processes, Biogeochemistry, 127, 273-289, doi:10.1007/s10533-015-0179-z, 2016.
Chadwick, O. A., Brimhall, G. H., and Hendricks, D. M.: From a black to a gray box — a mass balance interpretation of pedogenesis, Geomorphology, 3, 369-390, doi:10.1016/0169-555x(90)90012-f, 1990.
Chadwick, O. A., Derry, L. A., Vitousek, P. M., Huebert, B. J., and Hedin, L. O.: Changing sources of nutrients during four million years of ecosystem development, Nature, 397, 491-497, doi:10.1038/17276, 1999.
Chapin III, F. S.: The mineral nutrition of wild plants, Annu. Rev. Ecol. Syst., 11, 233-260, 1980.
Chapin III, F. S., Matson, P. A., and Vitousek, P. M.: Principles of Terrestrial Ecosystem Ecology, 2nd ed., 2011.
Chaudhuri, S., Clauer, N., and Semhi, K.: Plant decay as a major control of river dissolved potassium: A first estimate, Chem. Geol., 243, 178-190, doi:10.1016/j.chemgeo.2007.05.023, 2007.
Cleveland, C. C., Houlton, B. Z., Smith, W. K., Marklein, A. R., Reed, S. C., Parton, W., Del Grosso, S. J., and Running, S. W.: Patterns of new versus recycled primary production in the terrestrial biosphere, Proc Natl Acad Sci U S A, 110, 12733-12737, doi:10.1073/pnas.1302768110, 2013.
Dal Bo, I., Klotzsche, A., Schaller, M., Ehlers, T. A., Kaufmann, M. S., Fuentes Espoz, J. P., Vereecken, H., and van der Kruk, J.: Geophysical imaging of regolith in landscapes along a climate and vegetation gradient in the Chilean coastal cordillera, Catena, 180, 146-159, doi:10.1016/j.catena.2019.04.023, 2019.
Day, T. A., Guénon, R., and Ruhland, C. T.: Photodegradation of plant litter in the Sonoran Desert varies by litter type and age, Soil Biol. Biochem., 89, 109-122, doi:10.1016/j.soilbio.2015.06.029, 2015.
Delhaize, E., and Ryan, P. R.: Aluminum Toxicity and Tolerance in Plants, Plant Physiol., 107, 315-321, doi:10.1104/pp.107.2.315, 1995.
Dere, A. L., White, T. S., April, R. H., Reynolds, B., Miller, T. E., Knapp, E. P., McKay, L. D., and Brantley, S. L.: Climate dependence of feldspar weathering in shale soils along a latitudinal gradient, Geochim. Cosmochim. Acta, 122, 101-126, doi:10.1016/j.gca.2013.08.001, 2013.
Dixon, J. L., Heimsath, A. M., Kaste, J., and Amundson, R.: Climate-driven processes of hillslope weathering, Geology, 37, 975-978, doi:10.1130/g30045a.1, 2009.
Dixon, J. L., Hartshorn, A. S., Heimsath, A. M., DiBiase, R. A., and Whipple, K. X.: Chemical weathering response to tectonic forcing: A soils perspective from the San Gabriel Mountains, California, Earth. Planet. Sci. Lett., 323-324, 40-49, doi:10.1016/j.epsl.2012.01.010, 2012.
Dixon, J. L., Chadwick, O. A., and Vitousek, P. M.: Climate-driven thresholds for chemical weathering in postglacial soils of New Zealand, Journal of Geophysical Research: Earth Surface, 121, 1619-1634, doi:10.1002/2016jf003864, 2016.
Dosseto, A., Buss, H. L., and Suresh, P. O.: Rapid regolith formation over volcanic bedrock and implications for landscape evolution, Earth. Planet. Sci. Lett., 337-338, 47-55, doi:10.1016/j.epsl.2012.05.008, 2012.
Doughty, C. E., Taylor, L. L., Girardin, C. A. J., Malhi, Y., and Beerling, D. J.: Montane forest root growth and soil organic layer depth as potential factors stabilizing Cenozoic global change, Geophys. Res. Lett., 41, 983-990, doi:10.1002/2013gl058737, 2014.
Drever, J. I., and Zobrist, J.: Chemical weathering of silicate rocks as a function of elevation in the southern Swiss Alps, Geochim. Cosmochim. Acta, 56, 3209-3216, doi:10.1016/0016-7037(92)90298-w, 1992.
Drever, J. I.: The effect of land plants on weathering rates of silicate minerals, Geochim. Cosmochim. Acta, 58, 2325-2332, doi:10.1016/0016-7037(94)90013-2, 1994.
Eger, A., Yoo, K., Almond, P. C., Boitt, G., Larsen, I. J., Condron, L. M., Wang, X., and Mudd, S. M.: Does soil erosion rejuvenate the soil phosphorus inventory?, Geoderma, 332, 45-59, doi:10.1016/j.geoderma.2018.06.021, 2018.
Egli, M., Mirabella, A., Sartori, G., and Fitze, P.: Weathering rates as a function of climate: results from a climosequence of the Val Genova (Trentino, Italian Alps). Geoderma, 111, 99-121, doi:10.1016/S0016-7061(02)00256-2, 2003.

Fabian, J., Zlatanovic, S., Mutz, M., and Premke, K.: Fungal-bacterial dynamics and their contribution to terrigenous carbon turnover in relation to organic matter quality, ISME J, 11, 415-425, doi:10.1038/ismej.2016.131, 2017.
Fan, Y., Miguez-Macho, G., Jobbagy, E. G., Jackson, R. B., and Otero-Casal, C.: Hydrologic regulation of plant rooting depth, Proc Natl Acad Sci U S A, 114, 10572-10577, doi:10.1073/pnas.1712381114, 2017.
Ferrier, K. L., Kirchner, J. W., and Finkel, R. C.: Erosion rates over millennial and decadal timescales at Caspar Creek and Redwood Creek, Northern California Coast Ranges, Earth Surface Processes and Landforms, 30, 1025-1038, doi:10.1002/esp.1260, 2005.
Ferrier, K. L., Kirchner, J. W., Riebe, C. S., and Finkel, R. C.: Mineral-specific chemical weathering rates over millennial timescales: Measurements at Rio Icacos, Puerto Rico, Chem. Geol., 277, 101-114, doi:10.1016/j.chemgeo.2010.07.013, 2010.
Ferrier, K. L., Kirchner, J. W., and Finkel, R. C.: Weak influences of climate and mineral supply rates on chemical erosion rates: Measurements along two altitudinal transects in the Idaho Batholith, Journal of Geophysical Research: Earth Surface, 117, F02026, doi:10.1029/2011jf002231, 2012.
Finlay, R. D., Mahmood, S., Rosenstock, N., Bolou-Bi, E. B., Köhler, S. J., Fahad, Z., Rosling, A., Wallander, H., Belyazid, S., Bishop, K., and Lian, B.: Reviews and syntheses: Biological weathering and its consequences at different spatial levels – from nanoscale to global scale, Biogeosciences, 17, 1507-1533, doi:10.5194/bg-17-1507-2020, 2020.
Fisher, B. A., Rendahl, A. K., Aufdenkampe, A. K., and Yoo, K.: Quantifying weathering on variable rocks, an extension of geochemical mass balance: Critical zone and landscape evolution, Earth Surface Processes and Landforms, 42, 2457-2468, doi:10.1002/esp.4212, 2017.
Gallo, M. E., Sinsabaugh, R. L., and Cabaniss, S. E.: The role of ultraviolet radiation in litter decomposition in arid ecosystems, Applied Soil Ecology, 34, 82-91, doi:10.1016/j.apsoil.2005.12.006, 2006.
Gerrits, R., Pokharel, R., Breitenbach, R., Radnik, J., Feldmann, I., Schuessler, J. A., von Blanckenburg, F., Gorbushina, A. A., and Schott, J.: How the rock-inhabiting fungus K. petricola A95 enhances olivine dissolution through attachment, Geochim. Cosmochim. Acta, 282, 76-97, doi:10.1016/j.gca.2020.05.010, 2020.
Giehl, R. F., and von Wiren, N.: Root nutrient foraging, Plant Physiol., 166, 509-517, doi:10.1104/pp.114.245225, 2014.
Godoy, R., and Mayr, R.: Caracterización morfológica de micorrizas vesículo-arbusculares en coníferas endémicas del sur de Chile., Bosque, 10, 89-98, 1989.
Godsey, S. E., Hartmann, J., and Kirchner, J. W.: Catchment chemostasis revisited: Water quality responds differently to variations in weather and climate, Hydrological Processes, 33, 3056-3069, doi:10.1002/hyp.13554, 2019.
Green, E., Dietrich, W., and Banfield, J.: Quantification of chemical weathering rates across an actively eroding hillslope, Earth. Planet. Sci. Lett., 242, 155-169, doi:10.1016/j.epsl.2005.11.039, 2006.
Hahm, W. J., Riebe, C. S., Lukens, C. E., and Araki, S.: Bedrock composition regulates mountain ecosystems and landscape evolution, Proc Natl Acad Sci U S A, 111, 3338-3343, doi:10.1073/pnas.1315667111, 2014.
Hasenmueller, E. A., Gu, X., Weitzman, J. N., Adams, T. S., Stinchcomb, G. E., Eissenstat, D. M., Drohan, P. J., Brantley, S. L., and Kaye, J. P.: Weathering of rock to regolith: The activity of deep roots in bedrock fractures, Geoderma, 300, 11-31, doi:10.1016/j.geoderma.2017.03.020, 2017.
Hattenschwiler, S., Coq, S., Barantal, S., and Handa, I. T.: Leaf traits and decomposition in tropical rainforests: revisiting some commonly held views and towards a new hypothesis, New Phytol., 189, 950-965, doi:10.1111/j.1469-8137.2010.03483.x, 2011.
He, X. T., Logan, T. J., and Traina, S. J.: Physical and chemical characteristics of selected US municipal solid waste composts., Journal of Environmental Quality, 24, 543-552, doi:10.2134/jeq1995.00472425002400030022x, 1995.
Heartsill Scalley, T., Scatena, F. N., Moya, S., and Lugo, A. E.: Long-term dynamics of organic matter and elements exported as coarse particulates from two Caribbean montane watersheds, J. Trop. Ecol., 28, 127-139, doi:10.1017/s0266467411000733, 2012.
Heimsath, A. M., Dietrich, W. E., Nishiizumi, K., and Finkel, R. C.: The soil production function and landscape equilibrium, Nature, 388, 358-361, doi:10.1038/41056, 1997.
Hervé, F., Munizaga, F., Mantovani, M., and Hervé, M.: Edades Rb/Sr neopaleozoicas del basamento cristallino de la Cordillera de Nahuelbuta, Primer Congresso Geologico Chileno, Santiago, 1976.
Hervé, F.: Petrology of the crystalline basement of the Nahuelbuta Mountains, south-central Chile, Comparative studies on the Geology of the Circum-Pacific orogenic belt in Japan and Chile, edited by: Ishikava, I., and Aguirre, L., Japan Society for the Promotion of Science, 1977.
Hewawasam, T., von Blanckenburg, F., Bouchez, J., Dixon, J. L., Schuessler, J. A., and Maekeler, R.: Slow advance of the weathering front during deep, supply-limited saprolite formation in the tropical Highlands of Sri Lanka, Geochim. Cosmochim. Acta, 118, 202-230, doi:10.1016/j.gca.2013.05.006, 2013.
Houlton, B. Z., Morford, S. L., and Dahlgren, R. A.: Convergent evidence for widespread rock nitrogen sources in Earth's surface environment, Science, 360, 58-62, doi:10.1126/science.aan4399, 2018.
Ibarra, D. E., Caves, J. K., Moon, S., Thomas, D. L., Hartmann, J., Chamberlain, C. P., and Maher, K.: Differential weathering of basaltic and granitic catchments from concentration–discharge relationships, Geochim. Cosmochim. Acta, 190, 265-293, doi:10.1016/j.gca.2016.07.006, 2016.
Ibarra, D. E., Rugenstein, J. K. C., Bachan, A., Baresch, A., Lau, K. V., Thomas, D. L., Lee, J.-E., Boyce, C. K., and Chamberlain, C. P.: Modeling the consequences of land plant evolution on silicate weathering, Am. J. Sci., 319, 1-43, doi:10.2475/01.2019.01, 2019.

hat gelöscht: Faure, G., and Powell, J. L.: Strontium Isotope Geology, Isotopes in Geology, 1972.¶
Faure, G., and Mensing, T. M.: Isotopes: principles and applications, Wiley-Blackwell, 2005.¶

Jobbágy, E. G., and Jackson, R. B.: The uplift of soil nutrients by plants: Biogeochemical consequences across scales., Ecology, 85, 2380-2389, 2004.
Jobbágy, E. G. a. J., Robert B: The distribution of soil nutrients with depth: global patterns and the imprint of plants, Biogeochemistry, 53, 51-77, doi:10.1023/A:1010760720215, 2001.
Joos, O., Hagedorn, F., Heim, A., Gilgen, A. K., Schmidt, M. W. I., Siegwolf, R. T. W., and Buchmann, N.: Summer drought reduces total and litter-derived soil CO2 effluxes in temperate grassland – clues from a 13C litter addition experiment, Biogeosciences, 7, 1031-1041, doi:10.5194/bg-7-1031-2010, 2010.
Jung, M., Reichstein, M., Margolis, H. A., Cescatti, A., Richardson, A. D., Arain, M. A., Arneth, A., Bernhofer, C., Bonal, D., Chen, J., Gianelle, D., Gobron, N., Kiely, G., Kutsch, W., Lasslop, G., Law, B. E., Lindroth, A., Merbold, L., Montagnani, L., Moors, E. J., Papale, D., Sottocornola, M., Vaccari, F., and Williams, C.: Global patterns of land-atmosphere fluxes of carbon dioxide, latent heat, and sensible heat derived from eddy covariance, satellite, and meteorological observations, Journal of Geophysical Research, 116, doi:10.1029/2010jg001566, 2011.
Kalinowski, B. E., Liermann, L. J., Givens, S., and Brantley, S. L.: Rates of bacteria-promoted solubilization of Fe from minerals: a review of problems and approaches, Chem. Geol., 169, 357-370, doi:10.1016/s0009-2541(00)00214-x, 2000.
Kelly, A. E., and Goulden, M. L.: A montane Mediterranean climate supports year-round photosynthesis and high forest biomass, Tree Physiol, 36, 459-468, doi:10.1093/treephys/tpv131, 2016.
Kelly, E. F., Chadwick, O. A., and Hilinski, T. E.: The effect of plants on mineral weathering, Biogeochemistry, 42, 21-53, doi:10.1023/a:1005919306687, 1998.
Kleidon, A., Fraedrich, K., and Heimann, M.: A Green Planet Versus a Desert World: Estimating the Maximum Effect of Vegetation on the Land Surface Climate, Clim. Change, 44, 471-493, doi:10.1023/a:1005559518889, 2000.
Kronzucker, H. J., and Britto, D. T.: Sodium transport in plants: a critical review, New Phytol., 189, 54-81, doi:10.1111/j.1469-8137.2010.03540.x, 2011.
Kump, L. R., Brantley, S. L., and Arthur, M. A.: Chemical Weathering, Atmospheric CO2, and Climate, Annual Review of Earth and Planetary Sciences, 28, 611-667, doi:10.1146/annurev.earth.28.1.611, 2000.
Laliberte, E., Grace, J. B., Huston, M. A., Lambers, H., Teste, F. P., Turner, B. L., and Wardle, D. A.: How does pedogenesis drive plant diversity?, Trends Ecol. Evol., 28, 331-340, doi:10.1016/j.tree.2013.02.008, 2013.
Lambers, H., Raven, J. A., Shaver, G. R., and Smith, S. E.: Plant nutrient-acquisition strategies change with soil age, Trends Ecol. Evol., 23, 95-103, doi:10.1016/j.tree.2007.10.008, 2008.
Lambers, H., Brundrett, M. C., Raven, J. A., and Hopper, S. D.: Plant mineral nutrition in ancient landscapes: high plant species diversity on infertile soils is linked to functional diversity for nutritional strategies, Plant Soil, 348, 7-27, doi:10.1007/s11104-011-0977-6, 2011.
Lang, F., Bauhus, J., Frossard, E., George, E., Kaiser, K., Kaupenjohann, M., Krüger, J., Matzner, E., Polle, A., Prietzel, J., Rennenberg, H., and Wellbrock, N.: Phosphorus in forest ecosystems: New insights from an ecosystem nutrition perspective, J. Plant Nutr. Soil Sci., 179, 129-135, doi:10.1002/jpln.201500541, 2016.
Lang, F., Krüger, J., Amelung, W., Willbold, S., Frossard, E., Bünemann, E. K., Bauhus, J., Nitschke, R., Kandeler, E., Marhan, S., Schulz, S., Bergkemper, F., Schloter, M., Luster, J., Guggisberg, F., Kaiser, K., Mikutta, R., Guggenberger, G., Polle, A., Pena, R., Prietzel, J., Rodionov, A., Talkner, U., Meesenburg, H., von Wilpert, K., Hölscher, A., Dietrich, H. P., and Chmara, I.: Soil phosphorus supply controls P nutrition strategies of beech forest ecosystems in Central Europe, Biogeochemistry, 136, 5-29, doi:10.1007/s10533-017-0375-0, 2017.
Lee, J.-E., and Boyce, K.: Impact of the hydraulic capacity of plants on water and carbon fluxes in tropical South America, Journal of Geophysical Research, 115, doi:10.1029/2010jd014568, 2010.
Lenton, T. M., Crouch, M., Johnson, M., Pires, N., and Dolan, L.: First plants cooled the Ordovician, Nature Geoscience, 5, 86-89, doi:10.1038/ngeo1390, 2012.
Liang, Y., Sun, W., Zhu, Y. G., and Christie, P.: Mechanisms of silicon-mediated alleviation of abiotic stresses in higher plants: a review, Environ. Pollut., 147, 422-428, doi:10.1016/j.envpol.2006.06.008, 2007.
Lin, H.: Linking principles of soil formation and flow regimes, Journal of Hydrology, 393, 3-19, doi:10.1016/j.jhydrol.2010.02.013, 2010.
Lucas, Y.: The Role of Plants in Controlling Rates and Products of Weathering: Importance of Biological Pumping, Annual Review of Earth and Planetary Sciences, 29, 135-163, doi:10.1146/annurev.earth.29.1.135, 2001.
Luebert, F., and Pliscoff, P.: Sinópsis bioclimática y vegetacional de Chile., Editorial Universitaria, Santiago de Chile, 2006.
Ma, J. F., and Yamaji, N.: Functions and transport of silicon in plants, Cell. Mol. Life Sci., 65, 3049-3057, doi:10.1007/s00018-008-7580-x, 2008.
Maher, K.: The dependence of chemical weathering rates on fluid residence time, Earth. Planet. Sci. Lett., 294, 101-110, doi:10.1016/j.epsl.2010.03.010, 2010.
Maher, K., and Chamberlain, C. P.: Hydrologic regulation of chemical weathering and the geologic carbon cycle, Science, 343, 1502-1504, doi:10.1126/science.1250770, 2014.
McCulley, R. L., Jobbágy, E. G., Pockman, W. T., and Jackson, R. B.: Nutrient uptake as a contributing explanation for deep rooting in arid and semi-arid ecosystems, Oecologia, 141, 620-628, doi:10.1007/s00442-004-1687-z, 2004.

hat gelöscht: Marschner, H.: General introduction to the mineral nutrition of plants, Inorganic plant nutrition, 5-60, 1983.¶

Melnik, D.: Rise of the central Andean coast by Earthquakes straddling the Moho., Nature Geoscience, 9, 401-407, doi:10.1038/ngeo2683, 2016.
Información Oficial Hidrometeorológica y de Calidad de Aguas en Línea: http://snia.dga.cl/BNAConsultas/reportes, access: 12.06.2017, 2017.
Minyard, M. L., Bruns, M. A., Liermann, L. J., Buss, H. L., and Brantley, S. L.: Bacterial Associations with Weathering Minerals at the Regolith-Bedrock Interface, Luquillo Experimental Forest, Puerto Rico, Geomicrobiol. J., 29, 792-803, doi:10.1080/01490451.2011.619640, 2012.
Miralles González, C.: Evaluación de los factores que controllan la geoquímica de sedimentos fluviales de la cuenca del Río Elqui, Región de Coquimbo, Chile, Depeartamento de Geología, Universidad de Chile, 2013.
Molina, P. G., Parada, M. A., Gutiérrez, F. J., Ma, C., Li, J., Yuanyuan, L., Reich, M., and Aravena, Á.: Protracted late magmatic stage of the Caleu pluton (central Chile) as a consequence of heat redistribution by diking: Insights from zircon data and thermal modeling, Lithos, 227, 255-268, doi:10.1016/j.lithos.2015.04.008, 2015.
Mooney, H. A., Gulmon, S. L., Ehleringer, J., and Rundel, P. W.: Atmospheric water uptake by an Atacama Desert shrub, Science, 209, 693-694, 1980.
Moscoso, R., Nasi, C., and Salinas, P.: Hoja Vallenar y parte norte de La Serena: regiones de Atacama y Coquimbo: carta geológica de Chile 1: 250.000, Servicio Nacional de Geología y Minería Chile, 1982.
Moulton, K. L., West, J., and Berner, R. A.: Solute flux and mineral mass balance approaches to the quantification of plant effects on silicate weathering, Am. J. Sci., 300, 539-570, doi:10.2475/ajs.300.7.539, 2000.
Nier, A. O.: The Isotopic Constitution of Strontium, Barium, Bismuth, Thallium and Mercury, Physical Review, 54, 275-278, doi:10.1103/PhysRev.54.275, 1938.
Niklas, K. J., and Enquist, B. J.: Canonical rules for plant organ biomass partitioning and annual allocation., Am. J. Bot., 89, 812-819, 2002.
Oelkers, E. H., Benning, L. G., Lutz, S., Mavromatis, V., Pearce, C. R., and Plümper, O.: The efficient long-term inhibition of forsterite dissolution by common soil bacteria and fungi at Earth surface conditions, Geochim. Cosmochim. Acta, 168, 222-235, doi:10.1016/j.gca.2015.06.004, 2015.
Oelmann, Y., Richter, A. K., Roscher, C., Rosenkranz, S., Temperton, V. M., Weisser, W. W., and Wilcke, W.: Does plant diversity influence phosphorus cycling in experimental grasslands?, Geoderma, 167-168, 178-187, doi:10.1016/j.geoderma.2011.09.012, 2011.
Oeser, R. A., Stroncik, N., Moskwa, L.-M., Bernhard, N., Schaller, M., Canessa, R., van den Brink, L., Köster, M., Brucker, E., Stock, S., Fuentes, J. P., Godoy, R., Matus, F. J., Oses Pedraza, R., Osses McIntyre, P., Paulino, L., Seguel, O., Bader, M. Y., Boy, J., Dippold, M. A., Ehlers, T. A., Kühn, P., Kuzyakov, Y., Leinweber, P., Scholten, T., Spielvogel, S., Spohn, M., Übernickel, K., Tielbörger, K., Wagner, D., and von Blanckenburg, F.: Chemistry and Microbiology of the Critical Zone along a steep climate and vegetation gradient in the Chilean Coastal Cordillera., Catena, 170, 183-203, doi:10.1016/j.catena.2018.06.002, 2018.
Oeser, R. A., and von Blanckenburg, F.: Strontium isotopes trace biological activity in the Critical Zone along a climate and vegetation gradient, Chem. Geol., 2020a.
Oeser, R. A., and von Blanckenburg, F.: Dataset for evaluation element fluxes released by weathering and taken up by plants along the EarthShape climate and vegetation gradient, GFZ Data Services, doi:10.5880/GFZ.3.3.2020.003, 2020b.
OriginPro, OriginLab Corporation, Northampton, MA, USA, Version 2020.
Pagani, M., Caldeira, K., Berner, R., and Beerling, D. J.: The role of terrestrial plants in limiting atmospheric CO(2) decline over the past 24 million years, Nature, 460, 85-88, doi:10.1038/nature08133, 2009.
Parada, M. A., and Larrondo, P.: Thermochronology of the Lower Cretaceous Caleu Pluton in the coastal range of central Chile: tectonostratigraphic implications, Abstracts, 4th International Symposium of Andean Geodynamics, Göttingen, 1999, 563-566,
Parada, M. A., Larrondo, P., Guiresse, C., and Roperch, P.: Magmatic Gradients in the Cretaceous Caleu Pluton (Central Chile): Injections of Pulses from a Stratified Magma Reservoir, Gondwana Research, 5, 307-324, doi:10.1016/s1342-937x(05)70725-5, 2002.
Parada, M. A., López-Escobar, L., Oliveros, V., Fuentes, F., Morata, D., Calderón, M., Aguirre, L., Féraud, G., Espinoza, F., Moreno, H., Figueroa, O., Muñoz Bravo, J., Vásquez, R. T., and Stern, C. R.: Andean magmatism, in: The Geology of Chile, edited by: Moreno, T., and Gibbons, W., The Geological Society of London, 115-146, doi:10.1144/GOCH.4, 2007.
Pearce, C. R., Parkinson, I. J., Gaillardet, J., Chetelat, B., and Burton, K. W.: Characterising the stable (δ 88/86 Sr) and radiogenic (87 Sr/ 86 Sr) isotopic composition of strontium in rainwater, Chem. Geol., 409, 54-60, doi:10.1016/j.chemgeo.2015.05.010, 2015.
Perez-Fodich, A., and Derry, L. A.: Organic acids and high soil CO2 drive intense chemical weathering of Hawaiian basalts: Insights from reactive transport models, Geochim. Cosmochim. Acta, 249, 173-198, doi:10.1016/j.gca.2019.01.027, 2019.
Porada, P., Lenton, T. M., Pohl, A., Weber, B., Mander, L., Donnadieu, Y., Beer, C., Poschl, U., and Kleidon, A.: High potential for weathering and climate effects of non-vascular vegetation in the Late Ordovician, Nat Commun, 7, 12113, doi:10.1038/ncomms12113, 2016.
Porder, S., Vitousek, P. M., Chadwick, O. A., Chamberlain, C. P., and Hilley, G. E.: Uplift, Erosion, and Phosphorus Limitation in Terrestrial Ecosystems, Ecosystems, 10, 159-171, doi:10.1007/s10021-006-9011-x, 2007.
Porder, S., and Chadwick, O. A.: Climate and soil-age constraints on nutrient uplift and retention by plants, Ecology, 90, 623-636, doi:10.1890/07-1739.1, 2009.

hat gelöscht: Dataset for evaluation element fluxes released by weathering and taken up by plants

hat gelöscht: the EarthShape

hat gelöscht: GFZ Data Services, doi:10.5880/GFZ.3.3.2020.003,2020…

Porder, S.: How Plants Enhance Weathering and How Weathering is Important to Plants, Elements, 15, 241-246, doi:10.2138/gselements.15.4.241, 2019.
Powers, J. S., Becklund, K. K., Gei, M. G., Iyengar, S. B., Meyer, R., O'Connell, C. S., Schilling, E. M., Smith, C. M., Waring, B. G., and Werden, L. K.: Nutrient addition effects on tropical dry forests: a mini-review from microbial to ecosystem scales, Frontiers in Earth Science, 3, doi:10.3389/feart.2015.00034, 2015.
Quirk, J., Andrews, M. Y., Leake, J. R., Banwart, S. A., and Beerling, D. J.: Ectomycorrhizal fungi and past high CO2 atmospheres enhance mineral weathering through increased below-ground carbon-energy fluxes., Biol. Lett., 10, doi:10.1098/rsbl.2014.0375, 2014.
Rempe, D. M., and Dietrich, W. E.: Direct observations of rock moisture, a hidden component of the hydrologic cycle, Proceedings of the National Academy of Sciences, doi:10.1073/pnas.1800141115, 2018.
Riebe, C. S., Kirchner, J. W., Granger, D. E., and Finkel, R. C.: Strong tectonic and weak climatic control of long-term chemical weathering rates, Geology, 29, 511-514, doi:10.1130/0091-7613, 2001.
Riebe, C. S., and Granger, D. E.: Quantifying effects of deep and near-surface chemical erosion on cosmogenic nuclides in soils, saprolite, and sediment, Earth Surface Processes and Landforms, 38, 523-533, doi:10.1002/esp.3339, 2013.
Rundel, P. W., Ehleringer, J., Mooney, H. A., and Gulmon, S. L.: Patterns of drought response in leaf-succulent shrubs of the coastal Atacama Desert in Northern Chile, Oecologia, 46, 196-200, doi:10.1007/BF00540126, 1980.
Schaller, J., Turner, B. L., Weissflog, A., Pino, D., Bielnicka, A. W., and Engelbrecht, B. M. J.: Silicon in tropical forests: large variation across soils and leaves suggests ecological significance, Biogeochemistry, 140, 161-174, doi:10.1007/s10533-018-0483-5, 2018a.
Schaller, M., Ehlers, T. A., Lang, K. A. H., Schmid, M., and Fuentes-Espoz, J. P.: Addressing the contribution of climate and vegetation cover on hillslope denudation, Chilean Coastal Cordillera (26°–38°S), Earth. Planet. Sci. Lett., 489, 111-122, doi:10.1016/j.epsl.2018.02.026, 2018b.
Schuessler, J. A., Kämpf, H., Koch, U., and Alawi, M.: Earthquake impact on iron isotope signatures recorded in mineral spring water, Journal of Geophysical Research: Solid Earth, 121, 1-21, doi:10.1002/2016JB013408, 2016.
Schuessler, J. A., von Blanckenburg, F., Bouchez, J., Uhlig, D., and Hewawasam, T.: Nutrient cycling in a tropical montane rainforest under a supply-limited weathering regime traced by elemental mass balances and Mg stable isotopes, Chem. Geol., 497, 74-87, doi:10.1016/j.chemgeo.2018.08.024, 2018.
The Geobiology of Weathering: a 13th Hypothesis: https://arxiv.org/pdf/1509.04234.pdf, 2015.
Smeck, N. E., Runge, E., and Mackintosh, E.: Dynamics and genetic modeling of soil systems., in: Pedogenesis and soil taxonomy, edited by: Wilding, L. P., Elsevier, 51 - 81, 1983.
Smits, M. M., Bonneville, S., Benning, L. G., Banwart, S. A., and Leake, J. R.: Plant-driven weathering of apatite - the role of an ectomycorrhizal fungus., Geobiology, 10, 445-456, 2012.
Sohrt, J., Uhlig, D., Kaiser, K., von Blanckenburg, F., Siemens, J., Seeger, S., Frick, D. A., Krüger, J., Lang, F., and Weiler, M.: Phosphorus Fluxes in a Temperate Forested Watershed: Canopy Leaching, Runoff Sources, and In-Stream Transformation, Frontiers in Forests and Global Change, 2, doi:10.3389/ffgc.2019.00085, 2019.
Spohn, M., and Sierra, C. A.: How long do elements cycle in terrestrial ecosystems?, Biogeochemistry, 139, 69-83, doi:10.1007/s10533-018-0452-z, 2018.
Sprenger, M., Stumpp, C., Weiler, M., Aeschbach, W., Allen, S. T., Benettin, P., Dubbert, M., Hartmann, A., Hrachowitz, M., Kirchner, J. W., McDonnell, J. J., Orlowski, N., Penna, D., Pfahl, S., Rinderer, M., Rodriguez, N., Schmidt, M., and Werner, C.: The Demographics of Water: A Review of Water Ages in the Critical Zone, Rev. Geophys., 57, 800-834, doi:10.1029/2018rg000633, 2019.
Stock, S. C., Köster, M., Dippold, M. A., Nájera, F., Matus, F., Merino, C., Boy, J., Spielvogel, S., Gorbushina, A., and Kuzyakov, Y.: Environmental drivers and stoichiometric constraints on enzyme activities in soils from rhizosphere to continental scale, Geoderma, 337, 973-982, doi:10.1016/j.geoderma.2018.10.030, 2019.
Tessier, A., Campbell, P. G. C., and Bisson, M.: Sequential Extraction Procedure for the Speciation of Particulate Trace Metals, Anal. Chem., 51, 844-851, 1979.
Tielbörger, K., Bilton, M. C., Metz, J., Kigel, J., Holzapfel, C., Lebrija-Trejos, E., Konsens, I., Parag, H. A., and Sternberg, M.: Middle-Eastern plant communities tolerate 9 years of drought in a multi-site climate manipulation experiment, Nature Communications, 5, doi:10.1038/ncomms6102, 2014.
Tiessen, H., and Moir, J. O.: Characterization of available P by sequential extraction, in: Soil sampling and methods of analysis, Lewis Publishers Boca Raton, FL, USA, 5-229, 1993.
Tipping, E., Woof, C., Rigg, E., Harrison, A., Ineson, P., Taylor, K., Benham, D., Poskitt, J., Rowland, A., and Bol, R.: Climatic influences on the leaching of dissolved organic matter from upland UK moorland soils, investigated by a field manipulation experiment, Environ. Int., 25, 83-95, doi:10.1016/s0160-4120(98)00098-1, 1999.
Uhlig, D., Schuessler, J. A., Bouchez, J. L., Dixon, J., and von Blanckenburg, F.: Quantifying nutrient uptake as driver of rock weathering in forest ecosystems by magnesium stable isotopes, Biogeosci. Disc., 1-28, doi:10.5194/bg-2016-521, 2017.
Uhlig, D., and von Blanckenburg, F.: How Slow Rock Weathering Balances Nutrient Loss During Fast Forest Floor Turnover in Montane, Temperate Forest Ecosystems, Frontiers in Earth Science, 7, doi:10.3389/feart.2019.00159, 2019.

hat gelöscht: Poszwa, A., Dambrine, E., Ferry, B., Pollier, B., and Loubet, M.: Do deep tree roots provide nutrients to the tropical rainforest, Biogeochemistry, 60, 97-118, doi:10.1023/A:1016548113624, 2002.¶

Uhlig, D., Amelung, W., and von Blanckenburg, F.: Mineral nutrients sourced in deep regolith sustain long-term nutrition of mountainous temperate forest ecosystems, Global Biogeochem. Cycles, doi:10.1029/2019GB006513, 2020.
van der Heijden, M. G. A., Klironomos, J. N., Ursic, M., Moutoglis, P., Streitwolf-Engel, R., Boller, T., Wiemken, A., and Sanders, I. R.: Mycorrhizal fungal diversity determines plant biodiversity, ecosystem variability and productivity, Nature, 396, 69-72, doi:10.1038/23932, 1998.
van Dongen, R., Scherler, D., Wittmann, H., and von Blanckenburg, F.: Cosmogenic 10Be in river sediment: where grain size matters and why, Earth Surface Dynamics, 7, 393-410, doi:10.5194/esurf-7-393-2019, 2019.
van Schöll, L., Kuyper, T. W., Smits, M. M., Landeweert, R., Hoffland, E., and Breemen, N. v.: Rock-eating mycorrhizas: their role in plant nutrition and biogeochemical cycles, Plant Soil, 303, 35-47, doi:10.1007/s11104-007-9513-0, 2007.
Vitousek, P., Chadwick, O., Matson, P., Allison, S., Derry, L., Kettley, L., Luers, A., Mecking, E., Monastra, V., and Porder, S.: Erosion and the Rejuvenation of Weathering-derived Nutrient Supply in an Old Tropical Landscape, Ecosystems, 6, 762-772, doi:10.1007/s10021-003-0199-8, 2003.
Vitousek, P. M., and Reiners, W. A.: Ecosystem Succession and Nutrient Retention: A Hypothesis, Bioscience, 25, 376-381, doi:10.2307/1297148, 1975.
Vitousek, P. M., and Farrington, H.: Nutrient limitation and soil development: Experimental test of a biogeochemical theory, Biogeochemistry, 37, 63-75, doi:10.1023/a:1005757218475, 1997.
Vitousek, P. M., Hedin, L. O., Matson, P. A., Fownes, J. H., and Neff, J.: Within-System Element Cycles, Input-Output Budgets, and Nutrient Limitation, in: Successes, Limitations, and Frontiers in Ecosystem Science, Springer, New York, 432-451, doi:10.1007/978-1-4612-1724-4_18, 1998.
Vitousek, P. M.: Nutrient Cycling and Limitation: Hawai'i as a Model System, PRINCETON ENVIRONMENT AL INSTITUTE SERIES, 2004.
Vitousek, P. M., Porder, S., Houlton, B. Z., and Chadwick, O. A.: Terrestrial phosphorus limitation: mechanisms, implications, and nitrogen–phosphorus interactions, Ecol. Appl., 20, 5-15, doi:10.1890/08-0127.1, 2010.
Vitousek, P. M., and Chadwick, O. A.: Pedogenic Thresholds and Soil Process Domains in Basalt-Derived Soils, Ecosystems, 16, 1379-1395, doi:10.1007/s10021-013-9690-z, 2013.
von Blanckenburg, F., Wittmann, H., and Schuessler, J. A.: HELGES: Helmholtz Laboratory for the Geochemistry of the Earth Surface, Journal of large-scale research facilities JLSRF, 2, doi:10.17815/jlsrf-2-141, 2016.
Werner, C., Schmid, M., Ehlers, T. A., Fuentes-Espoz, J. P., Steinkamp, J., Forrest, M., Liakka, J., Maldonado, A., and Hickler, T.: Effect of changing vegetation and precipitation on denudation – Part 1: Predicted vegetation composition and cover over the last 21 thousand years along the Coastal Cordillera of Chile, Earth Surface Dynamics, 6, 829-858, doi:10.5194/esurf-6-829-2018, 2018.
White, A. F., Blum, A. E., Schulz, M. S., Vivit, D. V., Stonestrom, D. A., Larsen, M., Murphy, S. F., and Eberl, D.: Chemical Weathering in a Tropical Watershed, Luquillo Mountains, Puerto Rico: I. Long-Term Versus Short-Term Weathering Fluxes, Geochim. Cosmochim. Acta, 62, 209-226, doi:10.1016/s0016-7037(97)00335-9, 1998.
White, A. F., and Brantley, S. L.: The effect of time on the weathering of silicate minerals: why do weathering rates differ in the laboratory and field?, Chem. Geol., 202, 479-506, doi:10.1016/j.chemgeo.2003.03.001, 2003.
Wilcke, W., Yasin, S., Abramowski, U., Valarezo, C., and Zech, W.: Nutrient storage and turnover in organic layers under tropical montane rain forest in Ecuador, Eur. J. Soil Sci., 53, 15-27, 2002.
Wilcke, W., Velescu, A., Leimer, S., Bigalke, M., Boy, J., and Valarezo, C.: Biological versus geochemical control and environmental change drivers of the base metal budgets of a tropical montane forest in Ecuador during 15 years, Biogeochemistry, 136, 167-189, doi:10.1007/s10533-017-0386-x, 2017.
Winnick, M. J., and Maher, K.: Relationships between CO2, thermodynamic limits on silicate weathering, and the strength of the silicate weathering feedback, Earth. Planet. Sci. Lett., 485, 111-120, doi:10.1016/j.epsl.2018.01.005, 2018.

15 Figures

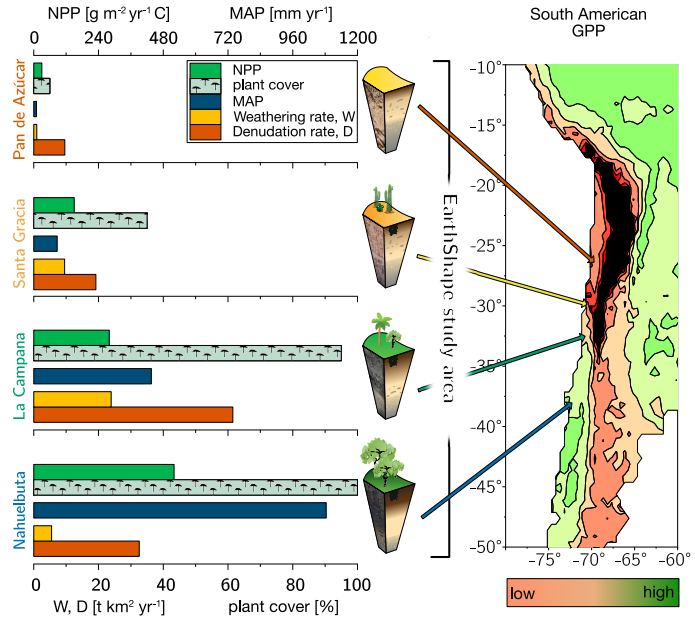

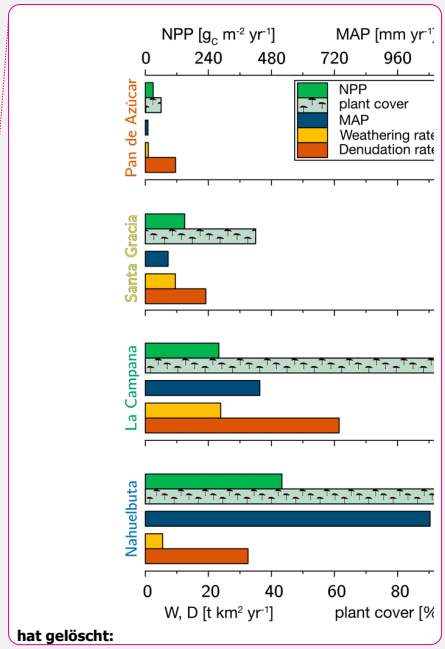

hat gelöscht:

Figure 1 The climate and vegetation gradient of the four EarthShape study sites (from arid to humid: Pan de Azúcar, Santa Gracia, La Campana, and Nahuelbuta). Left: Net primary productivity (NPP), plant cover, annual precipitation (MAP). Denudation rate (D) and weathering rate (W) were determined with cosmogenic ^{10}Be. Right: Position of the four study sites in South America and their respective gross primary productivity (GPP) derived from the FLUXNET data base (Jung et al., 2011). Black colour refers to very low GPP in the Atacama Desert. The uncertainties are not shown for clarity. They are provided in Table 1.

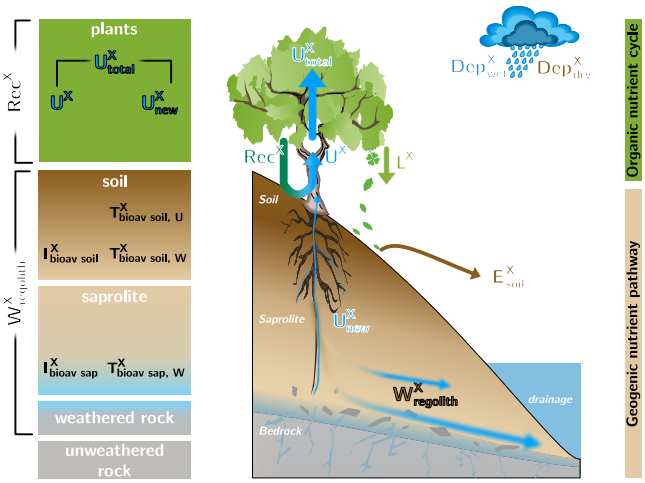

Figure 2 Conceptual framework of an ecosystem comprising the "geogenic nutrient pathway" and the "organic nutrient cycle" (modified after Uhlig and von Blanckenburg, 2019). Whereas the former is mainly set by mineral nutrient release by weathering ($W^X_{regolith}$) and to a minor extent by atmospheric wet- (Dep^X_{wet}) and dry deposition (Dep^X_{dry}), the organic nutrient cycle is mainly affected by nutrient re-utilization (i.e. recycling; Rec^X) from organic matter. Left: The different compartments (i.e. rock, saprolite, soil, and plants) are shown as boxes. They include the metrics used to quantify their properties such as the inventory I^X_{bulk} and turnover time $T^X_{i,j}$ of element X in compartment j. Right: The compartments are linked by fluxes (arrows) with the thickness of them denoting their relative proportions. E^X_{soil} denotes to erosion of soil.

hat gelöscht: to

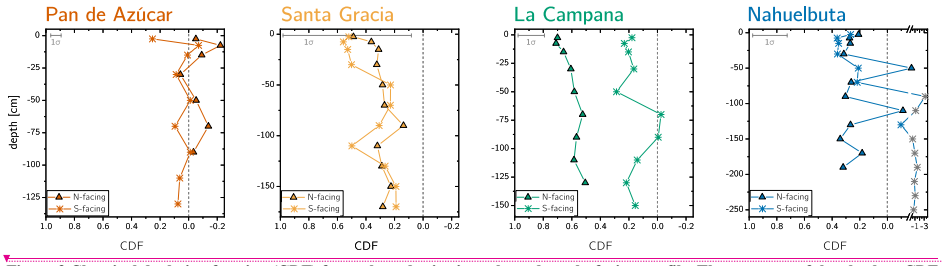

Figure 3 Chemical depletion fraction (CDF) for each study sites' north- and south- facing profile. The accuracy of the absolute CDF values is limited by the variability in the bedrocks' Zr concentration in the respective study sites and are indicated as grey 1 σ bar (Data Table S1). The grey symbols correspond mainly to saprolite samples in the south-facing regolith profile in Nahuelbuta and are excluded from further consideration. Note that in Nahuelbuta a different scaling compared to the other study sites applies after the axis break.

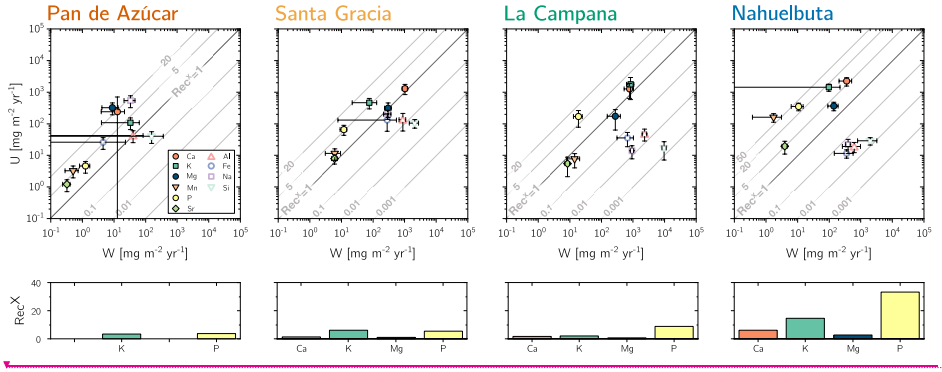

Figure 4 Chemical weathering flux ($W^X_{regolith}$) and plant nutrient-uptake fluxes (U^X_{total}) for Pan de Azúcar, Santa Gracia, La Campana, and Nahuelbuta (from left to right) for mineral nutrients. Grey contour lines emphasize the nutrient recycling factor (Rec^X), which is the ratio of U^X_{total} to $W^X_{regolith}$. Uncertainty bars show 1SD. Differences in nutrient recycling factors for Ca, K, Mg, and P among the four study sites are highlighted in the lower panels. Note that here we use the Rec^X calculated for $W^X_{regolith}$ from silicate weathering only. In Table 5 and Fig. A4 we also show Rec^X including atmospheric inputs. Because Pan de Azúcar Ca and Mg inputs are exclusively atmospheric their Rec^X are overestimated and thus not plotted on the lower left panel.

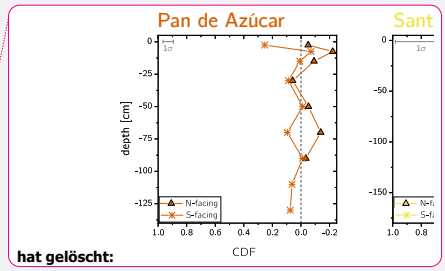

hat gelöscht:

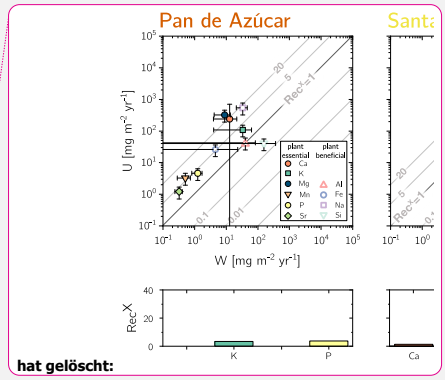

hat gelöscht:

hat gelöscht: plant-essential and plant-beneficial elements.

hat gelöscht: the plant essential elements

hat gelöscht: 7

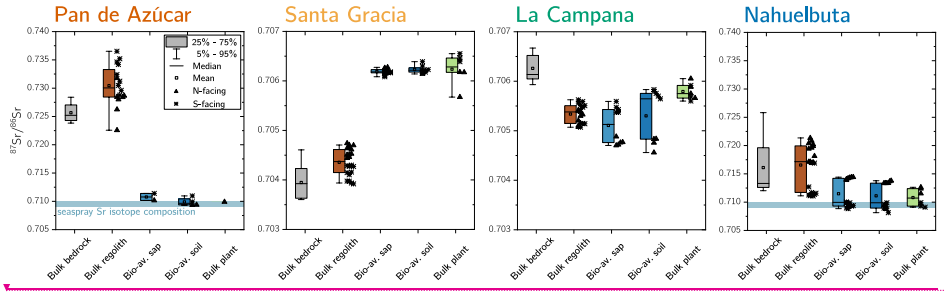

Figure 5 Average $^{87}Sr/^{86}Sr$ isotope composition of bedrock, bulk regolith, and the bio-available fraction in saprolite, soil, and plants in Pan de Azúcar, Santa Gracia, La Campana, and Nahuelbuta. The $^{87}Sr/^{86}Sr$ isotope ratios of bulk plant (green) are weighted according to the single species' organs relative growth rate (see Table 4 for weighting parameters). Whiskers span 90% of the respective data set. On the boxes' right-hand site, the differences between north- and south-facing regolith profiles are depicted. Note that bulk regolith samples in Nahuelbuta with anomalously low Zr concentrations have been excluded from this analysis as they are suspected to comprise a different parent rock. Y-axis covers broader range in Pan de Azúcar and Nahuelbuta than in Santa Gracia and La Campana.

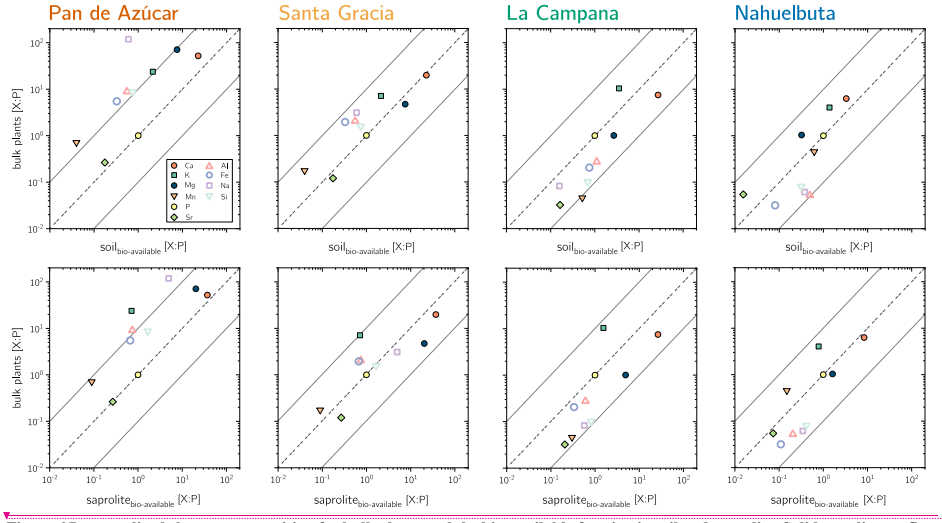

Figure 6 P-normalized element composition for bulk plants and the bio-available fraction in soil and saprolite. Solid grey lines reflect the 10 x P and 0.1 x P concentration, respectively. Note that with increasing recycling from Santa Gracia to Nahuelbuta, the bio-available fractions' X:P successively approaches X:P in vegetation.

hat gelöscht:

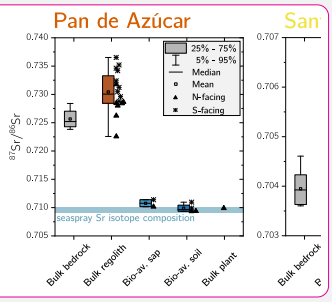

hat gelöscht: Table 5

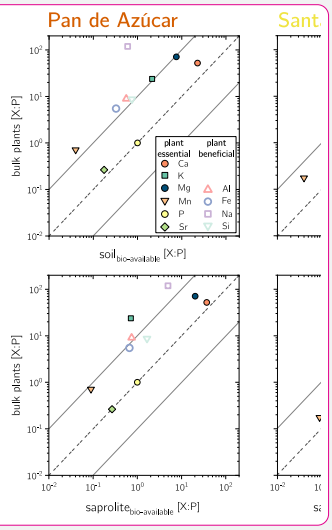

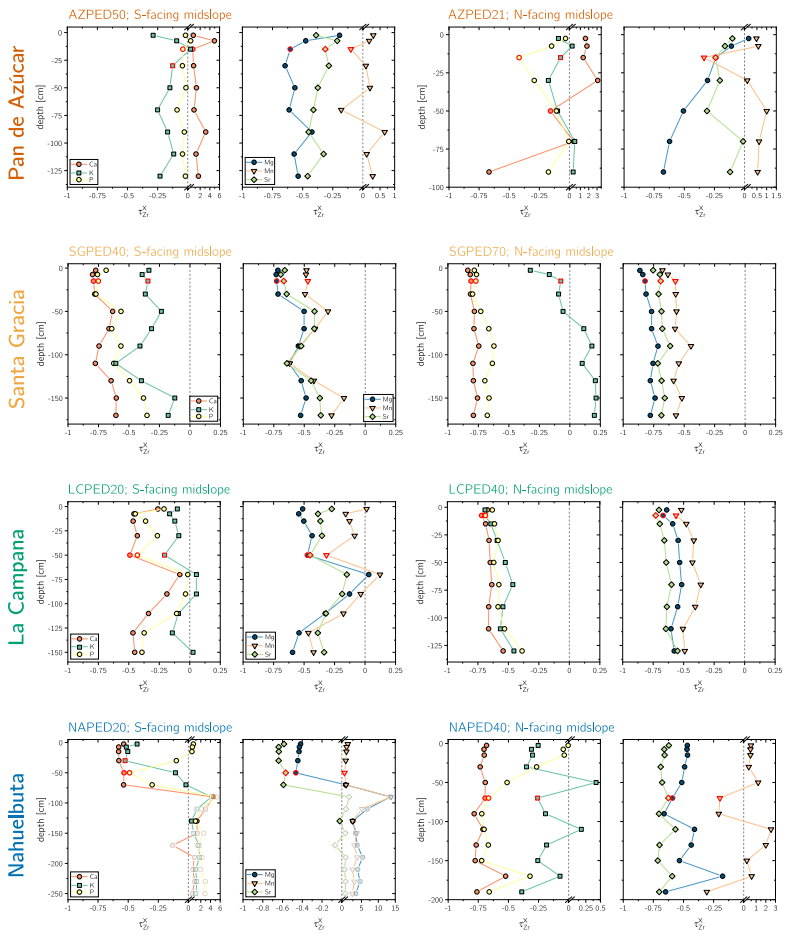

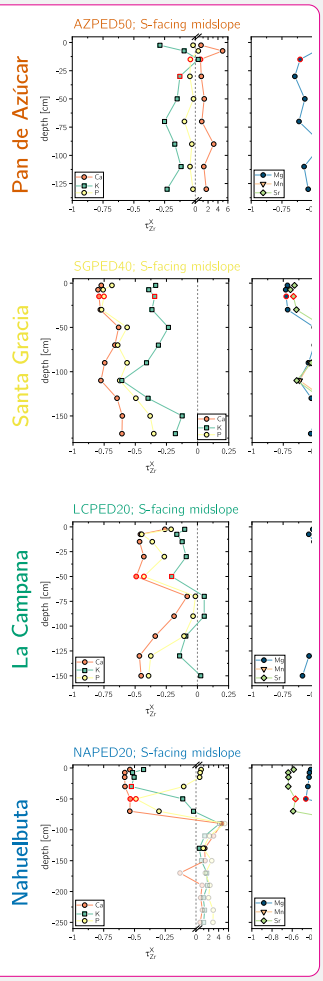

Figure A1. Depth distribution of the elemental loss and gain fractions (i.e. elemental mass transfer coefficient, τ). The vertical dashed line indicates $\tau^{X}_{Zr} = 0$ and represents unweathered parent bedrock. τ-values corresponding to the shallowest mineral soil samples are highlighted with a red rim. Grey symbols in Nahuelbuta are discarded due to the samples' anomalous low Zr concentration. Note that these τ-values differ from those reported in Oeser et al., 2018, because in this work they have been calculated relative to the initial bedrocks' chemical composition.

hat gelöscht:

hat gelöscht: deviate

hat gelöscht: such that

hat gelöscht: initial

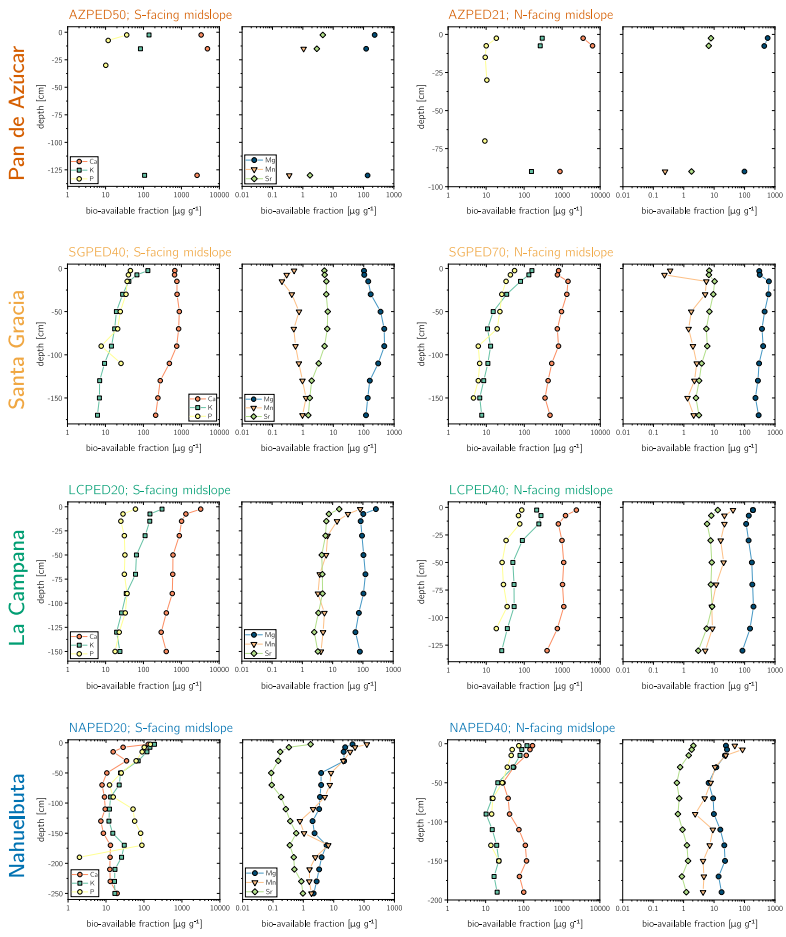

Figure A2. Depth distribution of the concentration of sequentially extracted bio-available fraction of mineral nutrients including Sr, comprised of the water soluble (18 MΩ Deionized H_2O) and the exchangeable (1 M NH_4OAc) fraction. P-accessibility in the bio-available fraction has been determined by Brucker and Spohn (2019) using a modified Hedley sequential P fractionation method. Note that in Pan de Azúcar the acquisition of the bio-available fraction was only possible on three samples per site. Data gaps do occur if both extractions of one sample were below limit of detection.

hat gelöscht:

hat verschoben (Einfügung) [1]

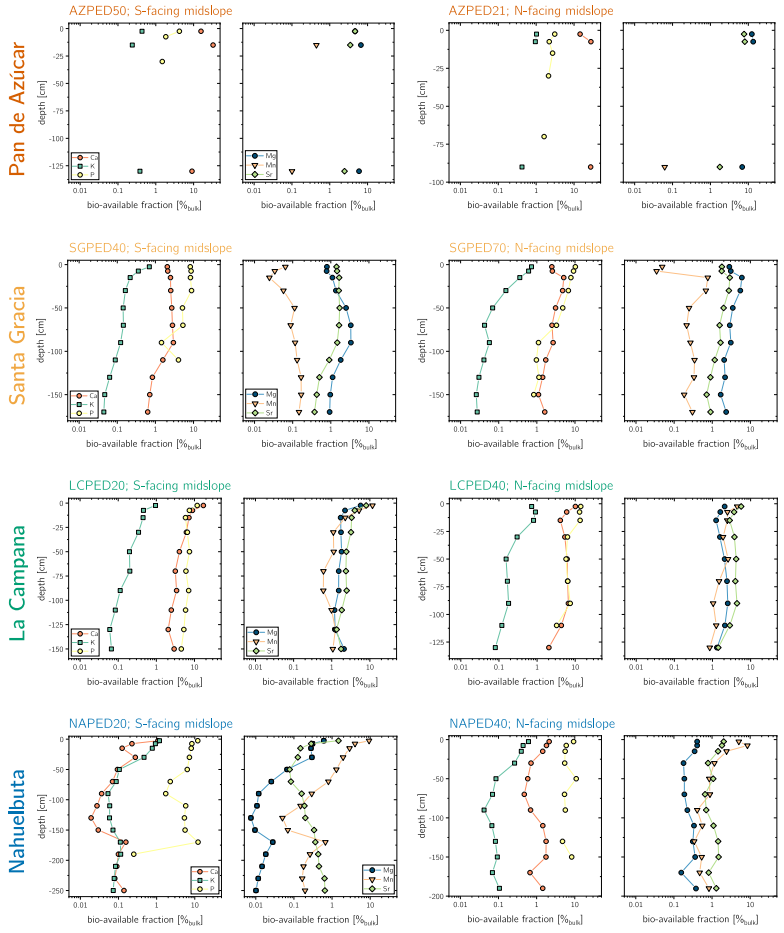

hat gelöscht: plant-essential elements including Sr, comprised of the water soluble (18 MΩ Milli-Q H_2O) and the exchangeable (1 M NH_4OAc) fraction.

Figure A3. Depth distribution of the sequentially extracted bio-available fraction of mineral nutrients including Sr relative to their respective amount contained in bulk regolith, comprised of the water soluble (18 MΩ Deionized H_2O) and the exchangeable (1 M NH_4OAc) fraction. P-accessibility in the bio-available fraction has been determined by Brucker and Spohn (2019) using a modified Hedley sequential P fractionation method. Note that in Pan de Azúcar the acquisition of the bio-available fraction was only possible on three samples per site. Data gaps do occur if both extractions of one sample were below limit of detection.

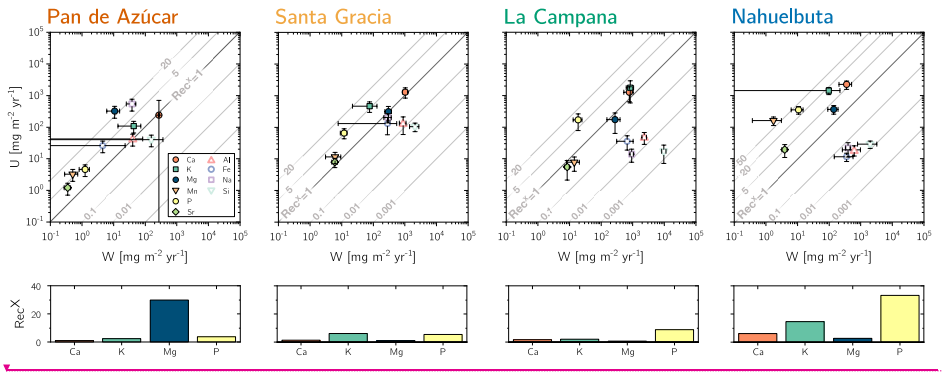

Figure A4. Chemical weathering flux ($W^X_{regolith}$) and ecosystem nutrient-uptake fluxes (U^X_{total}) for Pan de Azúcar, Santa Gracia, La Campana, and Nahuelbuta (from left to right). Weathering-release fluxes for Ca, K, Mg, Na, and Sr in Pan de Azúcar have been complemented by atmospheric depositional fluxes such that the total amount of available nutrients increase by 95, 22, 18, 12, and 10%, respectively. Grey contour lines emphasize the nutrient recycling factor (Rec^X), which is the ratio of U^X_{total} to $W^X_{regolith}$. Uncertainty bars show 1SD. Differences in nutrient recycling factors for Ca, K, Mg, and P among the four study sites are highlighted in the lower panels.

16 Tables

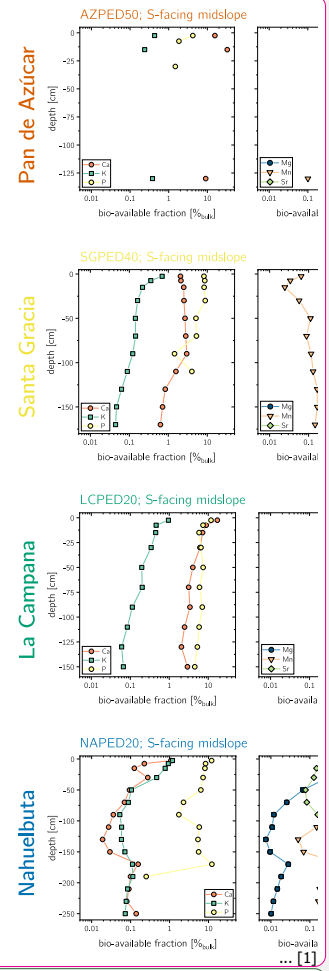

hat gelöscht: ... [1]

hat nach oben verschoben [1]: **P-accessibility in the bio-available fraction has been determined by Brucker and Spohn (2019) using a modified Hedley sequential P fractionation method. Note that in Pan de Azúcar the acquisition of the bio-available fraction was only possible on three samples per site. Data gaps do occur if both extractions of one sample were below limit of detection.** ¶

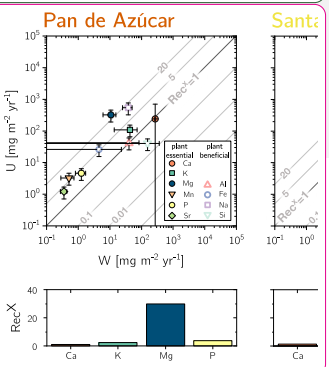

hat gelöscht:

hat gelöscht: **) for plant-essential (closed symbols) and plant-beneficial elements (open symbols)..... Weathering-release fluxes**

Table 1 Characteristics of the four EarthShape study sites and soil profile names in Pan de Azúcar, Santa Gracia, La Campana, and Nahuelbuta.

		Pan de Azúcar		Santa Gracia		La Campana		Nahuelbua		
		AZPED21	*AZPED50*	*SGPED70*	*SGPED40*	*LCPED40*	*LCPED20*	*NAPED40*	*NAPED20*	*Reference*
Latitude		26.1093 S	26.1102 S	29.7612 S	29.7574 S	32.9573 S	32.9559 S	37.8090 S	37.8077 S	†
Longitude		70.5491 W	70.5493 W	71.1656 W	71.1664 W	71.0643 W	71.0635 W	73.0138 W	73.0135 W	†
Altitude	[m a.s.l.]	343	330	690	682	734	730	1219	1239	*
Slope	[°]	25	40	15	25	12	23	13	15	‡
Aspect		N-facing	S-facing	N-facing	S-facing	N-facing	S-facing	N-facing	S-facing	†, ‡
Mean annual temperature (MAT)	[°C]	18.1		16.1		14.9		14.1		§
Mean annual precipitation (MAP)	[mm yr^{-1}]	10		87		436		1084		§
Lithology		granite		diorite		granodiorite		granodiorite		†
Mineralogy*	[Vol%]	Quartz xxx, Plagioclase x, K-feldspar xxx, Pyroxene -, Biotite x, Amphibole -		Quartz x, Plagioclase xx, K-feldspar xxx, Pyroxene xx, Biotite -, Amphibole x		Quartz xx, Plagioclase x, K-feldspar xxx, Pyroxene -, Biotite x, Amphibole -		Quartz xx, Plagioclase xx, K-feldspar xxx, Pyroxene x, Biotite x, Amphibole -		†
Soil type		Regosol	Regosol	Cambisol	Leptosol	Cambisol	Cambisol	umbric Podzol	orthodystric Umbrisol	‡
Soil thickness	[cm]	20	20	35	45	35	60	60	70	†
Soil pH**		8.1 ± 0.1	8.1 ± 0.1	6.0 ± 0.3	6.1 ± 0.3	5.2 ± 0.3	5.0 ± 0.3	4.7 ± 0.1	4.3 ± 0.2	‡
Cation exchange capacity (CEC)**	[µmolc g^{-1}]	-	-	108.5 ± 50.2	64.6 ± 23.4	86.4 ± 43.1	72.7 ± 62.1	21.0 ± 15.4	38.2 ± 24.7	‡
Catchment-wide denudation rate (D)	[t km^{-2} yr^{-1}]	7.7 ± 0.7		9.2 ± 0.8		200 ± 22		27.2 ± 2.4		‖
Soil denudation rate (D_{soil})	[t km^{-2} yr^{-1}]	8.2 ± 0.5	11.0 ± 0.7	15.9 ± 0.9	22.4 ± 1.5	69.2 ± 4.6	53.7 ± 3.4	17.7 ± 1.1	47.5 ± 3.0	†, #
Soil weathering rate (W)	[t km^{-2} yr^{-1}]	-1.0 ± 0.1***	0.9 ± 0.2	7.2 ± 4.7	11.9 ± 7.6	45.9 ± 8.0	20.0 ± 3.1	3.5 ± 0.9	7.5 ± 3.1	†, #
Soil erosion rate (E)	[t km^{-2} yr^{-1}]	9.1 ± 0.5	10.1 ± 0.7	8.7 ± 4.8	10.5 ± 7.7	23.4 ± 9.2	33.8 ± 4.6	14.2 ± 1.4	40.0 ± 4.3	†, #
Chemical depletion fraction (CDF)		-0.1 ± 0.0	0.1 ± 0.0	0.5 ± 0.3	0.5 ± 0.3	0.7 ± 0.1	0.4 ± 0.1	0.2 ± 0.1	0.2 ± 0.1	†, #
Vegetation cover	[%]	<5		30 – 40		95		100		‡
Vegetation types		*Cristaria integerrima*, *Nolana mollis*, *Perityle* sp., *Stipa plumosa*, *Tetragonia maritima*		*Adesmia* sp., *Cordia decandra*, *Cumulopuntia sphaerica*, *Eulychnia acida*, *Proustia cuneifolia*, *Senna cumingii*		*Aristeguietia salvia*, *Colliguaja odorifera*, *Cryptocarya alba*, *Jubaea chilensis*, *Lithraea caustica*		*Araucaria araucana*, *Chusquea culeou*, *Nothofagus antarctica*		‡
Net primary production (NPP)	[g_C m^{-2} yr^{-1}]	30 ± 10		150 ± 40		280 ± 50		520 ± 130		¶

* Estimation of mineral abundances based on thin section microscopy: -: absence, x: presence (<10 Vol%), xx: abundant (10-35 Vol%), xxx: very abundant (>35 Vol%)

** Denoting to regolith-profile averages

*** N-facing slope in Pan de Azúcar yield negative CDF and hence weathering rates due to the input of seaspray

† Oeser et al. (2018); ‡ Bernhard et al. (2018); § Ministerio de Obras Públicas (2017); ‖ van Dongen et al. (2019); # Schaller et al. (2018); ¶ Werner et al. (2018)

Table 2 Glossary of metrics for the parameterization of the geogenic nutrient pathway and organic nutrient cycle in terrestrial ecosystems after Uhlig and von Blanckenburg (2019).

Total mass fluxes (in e.g. t km^{-2} yr^{-1})		
Eq. (1)	$D = E + W$	denudation rate; the sum of chemical weathering and physical erosion
	E	physical erosion; physical removal of primary and secondary minerals along with biogenic material
Eq. (2)	$W = D \times CDF$	chemical weathering rate; net-chemical release flux from minerals as some fraction of which is being incorporated into secondary minerals and pedogenic (hydr-)oxides
	GPP	gross primary production; gross carbon input into biomass
	NPP	net primary productivity; net-carbon fixation by biomass
Elemental fluxes (in e.g. mg m^2 yr^{-1})		
Eq. (3)	$W^X_{regolith} = D \times [X]_{parent} \times (-\tau^X_{Xi})$	Chemical weathering flux of element X; release flux of X from minerals minus the flux of incorporation of X into secondary minerals and oxides
Eq. (4)	$U^X_{total} = \frac{NPP \times [X]_{plant}}{[C]_{plant}}$	Total nutrient uptake flux of element X; uptake of X by trees at the ecosystem scale, where $[C]_{plant}$ denotes the carbon concentration in dry mass, typically 50 weight%
	Dep^X_{dry}	Atmospheric dry deposition of element X
	Dep^X_{wet}	Atmospheric wet deposition of element X as rainfall
Elemental mass fractions and flux ratios (dimensionless)		
Eq. (5)	$CDF = 1 - \frac{[X_i]_{parent}}{[X_i]_{weathered}}$	chemical depletion fraction; fractional mass loss by dissolution of elements from the regolith
Eq. (6)	$\tau^X = \frac{[X]_{weathered}}{[X]_{parent}} \times \frac{[X_i]_{parent}}{[X_i]_{weathered}} - 1$	elemental mass transfer coefficient; elemental loss or gain relative to unweathered bedrock
Eq. (7)	$Rec^X = \frac{U^X_{total}}{W^X_{regolith}}$	nutrient recycling factor; number of times, element X is re-utilized from plant litter after its initial release from rock weathering
Elemental inventories (in e.g. g m^{-2} or kg m^{-2})		
Eq. (8)	$I_j = \int_{z=a}^{z=b} [X_j] \times \rho \, dz$	Inventory of element X in compartment j
	$I^X_{bio\text{-}av.\ soil}$	Inventory of element X in the bio-available fraction in soil
	$I^X_{bio\text{-}av.\ sap}$	Inventory of element X in the bio-available fraction in saprolite
	I^X_{bulk}	Inventory of element X in bulk regolith
Elemental turnover times (in e.g. yr)		
Eq. (9)	$T^X_{i,j} = \frac{I^X_i}{j}$	Turnover time of element X in compartment i with respect to input or output flux j; the ratio of total stock of element X in i to input or output flux j
	$T^X_{bio\text{-}av,\ U}$	Turnover time of element X in the forest floor with respect to uptake into trees; mean time a nutrient rest in the forest floor before re-utilization by forest trees
	$T^X_{bio\text{-}av,\ W}$	Turnover time of element X in the bio-available fraction in regolith with respect to adsorption onto clay minerals; mean time over which the inventory of the bio-available fraction is replenished by chemical silicate weathering in the absence of other gains or losses

Table 3 Elemental weathering fluxes ($W^{X}_{regolith}$) and ecosystem nutrient uptake fluxes (U^{X}_{total}) in Pan de Azúcar, Santa Gracia, La Campana, and Nahuelbuta along with the respective study site's average soil denudation rate (D) and net primary productivity (NPP).

Study site	D [t km^{-2} yr^{-1}]	NPP [g$_C$ m^{-2} yr^{-1}]	Al	Ca	Fe	K	Mg	Mn	Na	P	Si	Sr
			[mg m^{-2} yr^{-1}]									
Pan de Azúcar												
$W^{X}_{regolith}$	9.6		40	13*	5	30	9	0.5	33	1.3	160	0.3
SD	*0.6*		*43*	*9*	*18*	*30*	*5*	*0.2*	*13*	*0.4*	*210*	*0.1*
U^{X}_{total}	-	30	40	200	30	110	300	3	500	5	40	1.2
SD	-	*10*	*20*	*500*	*10*	*40*	*100*	*1*	*200*	*2*	*20*	*0.5*
Santa Gracia												
$W^{X}_{regolith}$	19.2		870	1030	280	80	300	6	290	12	2100	6.1
SD	*1.2*		*200*	*200*	*270*	*50*	*70*	*3*	*80*	*3*	*680*	*1.3*
U^{X}_{total}	-	150	140	1300	130	500	300	12	200	70	100	8
SD	-	*40*	*80*	*500*	*70*	*200*	*100*	*5*	*60*	*20*	*30*	*3*
La Campana												
$W^{X}_{regolith}$	61.5		2330	770	670	840	280	14	930	19	9700	8.5
SD	*4.0*		*370*	*250*	*350*	*220*	*120*	*6*	*110*	*6*	*1500*	*1.5*
U^{X}_{total}	-	280	50	1300	40	2000	200	8	14	170	17	6
SD	-	*50*	*20*	*600*	*20*	*1000*	*100*	*4*	*6*	*90*	*10*	*3*
Nahuelbuta												
$W^{X}_{regolith}$	32.6		620	360	360	100	140	1	400	11	2000	4.0
SD	*2.1*		*360*	*150*	*210*	*120*	*50*	*3*	*70*	*4*	*1200*	*0.7*
U^{X}_{total}	-	520	19	2200	12	1400	400	160	22	350	30	19
SD	-	*130*	*7*	*700*	*3*	*400*	*100*	*50*	*11*	*100*	*10*	*9*

* $W^{X}_{regolith}$ only includes information from AZPED21 (N-facing slope regolith profile) as atmospheric deposition of Ca in the S-facing slope led to (theoretically) negative weathering fluxes.

Uncertainties on weathering fluxes are estimated by Monte-Carlo simulations, where the SD of the respective profile's denudation rate, the SD of the bedrocks' element concentration of interest, and 3% relative uncertainty on the element concentration in regolith samples have been used.

Uncertainties on nutrient uptake fluxes are estimated by Monte-Carlo simulations, where the SD of the respective study site's net primary productivity (NPP) and the SD of the chemical composition of the weighted above-ground living ecosystem have been used (Table 4)

hat gelöscht: (Table 5)

660

Table 4 Chemical composition of the above ground living plants. Plant organs have been weighted according to Niklas and Enquist (2002), using the plant organs' relative growth rate (see Appendix A). Relative growth rates and relative abundance of the different plant species can be found in this table's footnotes. The unweighted chemical composition of each plant organ is listed in Data Table S5.

Study site	Al	Ca	Fe	K	Mg	Mn	Na	P	Si	Sr
					[µg g^{-1}]					
Pan de Azúcar[†]										
mean	2700	15200	1700	6900	20700	210	34600	290	2500	80
SD	*300*	*1500*	*200*	*700*	*2100*	*20*	*3500*	*30*	*300*	*10*
Santa Gracia[‡]										
mean	1880	17800	1800	6400	4200	160	2800	900	1400	110
SD	*920*	*4400*	*900*	*1600*	*1700*	*50*	*500*	*220*	*300*	*20*
SE (n=15)	*650*	*2900*	*600*	*1100*	*1000*	*30*	*400*	*140*	*200*	*20*
La Campana[§]										
mean	340	8900	250	12300	1200	50	100	1200	120	40
SD	*120*	*4100*	*110*	*8000*	*700*	*20*	*40*	*600*	*70*	*20*
SE (n=16)	*70*	*2300*	*70*	*5300*	*400*	*20*	*20*	*400*	*40*	*10*
Nahuelbuta[¶]										
mean	70	8500	40	5400	1400	610	80	1300	110	70
SD	*20*	*1400*	*10*	*500*	*250*	*110*	*30*	*200*	*10*	*30*
SE (n=10)	*10*	*1000*	*10*	*300*	*180*	*80*	*20*	*100*	*10*	*20*

Standard deviation and standard error relate to the variability within the data set of each ecosystem. Where natural replicates were not available (i.e. in Pan de Azúcar), 10% relative uncertainty has been assumed.

[†] Pan de Azúcar ecosystem composition: 100% Nolona mollis; 32% and 68% relative leaf and stem growth, respectively, accounting for 5% leaf and 95% stem standing biomass

[‡] Santa Gracia ecosystem composition: 25% each of Asterasia sp., Cordia decandra, Cumulopuntia sphaerica, Proustia cuneifolia; 32% and 68% relative leaf and stem growth assumed for all species, respectively, accounting for 5% leaf and 95% stem standing biomass

[§] La Campana ecosystem composition: 5% each for Aristeguieta salvia and Colliguaja odorifera and 45% each for Cryptocaria alba and Lithraea caustica; 32% and 68% relative leaf and stem growth assumed for all species, respectively, accounting for 5% leaf and 95% stem standing biomass

[¶] Nahuelbuta ecosystem composition: 60% Araucaria araucana, 10% Chusquea culeou, and 30% Nothofagus antarctica; 48% and 52% relative leaf and stem growth assumed for Araucaria araucana, respectively, accounting for 16% leaf and 84% stem standing biomass, 32% and 68% relative leaf and stem growth assumed for Chusquea culeou and Nothofagus antarctica, respectively, accounting for 5% leaf and 95% stem standing biomass.

hat nach unten verschoben [2]: Apart from phosphorus, the accessibility of these elements was determined using a sequential extraction method described by Arunachalam et al. (1996); Tessier et al. (1979); He et al. (1995). P-accessibility in the bio-available fraction has been determined by Brucker and Spohn (2019) using a modified Hedley sequential P fractionation method.

hat gelöscht: Table 4 Inventories of plant-essential and plant-beneficial elements in bulk regolith and the bio-available fraction in soil and saprolite.

hat nach unten verschoben [3]: Study site

hat gelöscht: Supplementary Tables S3 & S4 include depth-dependent concentration of the bio-available fraction (pooled) and the Milli-Q and NH4OAc extractions used for calculation of the inventories (Oeser and von Blanckenburg, 2020).¶

hat gelöscht: 5

hat gelöscht: The unweighted chemical composition of each plant organ is listed in Table S5 (Oeser and von Blanckenburg, 2020).…

Table 5. Nutrient recycling factors in Pan de Azúcar, Santa Gracia, La Campana, and Nahuelbuta. Shown in brackets are the Rec^X prior correction for atmospheric deposition.

	Rec^{Al}	Rec^{Ca}	Rec^{Fe}	Rec^{K}	Rec^{Mg}	Rec^{Mn}	Rec^{Na}	Rec^{P}	Rec^{Si}	Rec^{Sr}
Pan de Azúcar	1.1	1 (19)*	5.8	3 (3)*	30 (36)*	6	15 (16)*	4	0.26	3 (4)*
SD	*0.4*	*2*	*0.6*	*1*	*20*	*6*	*15*	*4*	*0.08*	*5*
Santa Gracia	0.1	1	0.4	6	1	1	1	5	0.04	1
SD	*0.5*	*4*	*0.5*	*3*	*3*	*3*	*1*	*13*	*0.07*	*3*
La Campana	0	2	0.1	2	1	0.5	0	9	0	1
SD	*0.1*	*2*	*0*	*5*	*1*	*0.6*	*0.1*	*15*	*0.01*	*2*
Nahuelbuta	0	6	0	15	3	190†	0.1	30	0.01	5
SD	*0*	*4*	*0*	*3*	*2*	*70*	*0.2*	*20*	*0.01*	*12*

* Rec^X in Pan de Azúcar has been corrected for atmospheric deposition of seaspray, ultimately decreases the recycling rates of weathering-derived nutrients by 95, 22, 18, 12, and 10% for Ca, K, Mg, Na, and Sr, respectively (see supporting information for further explanation and Fig. A6).

† values not being considered in the discussion as $W^{Mn}_{regolith}$ is potentially biased by high bedrock heterogeneities

690

hat gelöscht: ¶

hat verschoben (Einfügung) [4]

Table A1 Inventories of elements in bulk regolith and the bio-available fraction in soil and saprolite. Apart from phosphorus, the accessibility of these elements was determined using a sequential extraction method described by Arunachalam et al. (1996); Tessier et al. (1979); He et al. (1995). P-accessibility in the bio-available fraction has been determined by Brucker and Spohn (2019) using a modified Hedley sequential P fractionation method. Data Tables S3 & S4 include depth-dependent concentration of the bio-available fraction (pooled) and the Deionized and NH_4OAc extractions used for calculation of the inventories.

Study site		Extent* [m]	Al	Ca	Fe	K	Mg	Mn	Na	P	Si	Sr	Σ
Pan de Azúcar													
$I^X_{bio\text{-}av.\ soil}$	[g m^{-2}]	0.2	0.3	1440	n.c.	53	92	0.1	493	3.3	19	1.5	2100
$I^X_{bio\text{-}av.\ sap}$	[g m^{-2}]	1.0	1.7	3833	n.c.	253	244	0.6	682	0.0	75	3.5	5100
I^X_{bulk}	[kg m^{-2}]	1.0	136	21	44	65	8.6	0.5	39	1.3	636	0.2	950
Santa Gracia													
$I^X_{bio\text{-}av.\ soil}$	[g m^{-2}]	0.4	12	616	7.2	38	221	1.4	18	22	19	4.6	960
$I^X_{bio\text{-}av.\ sap}$	[g m^{-2}]	1.0	23	1179	21	23	651	2.9	159	21	53	8.5	2100
I^X_{bulk}	[kg m^{-2}]	1.0	183	130	75	29	42	1.5	61	1.6	532	1.0	1100
La Campana													
$I^X_{bio\text{-}av.\ soil}$	[g m^{-2}]	0.5	37	673	24	90	79	11	6.7	28	34	4.5	1000
$I^X_{bio\text{-}av.\ sap}$	[g m^{-2}]	1.0	51	1026	23	70	191	12	31	39	142	8.0	1600
I^X_{bulk}	[kg m^{-2}]	1.0	118	26	49	46	10	0.9	31	0.7	456	0.3	740
Nahuelbuta													
$I^X_{bio\text{-}av.\ soil}$	[g m^{-2}]	0.9	14	60	1.8	39	9.9	15	17	31	14	0.5	200
$I^X_{bio\text{-}av.\ sap}$	[g m^{-2}]	1.0	1.5	52	< 0.5	19	11	3.9	13	23	12	0.8	140
I^X_{bulk}	[kg m^{-2}]	1.0	95	15	47	22	13	1.0	10	0.7	309	0.1	510

$I^X_{bio\text{-}av,\ soil}$ = inventory of element X in the soil bio-available fraction; extent amounts to maximum soil depth

$I^X_{bio\text{-}av,\ sap}$ = inventory of element X in the saprolite bio-available fraction;

I^X_{bulk} = inventory of element X in bulk regolith

* the extent of the saprolite and regolith inventory have been scaled to 1.0 m for purposes of comparisons between the four study sites and the lack of an absolute measure of the depth of saprolite.

n.c. = not calculated as the respective bio-available fraction (Table S4) was below the limit of calibration of ICP-OES measurements

hat verschoben (Einfügung) [2]

hat verschoben (Einfügung) [3]

Table A2 Average $^{87}Sr/^{86}Sr$ ratio for bulk bedrock, bulk regolith, and the bio-available fraction in saprolite and soil. $^{87}Sr/^{86}Sr$ in bulk plants are weighted by the plant organs' relative growth rate and relative species abundance in the respective ecosystem (see Table 4). Radiogenic Sr composition for each single specimen are reported in Data Tables S2 (bulk regolith samples), S3 (bio-available fraction of saprolite and soil), and S5 (plant samples), respectively.

	bulk samples		bio-available samples		bulk living plants†	Seaspray input‡
	$^{87}Sr/^{86}Sr_{rock}$	$^{87}Sr/^{86}Sr_{regolith}$	$^{87}Sr/^{86}Sr_{sap}$	$^{87}Sr/^{86}Sr_{soil}$	$^{87}Sr/^{86}Sr_{plant}$	
Pan de Azúcar	0.7257	0.7305	0.7108	0.7099	0.7099	93%
SD	*0.0020*	*0.0036*	*0.0009*	*0.0007*		
Santa Gracia	0.7039	0.7044	0.7062	0.7062	0.7062	43%
SD	*0.0004*	*0.0003*	*0.0001*	*0.0001*	*0.0003*	
La Campana	0.7063	0.7053	0.7051	0.7053	0.7059	
SD	*0.0003*	*0.0002*	*0.0004*	*0.0005*	*0.0002*	
Nahuelbuta	0.7161	0.7162	0.7115	0.7111	0.7111	
SD	*0.0065*	*0.0036*	*0.0025*	*0.0023*	*0.0016*	
Seaspray*				0.7092		

* Seaspray composition from Pearce et al. (2015)

† Standard deviation corresponds to species-to-species differences in $^{87}Sr/^{86}Sr$

‡ Potential seaspray input into the bio-available fraction derived from a simple two-component mixing equation using bulk bedrock and seaspray as end-members. Substantial seaspray incorporation into the bio-available fraction in La Campana and Nahuelbuta is very unlikely (see text for discussion), therefore not shown.

hat gelöscht: 6

hat gelöscht: Table 5).

hat gelöscht: (Oeser and von Blanckenburg, 2020).

hat gelöscht: ¶
Table 7

Table A3

Turnover times for the soil and saprolite bio-available fraction with respect to the release by weathering and turnover times for bio-available fraction in soil with respect to uptake into plants.

study site	Al	Ca	Fe	K	Mg	Mn	Na	P	Si	Sr
						[yr]				
Pan de Azúcar										
$T^{X}_{bio-av.soil,U}$	10	6040	0	490	280	40	910	710	480	1250
$T^{X}_{bio-av.soil,W}$	10	n.d.	0	1590	10300	280	14800	2570	120	4670
$T^{X}_{bio-av.sap,W}$	40	n.d.	0	7570	27400	1240	20400	n.d.	490	10870
Santa Gracia										
$T^{X}_{bio-av.soil,U}$	90	480	50	80	710	120	90	330	180	590
$T^{X}_{bio-av.soil,W}$	10	600	30	510	730	230	60	1850	10	760
$T^{X}_{bio-av.sap,W}$	30	1150	80	300	2160	470	540	1760	30	1400
La Campana										
$T^{X}_{bio-av.soil,U}$	780	530	660	50	460	1420	480	160	1970	820
$T^{X}_{bio-av.soil,W}$	20	870	40	110	290	770	10	1470	3	530
$T^{X}_{bio-av.sap,W}$	20	1330	30	80	690	830	30	2050	10	950
Nahuelbuta										
$T^{X}_{bio-av.soil,U}$	760	30	160	30	30	90	790	90	490	20
$T^{X}_{bio-av.soil,W}$	20	170	10	400	70	17400	40	2900	10	120
$T^{X}_{bio-av.sap,W}$	0	150	0	190	80	4750	30	2130	10	210

$T^{X}_{bio-av.soil,U}$ = turnover time of element X in the soil bio-available fraction with respect to uptake into the ecosystem

$T^{X}_{bio-av.soil,W}$ = turnover time of element X in the soil bio-available fraction with respect to supply from dissolution of primary minerals and secondary precipitates

$T^{X}_{bio-av.sap,W}$ = turnover time of element X in the saprolite bio-available fraction with respect to supply from dissolution of primary minerals and secondary precipitates

n.d. = not determined; not determined turnover times because the respective inventory (Table A1) could not be determined

hat nach oben verschoben [4]: Nutrient recycling factors in Pan de Azúcar, Santa Gracia, La Campana, and Nahuelbuta. Shown in brackets are the Rec^{X} prior correction for atmospheric deposition.¶

hat gelöscht: Table 8

hat gelöscht: 4

hat gelöscht: ¶

Table A4 Correlation matrix with Pearson's correlation coefficients and significance (: p < 0.01, *: p < 0.05) for net primary productivity (NPP), denudation rate (D), mean annual precipitation (MAP), and indices of total and elemental degree and rate of weathering. Here we treat each regolith profile as independent, i.e. n = 8. Correlation coefficients involve the entire EarthShape study area.**

	MAP	NPP	CDF	W	$W^{Ca}_{regolith}$	$W^{K}_{regolith}$	$W^{Na}_{regolith}$	$W^{P}_{regolith}$	$W^{Si}_{regolith}$	τ^{Ca}	τ^{K}	τ^{Na}	τ^{P}	τ^{Si}
D	0.39	0.47	0.54	**0.86****	0.46	**0.80***	**0.94****	**0.87****	**0.86****	0.33	**0.66***	0.57	0.21	0.57
MAP		**0.98****	-0.15	0.06	-0.09	0.08	0.30	0.29	0.12	0.29	0.10	**0.63***	0.20	-0.05
NPP			0.01	0.15	0.08	0.14	0.38	0.41	0.20	0.45	0.17	**0.74***	0.34	0.10

CDF = chemical depletion fraction; W = soil weathering rate; $W^{X}_{regolith}$ = elemental weathering flux; τ^{X} = elemental mass transfer coefficient

Note that because CDF and τ^{X} are per definition different in sign (i.e. a CDF of +1 denote entire depletion, whereas a τ^{X} of -1 denote entire depletion), τ^{X} was multiplied by -1 for presentation purposes. Bold numbers denote significant correlation.

Table A5 Correlation matrix with Pearson's correlation coefficients and significance (: p < 0.01, *: p < 0.05) for net primary productivity (NPP), denudation rate (D), mean annual precipitation (MAP), and indices of total and elemental degree and rate of weathering. Correlation coefficients involve the study sites Pan de Azúcar, Santa Gracia, and Nahuelbuta. Here we treat each regolith profile as independent, i.e. n = 6. La Campana has been excluded because it features the steepest relief of all sites which causes elevated denudation rates.**

	MAP	NPP	CDF	W	$W^{Ca}_{regolith}$	$W^{K}_{regolith}$	$W^{Na}_{regolith}$	$W^{P}_{regolith}$	$W^{Si}_{regolith}$	τ^{Ca}	τ^{K}	τ^{Na}	τ^{P}	τ^{Si}
D	**0.68***	**0.72***	0.02	**0.54***	0.31	0.53	**0.94****	**0.76***	**0.81***	0.33	0.05	0.57	0.20	0.16
MAP		**0.99****	-0.24	0.09	-0.11	0.41	**0.64***	0.41	0.41	0.29	0.16	**0.72***	0.21	-0.11
NPP			-0.07	0.24	0.05	0.46	**0.72***	0.54	0.52	0.45	0.23	**0.82***	0.35	0.06

CDF = chemical depletion fraction; W = soil weathering rate; $W^{X}_{regolith}$ = elemental weathering flux; τ^{X} = elemental mass transfer coefficient

Note that because CDF and τ^{X} are per definition different in sign (i.e. a CDF of +1 denote entire depletion, whereas a τ^{X} of -1 denote entire depletion), τ^{X} was multiplied by -1 for presentation purposes. Bold numbers denote significant correlation.

hat gelöscht: Abschnittswechsel (Nächste Seite)

Table A6 ANOVAs evaluating variations in denudation rate (D), the chemical depletion fraction (CDF), soil weathering rate (W), and the elemental weathering rates for Ca, K, Na, P, and Si ($W^{Ca}_{regolith}$, $W^{K}_{regolith}$, $W^{Na}_{regolith}$, $W^{P}_{regolith}$, $W^{Si}_{regolith}$) among sites (single regolith profiles treated as independent from each other, n = 8). The Tukey HSD test for site comparison is shown below. Sig = 1 indicates significant differences between the sites. The comparison between Santa Gracia and Nahuelbuta is highlighted in bold because of their importance in the discussion.

		D		*CDF*		*W*		$W^{Ca}_{regolith}$		$W^{K}_{regolith}$		$W^{Na}_{regolith}$		$W^{P}_{regolith}$		$W^{Si}_{regolith}$	
		F ratio	***p > F***	***F ratio***	***p > F***	***F ratio***	***p > F***	***F ratio***	***p > F***	***F ratio***	***p > F***	***F ratio***	***p > F***	***F value***	***p > F***	***F value***	***p > F***
Overall ANOVA		*6.91*	*0.05*	*8.07*	*0.04*	*4.58*	*0.09*	*7.86*	*0.04*	*2.22*	*0.23*	*3.63*	*0.10*	*3.52*	*0.00*	*7.96*	*0.01*
Site 1	**Site 2**	***p value***	***Sig***	***p value***	***Sig***	***p value***	***Sig***	***p value***	***Sig***	***p value***	***Sig***	***p value***	***Sig***	***p value***	***Sig***	***p value***	***Sig***
Santa Gracia	Pan de Azúcar	0.86	0	0.07	1	0.80	0	0.04	1	1.00	0	0.80	0	0.34	0	0.80	0
La Campana	Pan de Azúcar	0.04	1	0.05	1	0.09	1	0.09	1	0.27	0	0.10	1	0.10	1	0.01	1
La Campana	Santa Gracia	0.08	1	0.99	0	0.20	0	0.70	0	0.30	0	0.25	0	0.62	0	0.30	0
Nahuelbuta	Pan de Azúcar	0.36	0	0.83	0	0.96	0	0.50	0	1.00	0	0.61	0	0.42	0	0.95	0
Nahuelbuta	**Santa Gracia**	**0.70**	**0**	**0.14**	**0**	**0.97**	**0**	**0.04**	**1**	**1.00**	**0**	**0.98**	**0**	**1.00**	**0**	**1.00**	**0**
Nahuelbuta	La Campana	0.22	0	0.11	0	0.13	0	0.38	0	0.31	0	0.35	0	0.51	0	0.29	0

F ratio = ratio of two mean square values.
P value ≤ 0.1 = Populations have significant different mean values
Sig = significance; 0: not significant, 1: significant

Seite 52: [1] hat gelöscht	**author**	**28.08.20 16:09:00**

Seite 52: [2] hat gelöscht	**author**	**28.08.20 16:09:00**

Seite 52: [2] hat gelöscht	**author**	**28.08.20 16:09:00**